

Quantum Quench in the Transverse Field Ising chain I: Time evolution of order parameter correlators

Pasquale Calabrese¹, Fabian H.L. Essler², and Maurizio Fagotti²

¹ Dipartimento di Fisica dell'Università di Pisa and INFN - Pisa 56127, Italy

² The Rudolf Peierls Centre for Theoretical Physics, University of Oxford - Oxford OX1 3NP, United Kingdom

Abstract. We consider the time evolution of order parameter correlation functions after a sudden quantum quench of the magnetic field in the transverse field Ising chain. Using two novel methods based on determinants and form factor sums respectively, we derive analytic expressions for the asymptotic behaviour of one and two point correlators. We discuss quenches within the ordered and disordered phases as well as quenches between the phases and to the quantum critical point. We give detailed account of both methods.

1. Introduction

The non-equilibrium dynamics of isolated quantum systems after a sudden “quench” of a parameter characterizing their respective Hamiltonians is a subject currently under intensive theoretical and experimental investigation. Recent experiments on trapped ultra-cold atomic gases [1, 2, 3, 4, 5, 6] have established that these systems are sufficiently weakly coupled to their environments as to allow the observation of essentially unitary non-equilibrium time evolution on very long time scales. This in turn provides the opportunity of investigating fundamental questions of many-body quantum mechanics, which in standard condensed matter systems are obscured by decoherence and dissipation. Two of the main questions raised in these works are (i) how fast correlations spread in quantum many-body systems and (ii) whether observables such as (multi-point) correlation functions generically relax to time independent values, and if they do, what principles determine their stationary properties. The first issue was addressed in a seminal work by Lieb and Robinson [7], which established that in lattice many-body systems information has a finite speed of propagation and provided a bound on the maximal group velocity. In recent years an effective light-cone scenario has been proposed theoretically [8, 9, 10, 11, 12], was tested in many numerical computations [13, 14, 15, 16, 17, 18] and was finally observed in cold-atom experiments [4].

The relaxation towards stationary behaviour at first appears very surprising, because unitary time evolution maintains the system in a pure state at all times. The resolution of this apparent paradox is that in the thermodynamic limit, (finite) *subsystems* can and do display correlations characterized by a mixed state, namely the one obtained by tracing out the degrees of freedom outside the subsystem itself. In other words, the system acts as its own bath.

In groundbreaking (“quantum Newton’s cradle”) experiments on the relaxation towards stationary states in systems of ultra-cold atoms Kinoshita, Wenger and Weiss [6] demonstrated the importance of dimensionality and conservation laws for many-body quantum dynamics out of equilibrium. In essence, these experiments show that three dimensional condensates relax quickly to a stationary state that is characterized by an effective temperature, a process known as “thermalization”, whereas the relaxation of quasi one-dimensional systems is slow and towards an unusual non-thermal distribution. This difference has been attributed to the existence of additional (approximate) local conservation laws in the quasi-1D case, which are argued to constrain the dynamics in analogy with classical integrable systems. The findings of Ref. [6] sparked a tremendous theoretical effort aimed at clarifying the effects of quantum integrability on the non-equilibrium evolution in many-particle quantum systems [19, 20, 21, 9, 22, 23, 24, 25, 26, 27, 28, 29, 30, 31, 32, 33, 34, 35, 36, 37, 38, 39, 40, 41, 42, 43, 44, 45, 46, 47, 48]. Many of these studies are compatible with the widely held belief (see e.g. [19] for a comprehensive summary) that the reduced density matrix of any finite subsystem (which determines correlation functions of any local observables within the subsystem) of an infinite system can be described in terms of either an effective thermal (Gibbs) distribution or a so-called generalized Gibbs ensemble [20]. It has been conjectured that the latter arises for integrable models, while the former is obtained for generic systems and evidence supporting this view has been obtained in a number of examples [20, 21, 22, 23, 24, 25, 26, 29, 31, 32, 33]. On the other hand, several numerical studies [34, 36, 37, 44, 45] suggest that the full picture may well be more complex.

Moreover, open questions remain even with regards to the very existence of stationary states. For example, the order parameter of certain mean-field models have been shown to display persistent oscillations [49, 50, 51, 52, 53, 54]. Non-decaying oscillations have also been observed numerically [36] in some non-integrable one-dimensional systems. This has given rise to the concept of “weak

thermalization”, which refers to a situation where time-averaged quantities are thermal, while oscillations persist on short time-scales. We note that questions related to thermalization and spreading of correlations have also been studied using holographic techniques [55, 56, 57].

Given that stationary behaviour is strictly speaking a property at infinite times in the thermodynamic limit (and these limits do not commute) it is important to have available analytic results that become exact in certain limits. To that end we consider here the non-equilibrium dynamics of the transverse field Ising chain

$$H(h) = -J \sum_{j=1}^L \left[\sigma_j^x \sigma_{j+1}^x + h \sigma_j^z \right], \quad (1)$$

where σ_j^α are the Pauli matrices at site j , $J > 0$ and we impose periodic boundary conditions $\sigma_{L+1}^\alpha = \sigma_1^\alpha$. The Hamiltonian (1) exhibits a \mathbb{Z}_2 symmetry of rotations around the z -axis in spin space by 180 degrees

$$\sigma_j^\alpha \rightarrow -\sigma_j^\alpha, \quad \alpha = x, y, \quad \sigma_j^z \rightarrow \sigma_j^z. \quad (2)$$

The model (1) is a crucial paradigm of quantum critical behaviour and quantum phase transitions [58]. At zero temperature and in the thermodynamic limit it exhibits ferromagnetic ($h < 1$) and paramagnetic ($h > 1$) phases, separated by a quantum critical point at $h_c = 1$. For $h < 1$ and $L \rightarrow \infty$ there are two degenerate ground states related by the \mathbb{Z}_2 symmetry (2). Spontaneous symmetry breaking selects a unique ground state, in which spins align along the x -direction. On the other hand, for magnetic fields $h > 1$ the ground state is non-degenerate and as the magnetic field h is increased spins align more and more along the z -direction. The order parameter for the quantum phase transition is the ground state expectation value $\langle \sigma_j^x \rangle$. In the following we will refer to the ferromagnetic phase as the ordered phase, and to the paramagnetic one as the disordered phase. We note that the model (1) is (approximately) realized both in solids [59] and in systems of cold Rubidium atoms confined in an optical lattice [60]. In the latter realization it is possible to investigate its non-equilibrium dynamics experimentally.

As shown in Appendix A, the model can be diagonalized by a Jordan-Wigner transformation which maps the model to spinless fermions with local annihilation operators c_j , followed by a Fourier transform and a Bogoliubov transformation. In terms of the momentum space Bogoliubov fermions α_k the Hamiltonian reads

$$H(h) = \sum_k \varepsilon_h(k) \alpha_k^\dagger \alpha_k, \quad \varepsilon_h(k) = 2J \sqrt{1 + h^2 - 2h \cos(k)}. \quad (3)$$

For details and more precise definitions see Appendix A.

1.1. Quench protocol and observables

In the following we focus on a *global quantum quench* of the magnetic field. We assume that the many-body system is prepared in the ground state $|\Psi_0\rangle$ of Hamiltonian $H(h_0)$. At time $t = 0$ the field h_0 is changed instantaneously to a different value h and one then considers the unitary time evolution of the system characterized by the new Hamiltonian $H(h)$, i.e. the initial state $|\Psi_0\rangle$ evolves as

$$|\Psi_0(t)\rangle = e^{-itH(h)} |\Psi_0\rangle. \quad (4)$$

The above protocol corresponds to an experimental situation, in which a system parameter has been changed on a time scale that is small compared to any other time scale in the system. We note that this can be achieved in cold-atom experiments [1, 3, 4].

In this paper we study the one and two-point functions of the order parameter

$$\rho^x(t) = \frac{\langle \Psi_0(t) | \sigma_\ell^x | \Psi_0(t) \rangle}{\langle \Psi_0(t) | \Psi_0(t) \rangle}, \quad (5)$$

$$\rho^{xx}(\ell, t) = \frac{\langle \Psi_0(t) | \sigma_{j+\ell}^x \sigma_j^x | \Psi_0(t) \rangle}{\langle \Psi_0(t) | \Psi_0(t) \rangle}, \quad \rho_c^{xx}(\ell, t) = \rho^{xx}(\ell, t) - (\rho^x(t))^2. \quad (6)$$

Although quantum quenches in the 1D Ising model have been the subject of many works [61, 62, 63, 64, 65, 66, 67, 68, 69, 70], results on the time evolution of order parameter correlation functions were reported only very recently by us in a short communication [71]. In the following we give detailed derivations on the *full asymptotic time and distance dependence* of one- and two-point order parameter correlation functions in the thermodynamic limit for quenches within the two phases. These have been obtained by two novel, complementary methods, and we discuss both of them in detail. The first method is based on the determinant representation of correlation functions characteristic of free-fermionic theories. The second is based on the form-factor approach [72, 73, 74, 75, 76] and is applicable more generally to integrable quenches in interacting quantum field theories [77, 32]. We stress that this approach is qualitatively different from numerical approaches based on quantum integrability [78, 79, 80, 44, 46]. In particular it allows us to obtain analytical results in the thermodynamic limit. New results not previously reported in [71] include expressions for the two-point function of the order parameter for quenches within the disordered phase and for quenches across the critical point.

1.2. The quench variables

As shown in Appendix A both the initial and final Hamiltonians can be diagonalized by combined Jordan-Wigner and Bogoliubov transformations with Bogoliubov angles θ_k^0 and θ_k respectively. The corresponding Bogoliubov fermions are related by a linear transformation (B.1) characterized by the difference $\Delta_k = \theta_k - \theta_k^0$. In order to parametrize the quench it is useful to introduce the quantity

$$\cos \Delta_k = \frac{hh_0 - (h + h_0) \cos k + 1}{\sqrt{1 + h^2 - 2h \cos(k)} \sqrt{1 + h_0^2 - 2h_0 \cos(k)}}. \quad (7)$$

We note that $\cos \Delta_k$ is invariant under the two transformations

$$(h_0, h) \rightarrow (h, h_0) \quad \text{and} \quad (h_0, h) \rightarrow \left(\frac{1}{h_0}, \frac{1}{h} \right). \quad (8)$$

However, we stress that the quantum quench itself is not invariant under the maps (8). In the form factor approach a more natural quantity to consider is

$$K(p) = \tan[\Delta_p/2]. \quad (9)$$

1.3. Time scales for two-point correlators.

In this manuscript we are mainly concerned with equal time correlation functions of spins separated by a distance ℓ , which we take to be much larger than the lattice spacing, i.e. $\ell \gg 1$. For fixed ℓ the time evolution is naturally divided into three regimes, which are determined by the propagation velocity of elementary excitations of the post-quench Hamiltonian $v(k) = \frac{d\varepsilon_h(k)}{dk}$. For a given final magnetic field h , the maximal propagation velocity is

$$v_{\max} = \max_{k \in [-\pi, \pi]} |\varepsilon'_h(k)| = 2J \min[h, 1]. \quad (10)$$

The three different regimes are:

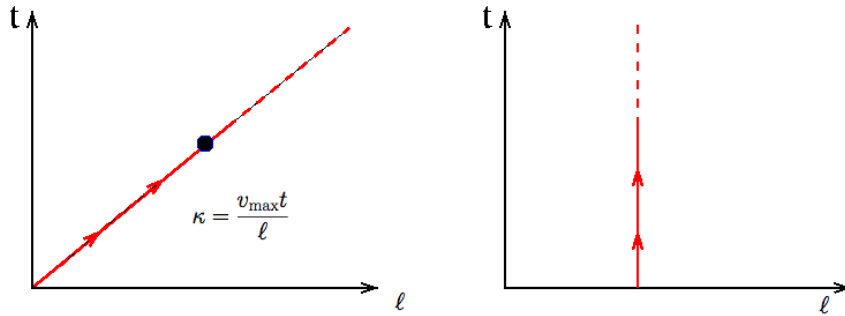


Figure 1. Left panel: for intermediate times $v_{\max}t \sim \ell$ the behaviour of $\rho^{\alpha\alpha}(\ell, t)$ is most conveniently determined by considering its asymptotic expansion around infinity (“space-time scaling limit”) along the ray $v_{\max}t = \kappa\ell$. This viewpoint is appropriate for any large, finite t and ℓ . Right panel: the asymptotic late-time regime is reached by considering time evolution at fixed ℓ . To describe this regime one should consider an asymptotic expansion of $\rho^{\alpha\alpha}(\ell, t)$ around $t = \infty$ at fixed ℓ .

- Short-times $v_{\max}t \ll \ell$.
- Intermediate times $v_{\max}t \sim \ell$. This regime is of particular importance for both experiments and numerical computations. A convenient way of describing this regime is to consider evolution along a particular “ray” $\kappa\ell = v_{\max}t$ in space-time, see Fig. 1. In order to obtain a very accurate description of the dynamics at a particular point along this ray, one may then construct an asymptotic expansion in the single variable ℓ around the *space-time scaling limit* $v_{\max}t, \ell \rightarrow \infty$, κ fixed.
- Late times $v_{\max}t \gg \ell$. This includes the limit $t \rightarrow \infty$ at fixed but large ℓ . In this regime it is no longer convenient to consider evolution along a particular ray in space-time. In order to obtain accurate results for the late time dynamics, one should construct an asymptotic expansion in t around infinity, see Fig. 1.

Because of the horizon effect [9, 22] the short-time regime does not display interesting features. We therefore focus on intermediate and late times. The most convenient way of analyzing the intermediate time regime is via the space-time scaling limit. It is important to note that taking the limit $\kappa \rightarrow 0$ of results obtained in the space-time scaling limit is *not* expected to reproduce the short-time regime. Similarly, in general taking $\kappa \rightarrow \infty$ in the space-time scaling limit does not necessarily reproduce the late time behaviour.

1.4. Organization of the manuscript.

This is the first in a series of two papers of the dynamics in the transverse field Ising chain after a sudden quench of the magnetic field. The second paper, henceforth referred to as “paper II”, gives a detailed account of properties in the stationary state, i.e. at $t = \infty$. The present manuscript deals with the time evolution of observables and is organized in the following way. In section 2 we present a detailed summary of our main results. In section 3 we discuss the determinant approach for calculating two-point functions after quantum quenches in models with free fermionic spectra. Section 4 introduces the form factor approach to correlation functions in integrable models after quantum quenches and gives a detailed account of its application to one and two point functions in the Ising chain. The scaling limit for quenches close to the critical point is constructed in section

5, and section 6 contains our conclusions. Our conventions for diagonalizing the Ising Hamiltonian with periodic boundary conditions are summarized in Appendix A and the initial state is expressed in terms of eigenstates of the post-quench Hamiltonian in Appendix B. Finally, Appendix C and Appendix D deal with certain technical issues.

2. Summary and discussions of the results

In this section we present a comprehensive summary of our main results. Our analytic results are valid in the thermodynamic limit $L \rightarrow \infty$ and are obtained by two different methods.

- (i) The first is based on representing correlation functions as determinants and then determining the asymptotic behaviour in the space-time scaling limit

$$t, \ell \rightarrow \infty, \frac{v_{\max} t}{\ell} \text{ fixed.} \quad (11)$$

Results obtained by this methods are exact.

- (ii) The second method employs a Lehmann representation for correlation functions, which provides an expansion of the correlator in powers of the functions $K(k)$ (9). The Lehmann representation is recast as a *low-density expansion* and then the dominant terms at late times and large distances are summed to all orders in $K(k)$. The method exploits the existence of a small parameter, namely the average densities $n(k)$ of elementary excitations of the post-quench Hamiltonian $H(h)$ with momentum k in the initial state $|\Psi_0(0)\rangle$

$$\frac{\langle \Psi_0(0) | n(k) | \Psi_0(0) \rangle}{\langle \Psi_0(0) | \Psi_0(0) \rangle} = \frac{K^2(k)}{1 + K^2(k)}. \quad (12)$$

A *small quench* is defined as being such that these densities are small for all k , i.e. $\max_k K^2(k) \ll 1$ (this does not necessarily imply that h and h_0 have to be very close to each other). The form factor approach provides accurate results for small quenches at late times and large distances. In practice the form factor method provides very good approximations to the exact result, except for quenches to or from the close vicinity of the critical point.

Analytic results obtained by the two methods are compared to a direct numerical evaluation of the determinant representations of correlation functions in the thermodynamic limit. Finite-size effects are concomitantly absent and for the purposes of the comparisons shown in the following figures the numerical results can therefore be considered to be exact.

2.1. One-point correlation function

For quenches starting in the disordered phase, i.e. $h_0 > 1$, the order parameter expectation value is zero for all times because the \mathbb{Z}_2 symmetry remains unbroken. For quenches that start and end in the ordered phase, i.e. $h_0, h < 1$, exact calculations based on the determinant approach show that the order parameter relaxes to zero exponentially at late times ($t \gg 1$) (note that since $\ln |\cos \Delta_k| < 0$ the exponential is always decreasing)

$$\langle \sigma_i^x(t) \rangle \simeq (\mathcal{C}_{\text{FF}}^x)^{\frac{1}{2}} \exp \left[t \int_0^\pi \frac{dk}{\pi} \varepsilon'_h(k) \ln |\cos \Delta_k| \right], \quad (13)$$

where

$$\mathcal{C}_{\text{FF}}^x = \frac{1 - hh_0 + \sqrt{(1 - h^2)(1 - h_0^2)}}{2\sqrt{1 - hh_0}(1 - h_0^2)^{\frac{1}{4}}}. \quad (14)$$

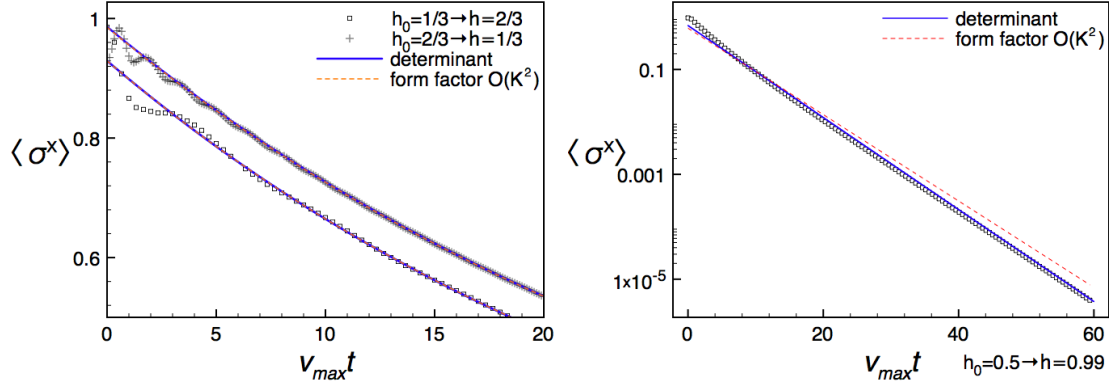


Figure 2. Expectation value of the order parameter after a quench within the ferromagnetic phase. Numerical data are compared with the asymptotic predictions from both determinants and form factors at order $O(K^2)$. The right panel shows the accuracy of the determinant result even very close to the critical point, while the form factor result ceases to be an accurate approximation because the density of excitations is no longer small. Numerical results are obtained by considering the cluster decomposition of the two-point function at distance $\ell = 180$. The left hand panel shows that the short-time behaviour after the quench is sensitive to whether the transverse field is increased or decreased. If $1 > h > h_0$ then $\langle \sigma^x(t) \rangle$ decreases for short times, while it initially increases if $1 > h_0 > h$.

This result is obtained by applying the cluster decomposition principle to the two-point function (19) (see Eq. (69) in Section 3 for the proof of Eq. (19)). The form factor approach gives (see Section 4.2)

$$\langle \sigma_i^x(t) \rangle \simeq (1 - h^2)^{\frac{1}{8}} \exp \left[-t \int_0^\pi \frac{dk}{\pi} \varepsilon'_h(k) 2K^2(k) \right]. \quad (15)$$

We note that

$$\begin{aligned} \ln |\cos \Delta_k| &= \ln \left[\frac{1 - K^2(k)}{1 + K^2(k)} \right] = -2K^2(k) - \frac{2}{3}K^6(k) + \dots, \\ (\mathcal{C}_{\text{FF}}^x)^{\frac{1}{2}} &\simeq (1 - h^2)^{\frac{1}{8}} + \frac{(h - h_0)^4}{64(1 - h^2)^{\frac{31}{8}}} + \dots, \end{aligned} \quad (16)$$

so that (15) is indeed the “low-density” approximation to (13).

Fig. 2 shows the comparison of the asymptotic result against exact numerical computation (obtained from cluster decomposition of the two-point function). It is evident that the asymptotic results become accurate already for small values of t . Eqn (13) is asymptotically valid also for quenches to the critical point as is shown in the left panel of Fig. 2.

For a quench from the ferromagnetic $h_0 < 1$ to the paramagnetic $h > 1$ phase, we *conjecture* that the expectation value of the order parameter at late times t is given by

$$\langle \sigma_i^x(t) \rangle = (\mathcal{C}_{\text{FP}}^x)^{\frac{1}{2}} [1 + \cos(2\varepsilon_h(k_0)t + \alpha) + \dots]^{\frac{1}{2}} \exp \left[t \int_0^\pi \frac{dk}{\pi} \varepsilon'_h(k) \ln |\cos \Delta_k| \right], \quad (17)$$

where k_0 is a solution of the equation $\cos \Delta_{k_0} = 0$, $\alpha(h, h_0)$ is an unknown constant, and

$$\mathcal{C}_{\text{FP}}^x = \left[\frac{h\sqrt{1 - h_0^2}}{h + h_0} \right]^{\frac{1}{2}}. \quad (18)$$

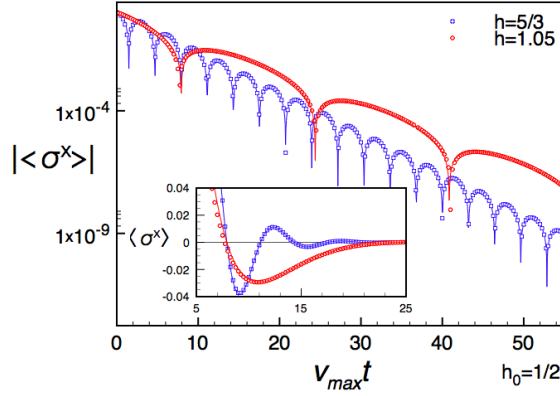


Figure 3. Expectation value of the order parameter after a quench from the ferromagnetic to the paramagnetic phase (inset) and its absolute value (main plot) in logarithmic scale to show the exponential decay of the correlation. Numerical data from $h_0 = 1/2$ to $h = 5/3$ and $h = 1.05$ are compared with the asymptotic conjecture in Eq. (17) which is reported as a continuous line. The asymptotic formula is valid all the way up to the critical point. Data are obtained by considering the cluster decomposition of the two-point function at distance $\ell = 180$.

The dots in eqn (17) indicate subleading contributions. The conjecture (17) is compared to the numerically calculated one-point function (the 1-point function is obtained by applying the cluster decomposition principle to the two-point function Eq. (32), see Section 3.2.1) in Fig. 3. The agreement is clearly excellent. From a mathematical point of view the oscillating factor is a correction to the asymptotic behaviour, as is most clearly seen by considering $\log |\langle \sigma_i^x(t) \rangle|$. However, by virtue of its oscillatory nature, its presence obscures the leading behaviour and needs to be included in order to have a good description of the quench dynamics. In the limit $h \rightarrow 1$, k_0 goes to 0 and $\varepsilon_1(k_0) = 0$, signaling that the crossover between (13) and (17) is smooth. In particular, when approaching the critical point, the oscillation frequency decreases as shown in Fig. 3.

2.2. Equal time two-point correlation function

2.2.1. Quench within the ferromagnetic phase. For a quench within the ordered phase, the determinant approach (detailed in Section 3) leads to the following result for the two-point function in the space-time scaling limit ($t, \ell \rightarrow \infty$ with $v_{\max} t / \ell$ fixed)

$$\begin{aligned} \rho_{FF}^{xx}(\ell, t) &\simeq C_{FF}^x \exp \left[\ell \int_0^\pi \frac{dk}{\pi} \ln |\cos \Delta_k| \theta_H(2\varepsilon'_h(k)t - \ell) \right] \\ &\quad \times \exp \left[2t \int_0^\pi \frac{dk}{\pi} \varepsilon'_h(k) \ln |\cos \Delta_k| \theta_H(\ell - 2\varepsilon'_h(k)t) \right]. \end{aligned} \quad (19)$$

Here $\theta_H(x)$ is the Heaviside step function

$$\theta_H(x) = \begin{cases} 1 & \text{if } x > 0, \\ 0 & \text{else.} \end{cases} \quad (20)$$

The constant C_{FF}^x (14) is fixed by matching (19) to the corresponding result at infinite time $t = \infty$, which is derived in paper II [81].

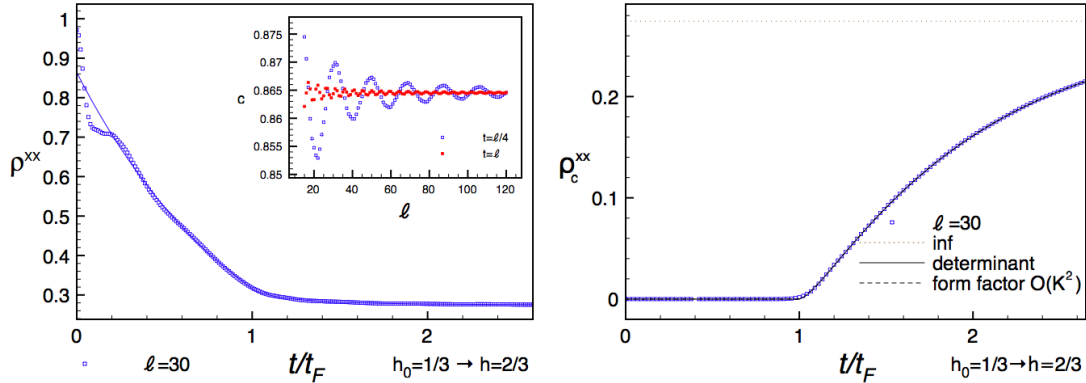


Figure 4. Numerical data for a quench within the ferromagnetic phase from $h_0 = 1/3$ to $h = 2/3$. Left: The two-point function against the asymptotic prediction Eq. (19) for $\ell = 30$ (up to a multiplicative factor) showing excellent agreement in the scaling regime. Inset: Ratio between the numerical data and asymptotic prediction (69). The leading correction is time independent, but subleading contributions oscillate. Right: The connected correlation function for the same parameters as on the left. For $t < t_F$, $\rho_c^{xx}(\ell, t)$ vanishes identically in the scaling regime.

In the limit $\ell \rightarrow \infty$ (19) gives the square of the result (13) for the one-point function. For times smaller than the Fermi time

$$t_F = \frac{\ell}{2v_{\max}}, \quad (21)$$

the first exponential factor in (19) equals 1. Thus, in the space-time scaling limit, connected correlations *vanish identically* for times $t < t_F$ and begin to form only after the Fermi time. This is a general feature of quantum quenches [9, 22] and has been recently observed in experiments on one dimensional cold-atomic gases [4]. We stress that this by no means implies that the connected correlations are exactly zero for $t < t_F$: in any model, both on the lattice or in the continuum there are exponentially suppressed terms (in ℓ) which vanish in the scaling limit. The form factor approach gives the following result for large t and ℓ (see Section 4.3)

$$\begin{aligned} \rho_{FF}^{xx}(\ell, t) &\simeq (1 - h^2)^{\frac{1}{4}} \exp \left[-2\ell \int_0^\pi \frac{dk}{\pi} K^2(k) \theta_H(2\varepsilon'_h(k)t - \ell) \right] \\ &\times \exp \left[-4t \int_0^\pi \frac{dk}{\pi} \varepsilon'_h(k) K^2(k) \theta_H(\ell - 2\varepsilon'_h(k)t) \right]. \end{aligned} \quad (22)$$

As expected, it gives the low density approximation to the full result (19).

A comparison (for a typical quench from $h_0 = 1/3$ to $h = 2/3$) between the asymptotic results (19) (22) and numerical results for the correlation function at a finite but large distance ($\ell = 30$) is shown in Fig. 4. The numerical results are obtained by expressing the two-point correlator in the thermodynamic limit as the determinant of an $\ell \times \ell$ matrix (see section 3) and then evaluating the determinant for different times. As we are concerned with equal time correlators only we do not need to extract the two-point function from a cluster decomposition of the 4-point function [61]. The agreement is clearly excellent. The ratio between the exact numerics and the analytic result (19) in the space-time scaling limit is shown in the inset of Fig. 4 for two values of $\kappa = v_{\max}t/\ell$. We see the ratio approaches a constant for large ℓ . The corrections to this constant are seen to

be oscillating. The right panel of Fig. 4 shows results for the connected two-point function for the same quench ($h_0 = 1/3 \rightarrow h = 2/3$). We see that the numerical data are fit very well by both (19) and the form factor result (22). The connected correlator is exponentially small for $t < t_F$ and correlations start forming at t_F .

In order to elucidate the relaxational behaviour of the two point function it is useful to follow Refs [9, 22] and rewrite (19) in the form

$$\frac{\rho_{FF}^{xx}(\ell, t)}{(\rho_{FF}^x(t))^2} \sim \exp \left[\int_0^\pi \frac{dk}{\pi} \left(\frac{2t}{\tau(k)} - \frac{\ell}{\xi(k)} \right) \theta_H \left(\frac{2t}{\tau(k)} - \frac{\ell}{\xi(k)} \right) \right]. \quad (23)$$

Here we have defined mode-dependent correlation lengths $\xi(k)$ and decay times $\tau(k)$ by

$$\xi^{-1}(k) = -\ln |\cos \Delta_k|, \quad \tau^{-1}(k) = -\varepsilon'_h(k) \ln |\cos \Delta_k|. \quad (24)$$

We observe that these quantities are related by the velocity $v_k = \varepsilon'_h(k)$ of the momentum k mode

$$v_k \tau(k) = \xi(k), \quad (25)$$

which allows us to rewrite the theta-function in (23) as $\theta_H(2v_k t - \ell)$. The physical interpretation of (23) is then clear: a given mode contributes to the relaxational behaviour only if the distance ℓ lies within its forward “light cone” (the factor of two multiplying the velocity is explained in Refs [9, 22]). The form of the remaining factor then follows from the stationary behaviour: the time dependent piece compensates the factor $(\rho_{FF}^x)^{-2}$, while the time-independent part is fixed by the $t \rightarrow \infty$ value of the correlator. As we already pointed out in our letter [71], this implies that the generalized Gibbs ensemble that characterizes the stationary state in fact determines the relaxational behaviour at late times as well.

Approach to infinite times within the space-time scaling regime. For the quench within the ferromagnetic phase, the infinite time limit at fixed ℓ gives the same result as the infinite time limit within the space-time scaling regime, i.e.

$$\lim_{t \rightarrow \infty} \frac{1}{\ell} \ln |\rho_{FF}^{xx}(\ell, t)| = \lim_{\kappa \rightarrow 0} \lim_{\substack{\ell, t \rightarrow \infty \\ t/\ell \text{ fixed}}} \frac{1}{\ell} \ln |\rho_{FF}^{xx}(\ell, t)|. \quad (26)$$

It is then useful to consider the approach to the stationary value within the space-time scaling regime result (19). In the limit $t \rightarrow \infty$, we have

$$\rho_{FF}^{xx}(\ell, t = \infty) \propto \exp \left[\ell \int_0^\pi \frac{dk}{\pi} \ln |\cos \Delta_k| \right]. \quad (27)$$

The corrections to (27) for large, finite times arise from the modes with $\varepsilon'_h(k) \sim 0$. For any $h \neq 1$, both modes with $k = 0$ and $k = \pi$ contribute to this correction and at the same order since both $\ln |\cos \Delta_k|$ and the dispersion relation itself are quadratic at both points. A straightforward calculation gives for any $h, h_0 < 1$

$$\frac{\rho_{FF}^{xx}(\ell, t \gg \ell)}{\exp \left[\ell \int_0^\pi \frac{dk}{\pi} \ln |\cos \Delta_k| \right]} \propto 1 + \frac{(h - h_0)^2 (1 - 2hh_0 + h_0^2)}{96\pi(1 - h_0^2)^2} \frac{\ell^4}{(v_{\max} t)^3} + \dots \quad (28)$$

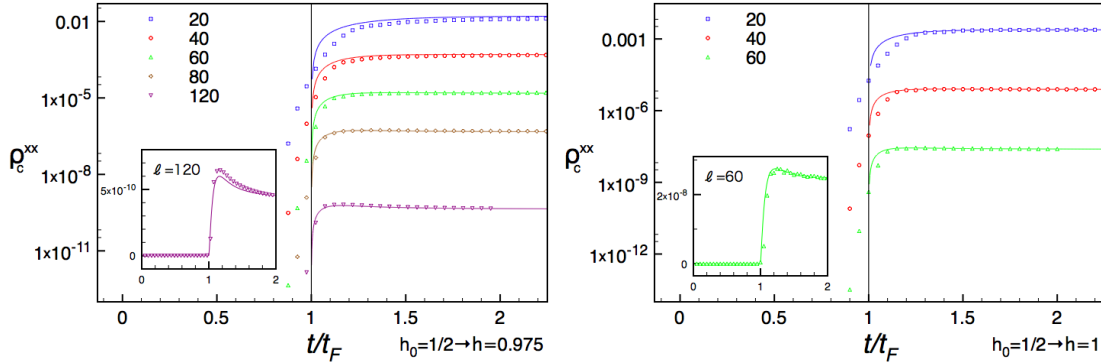


Figure 5. Numerical results for the connected two-point function for a quench from the ferromagnetic phase to a magnetic field very close to (left) and exactly at the critical point (right). The asymptotic behaviour agrees with the prediction (19) shown as continuous lines, but corrections are visible for smaller values of ℓ .

2.2.2. Quenches from the ferromagnetic phase to the quantum critical point. If we adjust the constant C_{FF}^x appropriately, equation (19) holds even for quenches to the quantum critical point. In Fig. 5 numerical results for the connected correlation function are compared with the asymptotic prediction for quenches very close to the critical point (left) and exactly to the critical point (right). In both cases, the asymptotic prediction is seen to become more accurate when ℓ is increased. However, it is clear from the figure that the asymptotic prediction works better for quenches exactly to the critical point than for quenches very close to it. This somewhat counterintuitive behaviour is readily understood as a property of subleading contributions to (19). We have already seen in the inset of Fig. 4 that there are subleading oscillating corrections. A more detailed analysis shows that they are power laws with an exponent that tends to zero upon approaching the critical point. This explains why the agreement of (19) with the numerical results is worse in Fig. 5 (left) than in Fig. 4. At the same time as the exponent of the power-law correction tends to zero upon quenching ever closer to the critical point, the oscillation frequency approaches zero as well. For quenches exactly to the critical point the leading oscillating corrections are therefore absent: they have morphed into a renormalization of the constant amplitude multiplying (19). This is the reason why (19) works better for quenches exactly to the critical point than for quenches close to it.

For a quench to the critical point at $h_c = 1$, the result (19) should be compared with conformal field theory (CFT) predictions of Refs [9, 22], which give the following result valid in the scaling limit of the Ising model

$$\lim_{h \rightarrow 1} \frac{\rho^{xx}(r, t)}{(1 - h^2)^{\frac{1}{4}}} \propto \begin{cases} e^{-\pi t/8\tau_0} & \text{for } vt < r/2 \\ e^{-\pi r/16v\tau_0} & \text{for } vt > r/2. \end{cases} \quad (29)$$

Here r is the physical distance, v the velocity characterizing the (strictly) linear dispersion relation $\varepsilon_q = vq$ at the critical point, and τ_0 the so-called extrapolation time. Eqn (29) is valid for times and distances such that $(x/v), t, (x/v) - t \gg \tau_0$. The scaling limit of the result (19) is constructed in section 5, and considering a quench to the critical point we obtain from (264)

$$\lim_{h \rightarrow 1} \frac{\rho^{xx}(r, t)}{(1 - h^2)^{\frac{1}{4}}} \propto \exp\left(-\frac{\Delta_0}{2v} \left[r\theta(2vt - r) + 2vt\theta(r - 2vt) \right]\right), \quad (30)$$

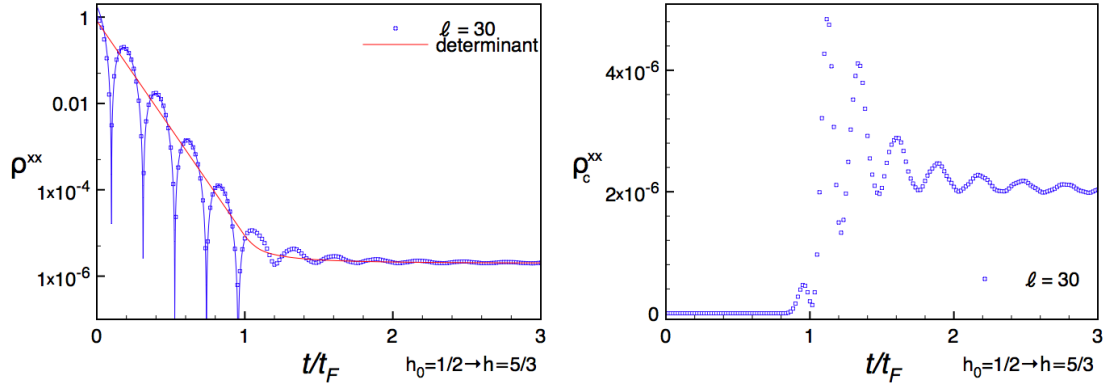


Figure 6. Numerical data for a quench from the ferromagnetic to the paramagnetic phase. Left: The two-point function against the asymptotic prediction Eq. (32) (valid for $t < t_F$) showing excellent agreement. Right: The connected correlation function for the same quench as on the left. For $t < t_F$, ρ_c^{xx} vanishes identically in the scaling regime. For $t > t_F$, ρ^{xx} (and so ρ_c^{xx}) approaches the asymptotic value Eq. (19), but subleading oscillating corrections are visible.

where $\Delta_0 = J(1 - h_0)$. Comparing (30) to (29) we see that the two expressions agree if we take the extrapolation time to be

$$\tau_0^{-1} = \frac{8\Delta_0}{\pi}. \quad (31)$$

Outside the scaling limit the CFT expression (29) is not expected to provide a good approximation to the full result (19) because the nonlinearity of the dispersion relation becomes important.

2.2.3. Quenches from the ferromagnetic to the paramagnetic phase. We have not been able to carry out a full analytical calculation of the time evolution of the two point function for a quench across the critical point. However, we conjecture \ddagger that (see Section 3.2.1)

$$\rho_{FP}^{xx}(\ell, t) \simeq \mathcal{C}_{FP}^x \exp \left[\int_0^\pi \frac{dk}{\pi} 2\varepsilon'_h(k) t \ln |\cos \Delta_k| \right] \times \begin{cases} \exp \left[\int_0^\pi \frac{dk}{\pi} (\ell - 2t\varepsilon'_h(k)) \ln |\cos \Delta_k| \theta_H(2\varepsilon'_h(k)t - \ell) \right] & t > t_F, \\ 1 + \cos(2\varepsilon_h(k_0)t + \alpha) + \dots & t < t_F, \end{cases} \quad (32)$$

where α and k_0 are the same as in (17) (see also Ref. [81]) and the constant factor \mathcal{C}_{FP}^x is given in (18). This prediction is compared with the numerically calculated correlation function in Fig. 6 (left) and the agreement is clearly very good. For $t < t_F$ (32) is simply the square of the corresponding one-point function, which ensures that connected correlations vanish for $t < t_F$ in the space-time scaling regime. This is in agreement with numerical results for the connected two-point function as shown in the right hand panel of Fig. 6. As can be seen in Fig. 6 oscillations are present for $t > t_F$ as well, but they display a rather fast decay in time towards the determinant result (19). Like for the one-point function, the oscillating factor is a correction to the leading asymptotic behaviour in

\ddagger Our conjecture is based on properties of the spectrum of the matrix Γ (50).

the space-time scaling limit, but it needs to be included to give a good description of the numerical data. Finally, we note that for $h = 1$ we have $\varepsilon_1(k_0) = 0$ and (32) reduces to (19).

2.2.4. Quench within the paramagnetic phase. For quenches within the paramagnetic phase the form factor approach gives the following result (see Section 4.5)

$$\begin{aligned} \rho_{PP}^{xx}(\ell, t) &\simeq \rho_{PP}^{xx}(\ell, \infty) + (h^2 - 1)^{\frac{1}{4}} \sqrt{4J^2 h} \int_{-\pi}^{\pi} \frac{dk}{\pi} \frac{K(k)}{\varepsilon_k} \sin(2t\varepsilon_k - k\ell) \\ &\times \exp \left[-2 \int_0^{\pi} \frac{dp}{\pi} K^2(p) (\ell + \theta_H(\ell - 2t\varepsilon'_p)[2t\varepsilon'_p - \ell]) \right] + \dots \end{aligned} \quad (33)$$

The regime of validity of (33) is sufficiently large values of ℓ and t and “small” quenches in the sense discussed in the beginning of section 2. We have not attempted to calculate the infinite time limit $\rho_{PP}^{xx}(\ell, \infty)$ within the framework of the form factor approach, because its exact large- ℓ asymptotics is known from the determinant approach to be [71, 81]

$$\rho_{PP}^{xx}(\ell, \infty) \simeq \mathcal{C}_{PP}^x(\ell) e^{-\ell/\xi}, \quad (34)$$

where $\mathcal{C}_{PP}^x(\ell)$ is determined in paper II [81] and

$$\xi^{-1} = \ln(\min[h_0, h_1]) - \ln \left[h_1 \frac{h + h_0}{2hh_0} \right], \quad h_1 = \frac{1 + hh_0 + \sqrt{(h^2 - 1)(h_0^2 - 1)}}{h + h_0}. \quad (35)$$

As discussed in our previous letter [71], (34) is described by a general Gibbs ensemble. Based on the form factor result (33) one may speculate that the full answer may have the structure

$$\begin{aligned} \rho^{xx}(\ell, t) &\simeq \left[\mathcal{C}_{PP}^x(\ell) + (h^2 - 1)^{\frac{1}{4}} \sqrt{4J^2 h} \int_{-\pi}^{\pi} \frac{dk}{\pi} \frac{K(k)}{\varepsilon_k} \sin(2t\varepsilon_k - k\ell) + \dots \right] \\ &\times \exp \left[- \int_0^{\pi} \frac{dp}{\pi} \ln \left[\frac{1 + K^2(p)}{1 - K^2(p)} \right] (\ell + \theta_H(\ell - 2t\varepsilon'_p)[2t\varepsilon'_p - \ell]) \right] + \dots \end{aligned} \quad (36)$$

In Fig. 7 we compare the analytic result (33) to numerical results obtained for two different quenches within the paramagnetic phase. The agreement is seen to be excellent.

For strong quenches the form factor result is not expected to be quantitatively accurate. This can be seen in Fig. 8. In all cases, the two-point function is seen to display slowly decaying oscillatory behaviour on the time scales shown. At sufficiently large t the decay is proportional to $t^{-3/2}$. This is in marked contrast to quenches within the ordered phase. The origin of this difference lies in the nature of the relaxational processes that drive the time evolution. The oscillatory behaviour seen in the paramagnetic phase arises from processes involving the annihilation of spin-flip excitations, while the smooth exponential behaviour seen in the ferromagnetic phase is related to the ballistic motion of domain wall excitations.

The structure of (33) implies the existence of a late time crossover scale t^* , at which the second contribution becomes smaller than $\rho_{PP}^{xx}(\ell, \infty)$. Using that $\rho_{PP}^{xx}(\ell, \infty) \propto e^{-\ell/\xi}$ and that the second contribution decays like $(Jt)^{-3/2}$ at late times we may estimate t^* as

$$Jt^* \sim e^{2\ell/(3\xi)}. \quad (37)$$

For the cases shown in Fig. 7 this gives $Jt^* \sim 4114$ and $Jt^* \sim 10^{20}$ respectively ($Jt_F = 7.5$ in both cases). This means that in both cases the stationary behaviour characterized by the generalized Gibbs ensemble is revealed only at *very late times*.

Finally, we note that so far we have not been able to analyze the time evolution of order parameter correlators for quenches within the paramagnetic phase by means of the determinant approach.

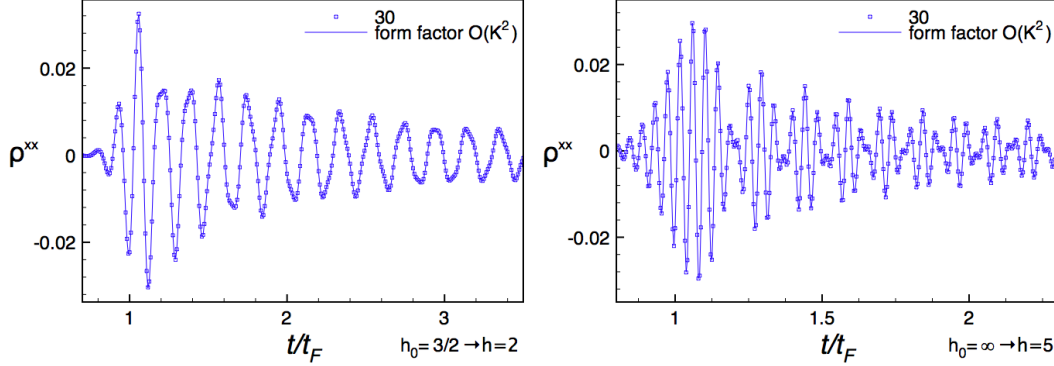


Figure 7. Time evolution of order parameter correlators for quenches within the paramagnetic phase. Left: $\rho_{PF}^{xx}(\ell = 30, t)$ for a quench from $h_0 = \frac{3}{2}$ to $h = 2$. Right: $\rho_{PF}^{xx}(\ell = 30, t)$ for a quench from $h_0 = \infty$ to $h = 5$. The two-point function is seen to exhibit oscillatory power-law decay at late times. The form factor result (solid lines) is seen to give a very good description of the numerical data (points). The short time regime is not shown as the correlators are exponentially small by virtue of the horizon effect.

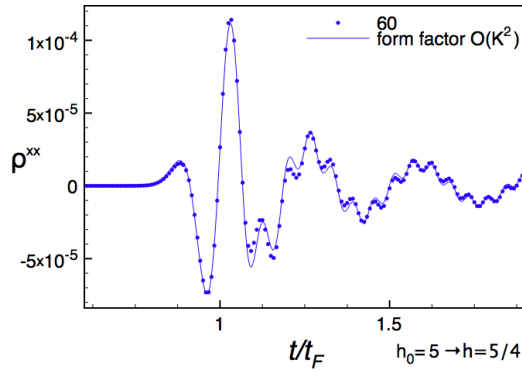


Figure 8. Time evolution of $\rho_{PF}^{xx}(\ell = 60, t)$ for a quench from $h_0 = 5$ to $h = 5/4$. As the quench is no longer small, deviations from the form factor result become more pronounced.

2.2.5. Quenches from the paramagnetic to the ferromagnetic phase. Here we have not been able to obtain analytic results by either the determinant or the form factor approach. However, observations within the framework of the determinant approach (see Section 3.2) suggest that for late times $t > t_F$ the leading asymptotic behaviour of the two-point function should be given by

$$\begin{aligned} \rho_{PF}^{xx}(\ell, t) &\simeq \mathcal{C}_{PF}^x(\ell) \exp \left[\ell \int_0^\pi \frac{dk}{\pi} \ln |\cos \Delta_k| \theta_H(2\varepsilon'_h(k)t - \ell) \right] \\ &\times \exp \left[2t \int_0^\pi \frac{dk}{\pi} \varepsilon'_h(k) \ln |\cos \Delta_k| \theta_H(\ell - 2\varepsilon'_h(k)t) \right], \quad t > t_F. \end{aligned} \quad (38)$$

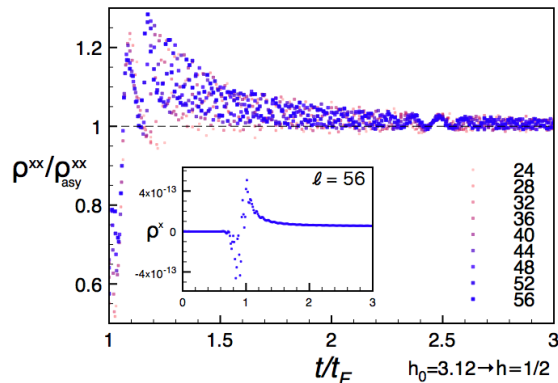


Figure 9. Order parameter two point function for a quench from the paramagnetic to the ferromagnetic phase (inset) and its ratio with the asymptotic prediction ρ_{PF}^{xx} given in eqn (38) (main plot). We consider a quench from $h_0 = (2 + 3\sqrt{2})/2$ to $h = 1/2$. For any $t > t_F$, the ratio approaches 1 with increasing ℓ .

Here the factor $\mathcal{C}_{\text{PF}}^x(\ell)$ is given by the $t = \infty$ results of [81]

$$\mathcal{C}_{\text{PF}}^x(\ell) = \left[\frac{h_0 - h}{\sqrt{h_0^2 - 1}} \right]^{\frac{1}{2}} \cos \left(\ell \arctan \left[\frac{\sqrt{(1 - h^2)(h_0^2 - 1)}}{1 + h_0 h} \right] \right). \quad (39)$$

We have tested this conjecture by comparing it to the numerical results and found it to hold. An example is shown in Fig. 9, where we plot the ratio of the numerically calculated correlation function and the analytic expression (19) for several values of the distance ℓ . The ratio clearly approaches 1 at late times. We note that the values of ℓ have been chosen in a way such that for the particular quench considered (i.e. $h_0 = 3.12$ to $h = 0.5$) oscillations in ℓ are suppressed in the $t \rightarrow \infty$ limit. Our analytic methods do not currently provide an understanding of the quench dynamics for times shorter than the Fermi time $t < t_F$.

2.3. Quenches to $h = 0$ or $h = \infty$.

These quenches are special, because the post-quench Hamiltonian is classical in both cases. As a result the dynamics is anomalous. For example, for quenches to $h = 0$ correlation functions involving only σ_j^x operators are time independent, because the final Hamiltonian $H(h)$ commutes with all σ_j^x . Correlation functions involving other operators do depend on time, but generally exhibit persistent oscillations. For instance, we have that

$$e^{iH(h=0)t} \sigma_j^z e^{-iH(h=0)t} = \cos^2(2Jt) \sigma_j^z + \frac{1}{2} \sin(4Jt) (\sigma_{j-1}^x + \sigma_{j+1}^x) \sigma_j^y - \sin^2(2Jt) \sigma_{j-1}^x \sigma_j^z \sigma_{j+1}^x, \quad (40)$$

and as a result $\langle \Psi(t) | \sigma_j^z | \Psi(t) \rangle$ does not approach a stationary value at late times.

3. Determinant approach: Analytic derivation of the asymptotic two-point function for a quench within the ordered phase.

In this section we present the analytic derivation of Eq. (19) for the asymptotic behaviour in the space-time scaling regime ($t, \ell \gg 1$, but t/ℓ arbitrary) of the two-point correlation function $\rho^{xx}(\ell, t)$.

Within this approach, it is convenient to replace the fermions c_j in Appendix A with the Majorana fermions

$$a_j^x = c_j^\dagger + c_j \quad a_j^y = i(c_j^\dagger - c_j), \quad (41)$$

which satisfy the algebra $\{a_l^x, a_n^x\} = 2\delta_{ln}$, $\{a_l^y, a_n^y\} = 2\delta_{ln}$, $\{a_l^x, a_n^y\} = 0$. In terms of these Majorana fermions, the operator σ_j^x has the nonlocal representation

$$\sigma_\ell^x = \prod_{j=1}^{\ell-1} (i a_j^y a_j^x) a_\ell^x. \quad (42)$$

The two-point function of σ^x is then the expectation value of a string of Majorana fermions

$$\rho^{xx}(\ell, t) = \left\langle \prod_{j=1}^{\ell} (-i a_j^y(t) a_{j+1}^x(t)) \right\rangle. \quad (43)$$

The Ising Hamiltonian (1) can be written as (see Appendix A)

$$H = \frac{1}{2} \left[1 - \prod_{l=1}^L \sigma_l^z \right] H_o + \frac{1}{2} \left[1 + \prod_{l=1}^L \sigma_l^z \right] H_e, \quad (44)$$

where H_o and H_e are quadratic Hamiltonians of the Jordan-Wigner fermions in the sectors with odd and even fermion number respectively ($H_{o/e}$ both commute with $\prod_{l=1}^L \sigma_l^z$). For finite chains, the ground state of the Ising Hamiltonian is an eigenstate of H_e . However, in the thermodynamic limit, the \mathbb{Z}_2 symmetry of H is spontaneously broken in the ordered phase $h_0 < 1$, where the ground state is a linear superposition of the ground states of H_e and H_o

$$|\Psi(0)\rangle = \frac{|B(0)\rangle_{\text{NS}} + |B(0)\rangle_{\text{R}}}{2}. \quad (45)$$

Thus, for a quench starting in the ordered phase free fermion techniques cannot be straightforwardly applied to the calculation of correlation functions involving generic operators. However, here we are interested only in the expectation value of even operators \hat{O}_e characterized by

$$\left[\prod_{j=1}^L \sigma_j^z \right] \hat{O}_e \left[\prod_{l=1}^L \sigma_l^z \right] = \hat{O}_e. \quad (46)$$

Hence we have

$$\begin{aligned} \lim_{L \rightarrow \infty} \langle \Psi(t) | \hat{O}_e | \Psi(t) \rangle &= \lim_{L \rightarrow \infty} \frac{{}_{\text{NS}} \langle B(t) | \hat{O}_e | B(t) \rangle_{\text{NS}} + {}_{\text{R}} \langle B(t) | \hat{O}_e | B(t) \rangle_{\text{R}}}{2} \\ &= \lim_{L \rightarrow \infty} {}_{\text{NS}} \langle B(t) | \hat{O}_e | B(t) \rangle_{\text{NS}}, \end{aligned} \quad (47)$$

Crucially, the expectation value ${}_{\text{NS}} \langle B(t) | \hat{O}_e | B(t) \rangle_{\text{NS}}$ can be evaluated using Wick's theorem. In contrast to even operators, expectation values of odd operators

$$\left[\prod_{j=1}^L \sigma_j^z \right] \hat{O}_o \left[\prod_{l=1}^L \sigma_l^z \right] = -\hat{O}_o \quad (48)$$

are significantly more difficult to determine [62]. The particular case of interest, $\rho^{xx}(\ell, t)$, involves an even operator (cf. Eq. (43)) and by straightforward application of Wick's theorem one obtains a representation as the Pfaffian of a $2\ell \times 2\ell$ antisymmetric matrix [62]

$$\rho^{xx}(\ell, t) = \text{pf}(\bar{\Gamma}), \quad (49)$$

where pf denotes the Pfaffian, $\bar{\Gamma}$ is given by

$$\bar{\Gamma} = \begin{bmatrix} \Gamma_0 & \Gamma_{-1} & \cdots & \Gamma_{1-\ell} \\ \Gamma_1 & \Gamma_0 & & \vdots \\ \vdots & & \ddots & \vdots \\ \Gamma_{\ell-1} & \cdots & \cdots & \Gamma_0 \end{bmatrix}, \quad \Gamma_l = \begin{pmatrix} -f_l & g_l \\ -g_{-l} & f_l \end{pmatrix}. \quad (50)$$

The elements of this matrix are the fermionic correlations[§]

$$\begin{aligned} g_n &\equiv i \langle a_l^x a_{l+n-1}^y \rangle, \\ f_n + i\delta_{n0} &\equiv i \langle a_l^x a_{l+n}^x \rangle = i \langle a_{l+n}^y a_l^y \rangle \quad \forall l. \end{aligned} \quad (52)$$

The matrix $\bar{\Gamma}$ is a block Toeplitz matrix because its constituent 2×2 blocks depend only on the difference between row and column indices. It is customary to introduce the (block) symbol of the matrix $\bar{\Gamma}$ via Fourier transform as follows

$$\Gamma_l = \begin{pmatrix} -f_l & g_l \\ -g_{-l} & f_l \end{pmatrix} = \int_{-\pi}^{\pi} \frac{dk}{2\pi} e^{ilk} \hat{\Gamma}(k), \quad \text{with} \quad \hat{\Gamma}(k) = \begin{pmatrix} -f(k) & g(k) \\ -g(-k) & f(k) \end{pmatrix}, \quad (53)$$

where the functions $f(k)$ and $g(k)$ are

$$\begin{aligned} f(k) &= i \sin \Delta_k \sin(2\varepsilon_h(k)t), \\ g(k) &= -e^{i\theta_k - ik} \left[\cos \Delta_k - i \sin \Delta_k \cos(2\varepsilon_h(k)t) \right]. \end{aligned} \quad (54)$$

The spectrum of block Toeplitz matrix $\bar{\Gamma}$ is the same of an $\ell \times \ell$ Toeplitz+Hankel matrix (Hankel matrices have elements which depend only on the sum of row and column indices, instead of the difference as in Toeplitz matrices). Indeed, being $\bar{\Gamma}$ a real antisymmetric matrix, its eigenvalues are complex conjugate pairs $\pm i\lambda_j$. Given an eigenvector \vec{V} of $\bar{\Gamma}$ with eigenvalue $i\lambda$, we can define the vector \vec{w} with ℓ components $w_i = V_{2i-1}$ (since $\Gamma_{-l} = \sigma_y \Gamma_l \sigma_y$, taking the even components would change the sign of λ). Thus, the ℓ vectors \vec{w}_i are solutions of the eigenvalue problem

$$(iT \pm H)\vec{w}_j = \mp i\lambda_j \vec{w}_j, \quad \begin{cases} T_{ln} = f_{l-n} \\ H_{ln} = g_{l+n-L-1} \end{cases}, \quad (55)$$

In particular, this means that

$$|\text{pf}(\bar{\Gamma})| = |\det[iT \pm H]|. \quad (56)$$

The sign of the Pfaffian can be fixed by observing that, for any given ℓ , both the determinant of the Toeplitz+Hankel matrix and the Pfaffian of the block Toeplitz matrix are polynomials in f_l and g_l of the same degree. Thus, the sign is independent of the actual values of the matrix elements and can be determined by considering the simplest case $T = 0$ (which occurs at the initial time and at asymptotically late times after the quench), obtaining

$$\rho^{xx}(\ell, t) = \text{pf}(\bar{\Gamma}) = (-1)^{\frac{\ell(\ell-1)}{2}} \det(H + iT) = (-1)^{\frac{\ell(\ell-1)}{2}} \det W, \quad (57)$$

[§] The identity in the second line of Eq. (52) is a consequence of reflection symmetry, which indeed implies that correlations should be invariant under the transformation

$$a_l^x \rightarrow i \left(\prod_l \sigma_l^z \right) a_{L+1-l}^y \quad a_l^y \rightarrow -i \left(\prod_l \sigma_l^z \right) a_{L+1-l}^x. \quad (51)$$

For example, the Dzyaloshinskii-Moriya interaction breaks this symmetry.

where $W = H + iT$. The matrix $\bar{\Gamma}$ is real and antisymmetric, so its eigenvalues are complex conjugate pairs of the form $\pm i\lambda_j$ with $j = 1 \dots \ell$. By construction $\lambda_j \in [-1, 1]$ (see e.g. [82]) and they are also the eigenvalues of the matrix $W = H + iT$. Thus we have

$$(\rho^{xx})^2 = \det \bar{\Gamma} = \det W^2 = \prod_{j=1}^{\ell} \lambda_j^2. \quad (58)$$

The evaluation of the correlation function $\rho^{xx}(\ell, t)$ for large ℓ is then equivalent to the asymptotic evaluation of the determinant of a block Toeplitz matrix or the sum of a Toeplitz and a Hankel matrices. Such matrices have been the subject of intense study by mathematicians and physicists for more than a century and standard, rigorous techniques for calculating their determinants such as Szëgo's lemma and the Fisher-Hartwig conjecture are available, see e.g. [83, 84]. However, these methods have been specifically designed for the evaluation of determinants of matrices whose elements do not depend explicitly on the matrix size. This is in contrast to our case, where we are interested in the scaling limit $\ell, t \rightarrow \infty$ with finite ratio ℓ/t . Under these circumstances, each element of the matrix Γ in the scaling limit depends on a parameter (namely t) which is proportional to the matrix dimension 2ℓ . This precludes the application of the aforementioned techniques for the asymptotic evaluation of these determinants. The two exceptions are the $t = 0$ case, where we recover the known equilibrium results, and the limit $t = \infty$. In order to deal with large values of t we developed a completely novel approach, which follows the one we proposed in Ref. [66] for the entanglement entropy and it is based on a multi-dimensional stationary phase approximation.

In the following we derive a rather general result valid for any block 2×2 block Toeplitz matrix Γ with a symbol $\hat{t}(k)$ that can be cast in the form

$$\hat{t}(k) = n_x(k) \sigma_x^{(k)} + \vec{n}_\perp(k) \cdot \vec{\sigma}^{(k)} e^{2i\varepsilon(k)t \sigma_x^{(k)}}, \quad \vec{n}_\perp(k) \cdot \hat{x} = 0. \quad (59)$$

Here the time t is the only parameter proportional to the matrix size 2ℓ , n_x, n_\perp are fixed but otherwise arbitrary and $\sigma^{(k)}$ denotes a local rotation of the Pauli matrices

$$\sigma_\alpha^{(k)} \sim e^{i\vec{w}(k) \cdot \sigma} \sigma_\alpha e^{-i\vec{w}(k) \cdot \sigma}. \quad (60)$$

Our particular case of interest (53) corresponds to having $n_x^2 + |\vec{n}_\perp|^2 = 1$.

We first consider $\text{Tr} \Gamma^{2n}$ for positive integer n . We note that the traces of odd powers of Γ vanish, because Γ is a real antisymmetric matrix (Γ is diagonalizable and for each non-zero eigenvalue there is another one with opposite sign). Our main result is that

$$\begin{aligned} \lim_{\substack{t, \ell \rightarrow \infty \\ t/\ell \text{ fixed}}} \frac{\text{Tr}[\Gamma^{2n}]}{2\ell} &= \int_{-\pi}^{\pi} \frac{dk_0}{2\pi} \max\left(1 - 2|\varepsilon'(k_0)| \frac{t}{\ell}, 0\right) \left(n_x(k_0)^2 + |\vec{n}_\perp(k_0)|^2\right)^n \\ &\quad + \int_{-\pi}^{\pi} \frac{dk_0}{2\pi} \min\left(2|\varepsilon'(k_0)| \frac{t}{\ell}, 1\right) n_x(k_0)^{2n}. \end{aligned} \quad (61)$$

Given the result (61) it is possible to infer the asymptotic behaviour of more complicated quantities such as

$$\text{Tr} \mathcal{F}(\Gamma^2) = \sum_n \mathcal{F}_n \text{Tr}[\Gamma^{2n}], \quad (62)$$

where $\mathcal{F}(z)$ is an analytic function with power series expansion $\mathcal{F}(z) = \sum_n \mathcal{F}_n z^n$ around $z = 0$. Using Eq. (61) and interchanging the order of sum and integration, we have

$$\lim_{\substack{t, \ell \rightarrow \infty \\ t/\ell \text{ fixed}}} \frac{\text{Tr}[\mathcal{F}(\Gamma^2)]}{2\ell} = \int_{-\pi}^{\pi} \frac{dk_0}{2\pi} \max\left(1 - 2|\varepsilon'(k_0)| \frac{t}{\ell}, 0\right) \mathcal{F}(n_x(k_0)^2 + |\vec{n}_\perp(k_0)|^2)$$

$$+ \int_{-\pi}^{\pi} \frac{dk_0}{2\pi} \min\left(2|\varepsilon'(k_0)|\frac{t}{\ell}, 1\right) \mathcal{F}(n_x(k_0)^2). \quad (63)$$

Clearly this approach is fully justified only as long as all eigenvalues of Γ fall within the radius of convergence of the expansion of the function $\mathcal{F}(z)$ around $z = 0$. For example, in the case of the entanglement entropy, we have $\mathcal{F}(z) = -\frac{1+iz}{2} \ln \frac{1+iz}{2}$ [66] and since the eigenvalues of Γ are of the form $\pm i\lambda_j$ with $\lambda_j \in [-1, 1]$ (63) holds (further generalizations to the entanglement of two blocks have also been considered [85]).

In the case at hand we have

$$(\rho^{xx})^2 = \det \Gamma = \exp[\text{Tr} \ln \Gamma], \quad \text{i.e.} \quad \ln(\rho^{xx})^2 = \frac{1}{2} \text{Tr} \ln \Gamma^2. \quad (64)$$

In order to use (62), (63) we are therefore led to consider the function $\mathcal{F}(z) = \frac{1}{2} \ln z$. The latter has a branch point at $z = 0$ and the previous approach appears not to be applicable. In order to circumvent this problem we employ a power series expansion of the logarithm around $z = 1$

$$\ln(\rho^{xx})^2 = \frac{1}{2} \text{Tr} \ln \Gamma^2 = \frac{1}{2} \text{Tr} \ln[1 + (\Gamma^2 - 1)] = \frac{1}{2} \sum_{m=1}^{\infty} \frac{(-1)^{m+1}}{m} \text{Tr}[(\Gamma^2 - 1)^m]. \quad (65)$$

Application of (63) to the function $\mathcal{F}(z) = (z - 1)^m$ then results in

$$\begin{aligned} \lim_{\substack{t, \ell \rightarrow \infty \\ t/\ell \text{ fixed}}} \frac{\text{Tr}[(\Gamma^2 - 1)^m]}{2\ell} &= \int_{-\pi}^{\pi} \frac{dk_0}{2\pi} \max\left(1 - 2|\varepsilon'(k_0)|\frac{t}{\ell}, 0\right) (n_x(k_0)^2 + |\vec{n}_{\perp}(k_0)|^2 - 1)^m \\ &+ \int_{-\pi}^{\pi} \frac{dk_0}{2\pi} \min\left(2|\varepsilon'(k_0)|\frac{t}{\ell}, 1\right) (n_x(k_0)^2 - 1)^m. \end{aligned} \quad (66)$$

Finally we can carry out the sum over m

$$\begin{aligned} \lim_{\substack{t, \ell \rightarrow \infty \\ t/\ell \text{ fixed}}} \frac{\text{Tr}[\ln \Gamma^2]}{2\ell} &= \int_{-\pi}^{\pi} \frac{dk_0}{2\pi} \max\left(1 - 2|\varepsilon'(k_0)|\frac{t}{\ell}, 0\right) \ln(n_x(k_0)^2 + |\vec{n}_{\perp}(k_0)|^2) \\ &+ \int_{-\pi}^{\pi} \frac{dk_0}{2\pi} \min\left(2|\varepsilon'(k_0)|\frac{t}{\ell}, 1\right) \ln(n_x(k_0)^2), \end{aligned} \quad (67)$$

which is exactly the same result we would have obtained applying (63) directly to the function $\mathcal{F}(z) = \frac{1}{2} \ln z$. The reason for this lies in the simple algebraic dependence of (61) on n . The specialization of (67) to the longitudinal correlator ρ^{xx} is now straightforward. The symbol $\hat{\Gamma}(k)$ of the block Toeplitz matrix $\bar{\Gamma}$ can be cast in the form (59) with

$$\vec{w}(k) = [\theta(k) - k]\hat{x}, \quad n_x^2(k) = \cos^2 \Delta_k, \quad |\vec{n}_{\perp}(k)|^2 = \sin^2 \Delta_k. \quad (68)$$

Eq. (67) then gives the asymptotic behaviour

$$\lim_{\substack{t, \ell \rightarrow \infty \\ t/\ell \text{ fixed}}} \frac{1}{\ell} \ln |\rho^{xx}(\ell, t)| = \int_{-\pi}^{\pi} \frac{dk_0}{2\pi} \min\left(2|\varepsilon'(k_0)|\frac{t}{\ell}, 1\right) \ln |\cos \Delta_{k_0}|. \quad (69)$$

This is a rewriting of (19) and represents one of our main results.

In the reasoning leading up to (67) we have assumed that the eigenvalues of $\Gamma^2 - 1$ lie within the unit circle so that we can expand the logarithm in a power series. This is equivalent to the requirement that the eigenvalues λ_j of Γ are such that $0 < \lambda_j^2 \leq 1$. More precisely, if there exists a $x_0 > 0$ such that for all ℓ the eigenvalues λ_j of Γ fulfil

$$x_0 < \lambda_j^2 \leq 1, \quad (70)$$

then the results (67) and (69) hold. In some cases of interest we find that even though λ_j are different from zero for any finite ℓ , one or several eigenvalues approach zero in the limit $\ell \rightarrow \infty$. In these circumstances the steps leading up to (67) and (69) are no longer justified. However, even then (69) can provide useful information about the asymptotics of $\rho^{xx}(\ell, t)$. On general grounds || we expect the latter to be of the form

$$\lim_{\substack{t, \ell \rightarrow \infty \\ t/\ell \text{ fixed}}} \ln |\rho^{xx}(\ell, t)| = -\ell\mu(t/\ell) - \alpha \ln(\ell) + c(t/\ell) + \dots, \quad (71)$$

and the question is under what circumstances $\mu(t/\ell)$ is given by (69). Under the assumption that the general structure (71) holds, this depends on the number N_0 of eigenvalues λ_j that approach zero for $\ell \rightarrow \infty$, as well as on how quickly they tend to zero. If N_0 is finite and the corresponding eigenvalues approach zero *sufficiently slowly* with ℓ , (69) will still be applicable. As an example let us consider the case where only a single pair $\pm i\lambda_1$ of eigenvalues approaches zero for $\ell \rightarrow \infty$ in such a way that for large ℓ we have $|\lambda_1| \sim \ell^{-\beta}$. Since $\rho^{xx}(\ell, t) = \prod_j \lambda_j^2$, the eigenvalue pair will contribute to subleading logarithmic term in (71), but will leave the function $\mu(t/\ell)$ unchanged. On the other hand, if our pair of eigenvalues were to approach zero exponentially fast $|\lambda_1| \sim e^{-\ell\bar{\mu}(t/\ell)}$, then it would contribute additively to the function $\mu(t/\ell)$ and (69) would cease to hold.

As far as our quench problem is concerned we do not have a criterion that would establish a priori whether eigenvalues exponentially close to zero will be present. We find that for quenches within the ferromagnetic phase they are always absent. In the other cases, the picture emerging from numerical studies of the spectrum of $\bar{\Gamma}$ suggests that only for quenches starting in the disordered phase eigenvalues approach zero exponentially fast, and then only a single pair $\pm i\lambda_0$ does so. Interestingly, we find that the contribution of all other eigenvalues is again captured by (67). At present we are not able to determine λ_0 analytically.

3.1. Proof of the formula for the trace of integer powers of Γ .

The first step of our calculation is to derive an appropriate integral representation for $\text{Tr} \Gamma^{2n}$ by trading matrix multiplications for additional integrations. The basic idea is easily explained for a product of two Γ matrices. Each block element is given by

$$\Gamma_{ln} = \int_{-\pi}^{\pi} \frac{dk}{2\pi} e^{i(l-n)k} \hat{t}(k), \quad (72)$$

where the 2×2 block $\hat{t}(k)$ is of the form (59). Hence the block matrix elements of Γ^2 can be written as

$$(\Gamma^2)_{lm} = \sum_{m=1}^{\ell} \Gamma_{lm} \Gamma_{mn} = \int_{[-\pi, \pi]^2} \frac{dk_1}{2\pi} \frac{dk_2}{2\pi} e^{i(lk_1 - nk_2)} \hat{t}(k_1) \cdot \hat{t}(k_2) \sum_{m=1}^{\ell} e^{im(k_1 - k_2)}. \quad (73)$$

The sum over m can now be replaced by an integral using

$$e^{-i(\ell+1)k/2} \sum_{m=1}^{\ell} e^{imk} = \frac{\ell}{2} \int_{-1}^1 d\xi \frac{k}{2 \sin(k/2)} e^{i\ell\xi k/2}. \quad (74)$$

The generalization to Γ^{2n} is straightforward, and replacing the trace in an analogous way we obtain the following integral representation

$$\text{Tr}[\Gamma^{2n}] = \left(\frac{\ell}{2}\right)^{2n} \int_{[-\pi, \pi]^n} \frac{d^{2n}k}{(2\pi)^{2n}} \int_{[-1, 1]^{2n}} d^{2n}\xi C(\{k\}) e^{i\ell \sum_{j=0}^{2n-1} \xi_j (k_{j+1} - k_j)/2} F(\{k\}). \quad (75)$$

|| This form has been observed in various examples, see e.g. [22, 34, 66, 61, 77, 36, 56], even with oscillating factors.

Here the functions appearing under the integrals are

$$C(\{k\}) \equiv \prod_{j=0}^{2n-1} \frac{k_j - k_{j-1}}{2 \sin[(k_j - k_{j-1})/2]}, \quad (76)$$

$$F(\{k\}) = \text{Tr} \left[\prod_{i=0}^{2n-1} n_x(k_i) \sigma_x^{(k)} + \vec{n}_\perp(k_i) \cdot \vec{\sigma}^{(k)} e^{2i\varepsilon_i t \sigma_x^{(k)}} \right], \quad (77)$$

the trace is over the remaining 2×2 blocks and $\varepsilon_i = \varepsilon(k_i)$. Performing the change of variables

$$\begin{aligned} \zeta_0 &= \xi_1, \\ \zeta_i &= \xi_{i+1} - \xi_i \quad i \in [1, n-1], \end{aligned} \quad (78)$$

Eq. (75) can be rewritten in the form

$$\text{Tr}[\Gamma^{2n}] = \left(\frac{\ell}{2}\right)^{2n} \int_{[-\pi, \pi]^{2n}} \frac{d^{2n}k}{(2\pi)^{2n}} \int_{R_\zeta} d^{2n}\zeta C(\{k\}) e^{-i\ell \sum_{j=1}^{2n-1} \zeta_j (k_j - k_0)/2} F(\{k\}). \quad (79)$$

Here the domain of integration R_ζ is determined by the conditions

$$R_\zeta : \quad -1 \leq \sum_{j=0}^{k-1} \zeta_j \leq 1 \quad \forall k \in [1, 2n]. \quad (80)$$

As the integrand in Eq. (79) is independent of ζ_0 , we can carry out the ζ_0 integration, which gives

$$\text{Tr}[\Gamma^{2n}] = \left(\frac{\ell}{2}\right)^{2n} \int_{[-\pi, \pi]^{2n}} \frac{d^{2n}k}{(2\pi)^{2n}} \int d^{2n-1}\zeta \mu(\{\zeta\}) C(\{k\}) e^{-i\ell \sum_{j=1}^{2n-1} \zeta_j (k_j - k_0)/2} F(\{k\}). \quad (81)$$

Here the function $\mu(\{\zeta\})$ is the measure of the domain of ζ_0 under the constraints (80)

$$\mu(\{\zeta\}) = \max \left[0, \min_{j \in \{0, 2n-1\}} \left[1 - \sum_{k=1}^j \zeta_k \right] + \min_{j \in \{0, 2n-1\}} \left[1 + \sum_{k=1}^j \zeta_k \right] \right]. \quad (82)$$

It can be shown that $\mu(\{\zeta\})$ is symmetric with respect to an arbitrary permutation of the variables ζ_i . Since we are interested in the behaviour for $\ell \gg 1$ and the phase in the integral is proportional to the large parameter ℓ , the asymptotic behaviour can be obtained using a multi-dimensional stationary phase approximation. The main idea behind this method is that the leading contribution to the integral arises from the neighborhoods of the points in which the phase is stationary. As the symbol is independent of the integration variables ζ_i , the stationarity of these variables implies

$$k_j \approx k_0, \quad j = 1, \dots, 2n-1. \quad (83)$$

We may replace any k_j with k_0 everywhere except in rapidly oscillating terms such as the $e^{2i\varepsilon_i t}$ factors in the symbol. We call this the *localization rule*. This rule allows us in particular to drop the factor $C(\{k\})$, cf. (76), as it is equal to one at the stationary points $C(\{k\}) \simeq 1$

$$\text{Tr}[\Gamma^{2n}] \simeq \left(\frac{\ell}{2}\right)^{2n} \int_{[-\pi, \pi]^{2n}} \frac{d^{2n}k}{(2\pi)^{2n}} \int d^{2n-1}\zeta \mu(\{\zeta\}) e^{-i\ell \sum_{j=1}^{2n-1} \zeta_j (k_j - k_0)/2} F(\{k\}). \quad (84)$$

The localization rule furthermore allows us to substitute the integration variables in n_x and \vec{n}_\perp with k_0 , and to remove the local rotation in $f(\{k\})$, i.e. under the integral we may replace

$$F(\{k\}) \rightarrow G(\{k\}) \equiv \text{Tr} \prod_{i=0}^{2n-1} \left[n_x(k_0) \sigma_x + \vec{n}_\perp(k_0) \cdot \vec{\sigma} e^{2i\varepsilon_i t \sigma_x} \right]. \quad (85)$$

As is shown in Appendix C, the product under the trace can be rewritten as

$$\sum_{p=0}^{2n} n_x^{2n-p} |n_\perp|^p (i\sigma_z)^p \sum_{1 \leq j_1 < j_2 < \dots < j_p \leq 2n} (-1)^{\sum_{m=1}^p j_m} e^{2it\sigma_x \sum_{m=1}^p (-1)^{p-m} \varepsilon_{j_{m-1}}}. \quad (86)$$

Each term in the sums over $j_1 \dots j_p$ gives the same contribution to the integral (84) as can be shown by changing integration variables

$$\begin{aligned} k'_1 &= k_{j_1}, k'_2 = k_{j_2}, \dots, k'_{j_p} = k_p, k'_l = k_l \text{ for all } l \notin \{j_1, \dots, j_p\}, \\ \zeta'_1 &= \zeta_{j_1}, \zeta'_2 = \zeta_{j_2}, \dots, \zeta'_{j_p} = \zeta_p, \zeta'_l = \zeta_l \text{ for all } l \notin \{j_1, \dots, j_p\}, \end{aligned} \quad (87)$$

and then invoking the invariance of $\mu(\{\zeta\})$ in Eq. (82) under any permutation of its variables. When evaluating the trace in (86) we may therefore replace $j_m \rightarrow m$. We call this the *contraction rule*. Noting that only the terms with even p have a non-vanishing trace (because $\text{Tr} \sigma_z e^{ia\sigma_x} = 0$) and then applying the contraction rule allows us to replace

$$G(\{k\}) \rightarrow \sum_{p=0}^n \binom{n}{p} n_x^{2n-2p} n_\perp^{2p} 2 \cos \left(2t \sum_{m=1}^{2p} (-1)^m \varepsilon_{m-1} \right). \quad (88)$$

Here the binomial takes into account the number of terms giving identical contributions to the integral and we have used that $\text{Tr} e^{ia\sigma_x} = 2 \cos a$. Inserting this expression into (84) we arrive at

$$\begin{aligned} \text{Tr}[\Gamma^{2n}] &= \ell \left(\frac{\ell}{2} \right)^{2n-1} \sum_{p=0}^n \binom{n}{p} \int_{[-\pi, \pi]^{2n}} \frac{d^{2n} k}{(2\pi)^{2n}} \int d^{2n-1} \zeta \mu(\{\zeta\}) \\ &\quad \times n_x^{2n-2k} n_\perp^{2k} e^{-i\ell \sum_{j=1}^{2p-1} \zeta_j \frac{k_j - k_0}{2} + 2it \sum_{j=0}^{2p-1} (-1)^j \varepsilon_j}, \end{aligned} \quad (89)$$

where we replaced the cosine with a complex exponential using the symmetry of the integral under the change of variables $\vec{k} \rightarrow -\vec{k}$ and $\vec{\zeta} \rightarrow -\vec{\zeta}$.

We are now in a position to employ a stationary phase approximation in order to extract an exact asymptotic result in the limit of large ℓ . As the phase of the integral is stationary along a one-dimensional smooth curve, application of the stationary phase method is not a simple matter. For a two-dimensional integral whose phase is stationary on a one-dimensional variety, the solution can be found in Ref. [86]. Higher-dimensional integrals with a curve of stationary points are only partially treated in Ref. [87], where it is demonstrated that it is possible to isolate the integration in k_0 and perform a standard multi-dimensional stationary phase approximation for the remaining integrals. To apply this idea to our case, we rewrite Eq. (89) as

$$\text{Tr}[\Gamma^{2n}] = \ell \left(\frac{\ell}{2} \right)^{2n-1} \sum_{l=0}^n \binom{n}{l} \int_{-\pi}^{\pi} \frac{dk_0}{2\pi} n_x(k_0)^{2n-2l} n_\perp(k_0)^{2l} \Lambda_{n;l}(k_0), \quad (90)$$

where the functions $\Lambda_{n;l}$ are given by

$$\Lambda_{n;l}(k_0) = \int_{[-\pi, \pi]^{2n-1}} \frac{d^{2n-1} k}{(2\pi)^{2n-1}} \int d^{2n-1} \zeta \mu(\{\zeta\}) e^{-i\ell \sum_{j=1}^{2n-1} \zeta_j \frac{k_j - k_0}{2} + 2it \sum_{j=0}^{2l-1} (-1)^j \varepsilon_j}. \quad (91)$$

We now use the standard multi-dimensional phase approximation to evaluate $\Lambda_{n;l}(k_0)$.

The general result for the large- ℓ asymptotic behaviour of a multi-dimensional integral over rapidly oscillating functions, whose phase is stationary at an *isolated point* \vec{x}_0 detached from the boundary is [86]

$$\int_D d^N x p(\vec{x}) e^{i\ell q(\vec{x})} = \left(\frac{2\pi}{\ell} \right)^{N/2} p(\vec{x}_0) |\det A|^{-1/2} \exp \left[i\ell q(\vec{x}_0) + \frac{i\pi \sigma_A}{4} \right], \quad (92)$$

where $A_{ij} = \partial_{x_i} \partial_{x_j} q|_{\vec{x}_0}$ is the Hessian matrix of $f(\vec{x})$ evaluated in \vec{x}_0 , and σ_A is the signature of the matrix A , *i.e.* the difference between the number of the positive and negative eigenvalues. The stationarity conditions for the phases of the integrands in $\Lambda_{n;l}(k_0)$ are

$$\begin{aligned} \bar{k}_j &= k_0, & j &= 1, \dots, 2n-1, \\ \bar{\zeta}_j &= 4^{\frac{j}{\ell}} (-1)^j \varepsilon'_j, & j &= 1, \dots, 2l-1, \\ \bar{\zeta}_j &= 0, & j &= 2l, \dots, 2n-1. \end{aligned} \quad (93)$$

Using an ordering of integration variables where the ζ 's are placed before the k 's, the Hessian is of the form

$$A = \frac{1}{2} \begin{pmatrix} 0 & \mathbf{I} \\ \mathbf{I} & M \end{pmatrix}. \quad (94)$$

Hence the eigenvalues $a_{\pm}^{(i)}$ of A are related to the eigenvalues μ_i of the matrix M by $a_{\pm}^{(i)} = (\mu_i \pm \sqrt{\mu_i^2 + 4})/4$. The signature of A is $\sigma_A = 0$ and its determinant is $\det A = -4^{1-2n}$. At the stationary point the phase in the integral vanishes, because there is an even number of ε 's with alternating signs. Finally, the value of $\mu(\{\bar{\zeta}\})$ at the stationary point is found to be

$$\mu(\{\bar{\zeta}\}) = \begin{cases} \frac{2}{\ell} \max[0, \ell - 2|\varepsilon'(k_0)|t] & l \neq 0, \\ 2 & l = 0. \end{cases} \quad (95)$$

Putting everything together, the stationary phase approximation gives the following result for the functions $\Lambda_{n;l}(k_0)$

$$\Lambda_{n;l}(k_0) = \left(\frac{2}{\ell}\right)^{2n-1} \mu(\{\bar{\zeta}\}). \quad (96)$$

Inserting (96) into (90) then gives

$$\text{Tr}[\Gamma^{2n}] = \ell \sum_{l=0}^n \binom{n}{l} \int_{-\pi}^{\pi} \frac{dk_0}{2\pi} n_x(k_0)^{2n-2l} n_{\perp}(k_0)^{2l} \mu(\{\bar{\zeta}\}), \quad (97)$$

and substituting the value (95) for $\mu(\{\bar{\zeta}\})$ we arrive at

$$\begin{aligned} \text{Tr}[\Gamma^{2n}] &= 2 \int_{-\pi}^{\pi} \frac{dk_0}{2\pi} \max(\ell - 2|\varepsilon'(k_0)|t, 0) \left(n_x(k_0)^2 + |\vec{n}_{\perp}(k_0)|^2 \right)^n \\ &\quad + 2 \int_{-\pi}^{\pi} \frac{dk_0}{2\pi} (\ell - \max(0, \ell - 2|\varepsilon'(k_0)|t)) n_x(k_0)^{2n}. \end{aligned} \quad (98)$$

This is equivalent to (61). A less general version of this result was previously presented in Ref. [66].

3.2. On the applicability of stationary phase method.

Eq. (69) is our main result obtained with the determinant approach. It is based on a multi-dimensional stationary phase approximation for $\text{Tr}[\bar{\Gamma}^{2n}]$. The result (98) is then used in combination with a series expansion in order to obtain the asymptotic behaviour of $\det \bar{\Gamma}$, which in turn gives the square of the longitudinal correlation function ρ^{xx} . As we have already discussed, this series expansion is possible only if there is no eigenvalue of the matrix $\bar{\Gamma}$ that approaches zero in the large ℓ limit. While this restriction appears to be quite simple, we do not have an analytic method that allows us to predict for what kind of quenches zero eigenvalues exist in the $\ell \rightarrow \infty$ limit. To address this question we therefore have carried out numerical studies of the spectrum of W (which is related to the spectrum of $\bar{\Gamma}$ by (58)) for different quenches. We have to distinguish between four

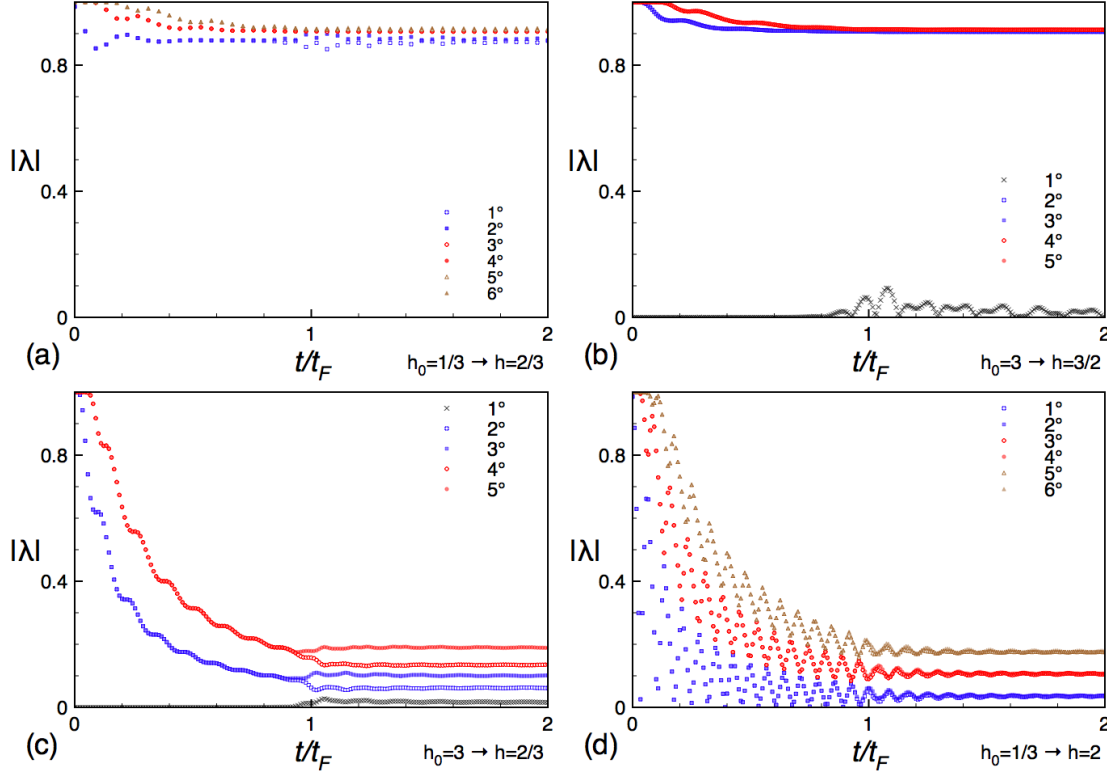


Figure 10. Typical absolute values of the low lying eigenvalues of the matrix W in the four kind of quenches. In (a) and (b) $\ell = 30$, while in (c) and (d) $\ell = 60$. (a) For a quench within the ordered phase, all eigenvalues are well separated from zero. Before the Fermi time (up to finite distance corrections to t_F) the eigenvalues are almost degenerate in pairs. (b) For a quench within the disordered phase, a *single* eigenvalue is very close to the real axis (exponentially close for $t < t_F$ and as a power law for $t > t_F$). (c) Quench from the disordered to the ordered phase. For $t < t_F$ a *single* eigenvalue is exponentially close to the real axis. For $t > t_F$ the distance of the smaller eigenvalue from the real axis scales like a power law. (d) Quench from the ordered to the disordered phase. All eigenvalues are doubly degenerate. All the smallest eigenvalues approach zero as a power in ℓ for any time. For $t < t_F$ the smallest eigenvalue crosses periodically zero.

cases: (1) FM \rightarrow FM; (2) PM \rightarrow PM; (3) PM \rightarrow FM and (4) FM \rightarrow PM, where FM and PM denote the ferromagnetic and paramagnetic phases respectively. In Fig. 10 we report the (absolute values of) smallest eigenvalues of the matrix W for particular examples of the four cases. Extensive numerical studies suggest that the spectra are similar for all quenches of a given type, i.e. (1)-(4). The qualitative features emerging from Fig. 10 can be summarized as

- (1) FM \rightarrow FM: all eigenvalues are well separated from zero;
- (2) PM \rightarrow PM: a *single* eigenvalue of W is close to zero. For $t < t_F$ it approaches zero exponentially fast in ℓ , while for $t > t_F$ it tends to zero only as a power-law;
- (3) PM \rightarrow FM: for both $t < t_F$ and $t > t_F$ several eigenvalues scale to zero like power laws in ℓ . For $t < t_F$ the smallest eigenvalue approaches zero exponentially fast in ℓ .

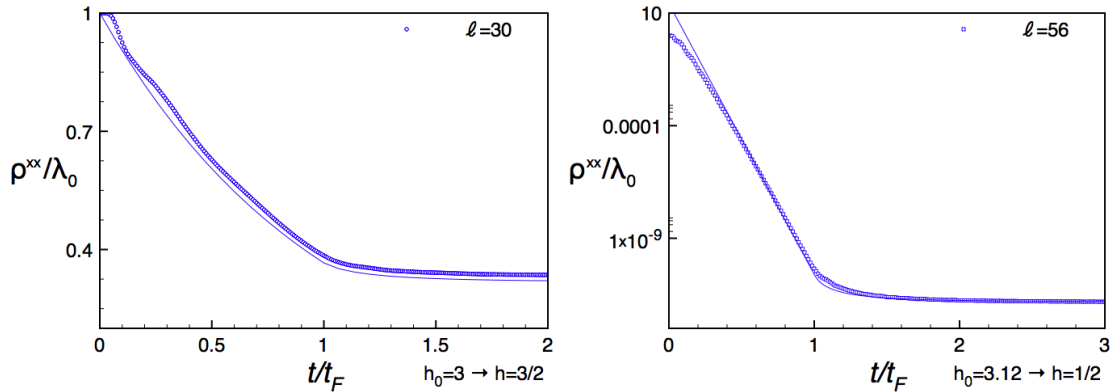


Figure 11. Ratio between the numerically evaluated two point function $\rho^{xx}(\ell, t)$ and the smallest eigenvalue of the matrix W . Left: Numerical data for a quench within the paramagnetic phase from $h_0 = 3$ to $h = 3/2$. The data are in perfect agreement with the prediction (69) and the leading correction is a stationary multiplicative factor. Right: The same plot for a quench from the paramagnetic $h_0 = (2 + 3\sqrt{2})/2$ to the ferromagnetic $h = 1/2$ phase.

- (4) FM \rightarrow PM: several eigenvalues tend to zero in a power-law fashion in ℓ for both $t > t_F$ and $t < t_F$. For $t < t_F$ the smallest eigenvalue crosses zero periodically.

The numerical analysis suggests that (69) can be applied for all quenches of type (1) for large t and all corrections to (69) are small. In case (4) our result (69) still gives the dominant behaviour, but there are additional important oscillating power-law corrections to $\rho^{xx}(\ell, t)$ that we have not been able to determine analytically. For quenches originating in the paramagnetic phase (69) gives the dominant contribution only if $t > t_F$, but there are important power-law corrections to $\rho^{xx}(\ell, t)$ beyond the accuracy of our analysis.

These properties of the spectrum suggest that, for quenches starting from the disordered phase, the product of all eigenvalues except the only one which is close to zero (i.e. ρ^{xx}/λ_0) should be given by Eq. (69). Fig. 11 shows that indeed this is the case for quenches to both disordered and ordered phases for any t . Thus, if we were able to obtain a prediction for the smallest eigenvalue, we would completely characterize these quenches as well.

Finally, we note that the gross features of the spectrum of W (and hence $\bar{\Gamma}$) appear to be related to the winding number (around zero) of the (block) symbol (53). We observe that the winding number of $g(k)$ (which is only a part of $\hat{\Gamma}(k)$) depends on the quench parameters in the following way:

- (1) If $|h|, |h_0| < 1$, the winding number is zero;
- (2) if $|h_0|, |h| > 1$, the winding number is equal to 1;
- (3) If $|h_0| < 1$ and $|h| > 1$, the winding number oscillates with t between 0 and 1. In particular it remains 0 for any $t > t_F$.
- (4) If $|h_0| > 1$ and $|h| < 1$, the winding number oscillates with t between -1 and 1.

We see that the winding number vanishes when there is no eigenvalue exponentially close to zero, but the reverse does not hold. For (block) Toeplitz matrices with ℓ independent elements the generalization of the Szëgo lemma to symbols with non vanishing winding number is complicated and not known in general (see e.g. [83, 84]).

3.2.1. *A closer look to quenches from the ordered to the disordered phases.* For quenches from the ordered to the disordered phase, the last panel of Fig. 10 shows that all eigenvalues of W move coherently in time. In particular, the eigenvalues closest to zero oscillate with the same frequency about zero until the Fermi time t_F . After t_F they do not cross zero anymore and the smallest one remains separated from zero as a power law in ℓ . These qualitative features of the spectrum would suggest that for $t < t_F$ $\rho^{xx}(t, \ell)$ should oscillate in time with the same frequency of the smallest eigenvalues. While it is not easy to put this on a solid ground, we have been able to identify it as the frequency with which the winding number of $g(k)$ changes. We indeed find that the frequency is determined by the mode k_0 such that $\cos \Delta_{k_0} = 0$. Thus for $t < t_F$ we heuristically predict

$$\langle \sigma_1^x(t) \sigma_{\ell+1}^x(t) \rangle \sim C_{\text{FP}}^x [1 + \cos(2\varepsilon_{k_0} t + \alpha)] \exp \left[\int_{-\pi}^{\pi} \frac{dk_0}{2\pi} 2|\varepsilon'_k| t \ln |\cos \Delta_k| \right] \quad t < t_F, \quad (99)$$

where α is an undetermined phase shift. The comparison of this prediction with the direct computation of the determinant has already been shown in Fig. 6. For times larger than t_F , Eq. (69) matches well the evolution of the two-point function, up to oscillatory decaying corrections (see Fig. 6) which is consistent with the presence of one eigenvalue exponentially close to zero.

4. Form-factor approach

While the procedure set out in Section 3 can be generalized to any model with a free-fermion representation [88], it cannot be applied to quenches in *interacting* integrable models. In order to overcome these limitations we have generalized the form-factor approach to correlation functions in integrable quantum field theories [72, 73, 74, 75, 76] to quantum quenches. A characteristic feature of integrable models is the existence of a basis of scattering states of elementary excitations, which are simultaneous exact eigenstates of the Hamiltonian and the momentum operator. These states can be characterized by n momenta k_1, \dots, k_n and in general also other quantum numbers a_1, \dots, a_n

$$\begin{aligned} H|k_1, \dots, k_n\rangle_{a_1, \dots, a_n} &= \left[\sum_{j=1}^n \varepsilon_{a_j}(k_j) \right] |k_1, \dots, k_n\rangle_{a_1, \dots, a_n}, \\ P|k_1, \dots, k_n\rangle_{a_1, \dots, a_n} &= \left[\sum_{j=1}^n k_j \right] |k_1, \dots, k_n\rangle_{a_1, \dots, a_n}. \end{aligned} \quad (100)$$

Ground state correlators of local operators \mathcal{O} can be expressed in a Lehmann representation

$$\begin{aligned} \langle 0|\mathcal{O}(t, x)\mathcal{O}^\dagger(0, 0)|0\rangle &= \sum_{n=0}^{\infty} \frac{1}{n!} \sum_{\substack{k_1, \dots, k_n \\ a_1, \dots, a_n}} |\langle 0|\mathcal{O}(0, 0)|k_1, \dots, k_n\rangle_{a_1, \dots, a_n}|^2 \\ &\quad \times e^{-i \sum_{j=1}^n \varepsilon_{a_j}(k_j)t - k_j x}, \end{aligned} \quad (101)$$

where $|0\rangle$ denotes the ground state and in our notations corresponds to particle number zero. Using the known expressions for the form factors $\langle 0|\mathcal{O}(0, 0)|k_1, \dots, k_n\rangle_{a_1, \dots, a_n}$ the spectral sum can be calculated to very high accuracy (for large t and x) by taking into account only terms involving a small number n of particles. Recently the form factor approach has been generalized to low temperature correlation functions [89, 90] (see also [91, 92] for related work)

$$\frac{\text{Tr} [e^{-\beta H} \mathcal{O}(t, x) \mathcal{O}^\dagger(0, 0)]}{\text{Tr} [e^{-\beta H}]}. \quad (102)$$

The numerator in (102) can now be expanded in a Lehmann representation as follows

$$\begin{aligned} & \sum_{n,m=0}^{\infty} \sum_{\substack{k_1, \dots, k_n \\ a_1, \dots, a_n}} \sum_{\substack{p_1, \dots, p_m \\ b_1, \dots, b_m}} |b_m, \dots, b_1 \langle p_m, \dots, p_1 | \mathcal{O}(0, 0) | k_1, \dots, k_n \rangle_{a_1, \dots, a_n}|^2 \\ & \times e^{-\beta \sum_{l=1}^m \varepsilon_{b_l}(p_l)} e^{-i \sum_{j=1}^n \varepsilon_{a_j}(k_j)t - k_j x} e^{i \sum_{l=1}^m \varepsilon_{b_l}(p_l)t - p_l x}. \end{aligned} \quad (103)$$

Using exact results for the form factors $b_m, \dots, b_1 \langle p_m, \dots, p_1 | \mathcal{O}(0, 0) | k_1, \dots, k_n \rangle_{a_1, \dots, a_n}$ [72, 93], one needs to sum an infinite number of terms in the Lehmann expansion in order to obtain the correlation function at late times and large distances. Such a resummation is possible at low temperatures $T \ll \Delta$, where Δ is the spectral gap, because the density of excitations in the state of thermal equilibrium constitutes a natural small parameter in this case [89]. The situation after a quantum quench bears many similarities to the finite temperature case. When dealing with a ‘‘small’’ quench in a gapped theory there exists a regime in which the density of excitations (of the post-quench Hamiltonian) in the initial state is small. It is then natural to use this small parameter in order to carry out a low-density expansion for the observables of interest. Let us consider a quantum quench $H_0 \rightarrow H$, where H describes an integrable scattering theory: we prepare the system in the ground state $|\Psi_0\rangle$ of H_0 and then consider time evolution by H . We are interested in observables such as

$$\frac{\langle \Psi_0(t) | \mathcal{O}(x) \mathcal{O}^\dagger(0) | \Psi_0(t) \rangle}{\langle \Psi_0 | \Psi_0 \rangle}. \quad (104)$$

Any translationally invariant initial state can be expressed in terms of the eigenstates of H as

$$\begin{aligned} |\Psi_0(t)\rangle &= \sum_{n=0}^{\infty} \sum_{\substack{k_1, \dots, k_n \\ a_1, \dots, a_n}} e^{-i \sum_{j=1}^n \varepsilon_{a_j}(k_j)t} F_n(\{k_j, a_j\}) |k_1, \dots, k_n\rangle_{a_1, \dots, a_n}, \\ F_n(\{k_j, a_j\}) &= a_n, \dots, a_1 \langle k_n, \dots, k_1 | \Psi(0) \rangle. \end{aligned} \quad (105)$$

A particular class of initial states is given by

$$|\Psi_0(0)\rangle = \sum_{n=0}^{\infty} \frac{i^n}{n!} \sum_{p_1, \dots, p_n} \left[\prod_{j=1}^n K^{a_j b_j}(p_j) \right] | -p_1, p_1, \dots, -p_n, p_n \rangle_{a_1, b_1, \dots, a_n, b_n}, \quad (106)$$

where summation over the indices a_j, b_k is implied. As is shown in Appendix B quantum quenches of the transverse field in the TFIM automatically lead to initial states of the form (106). For general integrable quantum field theories (106) are known to describe boundary-states [94] and correspond to situations where the initial state can be viewed as a boundary condition (in Euclidean space) that is compatible with quantum integrability. Given an initial state of the form (106), the basic idea is to employ a Lehmann representation in terms of the exact eigenstates of the post-quench Hamiltonian H . For a two-point function we have

$$\begin{aligned} \langle \Psi_0(t) | \mathcal{O}(x) \mathcal{O}^\dagger(0) | \Psi_0(t) \rangle &= \sum_{m=0}^{\infty} \sum_{n=0}^{\infty} \frac{i^{n-m}}{n! m!} \sum_{\substack{p_1, \dots, p_n \\ k_1, \dots, k_m}} \left[\prod_{j=1}^n K^{a_j b_j}(p_j) \right] \left[\prod_{l=1}^m K^{c_l d_l}(k_l) \right]^* \\ &\times \sum_{s=0}^{\infty} \sum_{q_1, \dots, q_s} \frac{1}{s!} c_{m, d_m, \dots, c_1, d_1} \langle k_m, -k_m, \dots, k_1 - k_1 | \mathcal{O}(t, x) | q_1, \dots, q_s \rangle_{f_1, \dots, f_s} \\ &\times \sum_{f_s, \dots, f_1} \langle q_s, \dots, q_1 | \mathcal{O}^\dagger(t, 0) | -p_1, p_1, \dots, -p_n, p_n \rangle_{a_1, b_1, \dots, a_n, b_n}. \end{aligned} \quad (107)$$

The form factors entering this expression are known, both for the TFIM and a variety of integrable quantum field theories [72, 93]. The normalization itself has the following Lehmann representation

$$\begin{aligned} \langle \Psi_0(t) | \Psi_0(t) \rangle &= \sum_{n=0}^{\infty} \frac{(-1)^n}{(n!)^2} \sum_{\substack{p_1, \dots, p_n \\ k_1, \dots, k_n}} \prod_{j=1}^n K^{a_j b_j}(p_j) [K^{c_j d_j}(k_j)]^* \\ &\times c_n, d_n, \dots, c_1, d_1 \langle k_n, -k_n, \dots, k_1 - k_1 | -p_1, p_1, \dots, -p_n, p_n \rangle_{a_1, b_1, \dots, a_n, b_n}. \end{aligned} \quad (108)$$

In order to extract the large time and distance asymptotics of (107) it is necessary to sum an infinite number of terms. In analogy to the finite temperature case we proceed as follows.

- Consider all contributions at a given order in the functions $K^{ab}(q)$.
- At each order we encounter two types of divergences: (i) infinite volume divergences that arise because in the thermodynamic limit the scattering states are normalized to delta functions. These singular contributions are ultimately compensated by corresponding divergences in the normalization (108) and are dealt with by an appropriate subtraction procedure, cf. [89] for the finite temperature case; (ii) “infrared” divergences, i.e. contributions that diverge as $t \rightarrow \infty$ or $x \rightarrow \infty$.
- We isolate the terms with the strongest infrared divergences at each order in $K^{ab}(q)$ and then sum up all these contributions, *c.f.* [95] for a similar calculation in the finite-temperature case.

4.1. Finite Volume Form Factors for the TFIM

As is clear from the above discussion the basic building blocks are the form factors. For the case of the transverse field Ising chain these naturally depend on the precise choice of basis of free fermion scattering states $|k_1, \dots, k_n\rangle_{\text{R,NS}}$. For a particular such choice, the finite-volume form factors of the spin operators σ_ℓ^x have been determined in Refs [96, 97, 98]. The non-vanishing matrix elements are

$$\begin{aligned} \text{NS} \langle q_1, \dots, q_{2n} | \sigma_\ell^x | p_1, \dots, p_m \rangle_{\text{R}} &= e^{-i\ell[\sum_{j=1}^{2n} q_j - \sum_{l=1}^m p_l]} \\ &\times i^{\lfloor n + \frac{m}{2} \rfloor} (4J^2 h)^{\frac{(m-2n)^2}{4}} \sqrt{\xi \xi_T} \prod_{j=1}^{2n} \left[\frac{e^{\eta q_j}}{L \varepsilon_{q_j}} \right]^{\frac{1}{2}} \prod_{l=1}^m \left[\frac{e^{-\eta p_l}}{L \varepsilon_{p_l}} \right]^{\frac{1}{2}} \\ &\times \prod_{j < j'=1}^{2n} \left[\frac{\sin(\frac{q_j - q_{j'}}{2})}{\varepsilon_{q_j q_{j'}}} \right] \prod_{l < l'=1}^m \left[\frac{\sin(\frac{p_l - p_{l'}}{2})}{\varepsilon_{p_l p_{l'}}} \right] \prod_{j=1}^{2n} \prod_{l=1}^m \left[\frac{\varepsilon_{q_j p_l}}{\sin(\frac{q_j - p_l}{2})} \right] \end{aligned} \quad (109)$$

where m is even (odd) for $h < 1$ ($h > 1$) and

$$\begin{aligned} \varepsilon_k &= 2J \sqrt{1 + h^2 - 2h \cos k}, \quad \varepsilon_{k, k'} \equiv \frac{\varepsilon_k + \varepsilon_{k'}}{2}, \quad \xi = |1 - h^2|^{1/4}, \\ \xi_T &= \prod_{\substack{q \in \text{NS} \\ p \in \text{R}}} (\varepsilon_{q, p})^{\frac{1}{2}} \prod_{q, q' \in \text{NS}} (\varepsilon_{q, q'})^{-\frac{1}{4}} \prod_{p, p' \in \text{R}} (\varepsilon_{p, p'})^{-\frac{1}{4}}, \quad e^{\eta k} = \frac{\prod_{q \in \text{NS}} \varepsilon_{k, q}}{\prod_{p \in \text{R}} \varepsilon_{k, p}}. \end{aligned} \quad (110)$$

For large L we have with exponential accuracy (in L)

$$e^{\eta k} \approx 1 \quad e^{\eta k} \approx 1. \quad (111)$$

As we are interested in the thermodynamic limit we will set these terms equal to 1 in what follows (their deviations from 1 give rise to subleading contributions). We stress that as a consequence of

the different quantization conditions of R and NS momenta there are no singularities in Eq. (109) as long as L is (large but) finite. The free fermionic basis used in Ref. [98] differs from the one discussed in Appendix A. However, the initial state can still be represented in terms of eigenstates of the post quench Hamiltonian $H(h)$ using (B.8) and (B.10), provided that $K(k)$ is chosen appropriately.

4.2. Quench within the ferromagnetic phase: time evolution of the order parameter

We now consider a quench within the ordered phase: we prepare the system in the ground state of the Hamiltonian $H(h_0)$ and at time $t = 0$ suddenly change the magnetic field from h_0 to h , where $h_0, h < 1$. We are interested in the case where the \mathbb{Z}_2 symmetry of $H(h_0)$ is broken spontaneously in the ground state $|\Psi_0\rangle$. This is possible only in the thermodynamic limit. On the other hand, we would like to keep the length L of the system very large but finite in our calculations for technical reasons. In order to be able to work in a large, finite volume, we therefore take our initial state to be of the form

$$|\Psi_0\rangle = \frac{1}{\sqrt{2}} \left\{ |0; h_0\rangle_{\text{NS}} + |0; h_0\rangle_{\text{R}} \right\}, \quad (112)$$

where $|0; h_0\rangle_{\text{NS}}$ and $|0; h_0\rangle_{\text{R}}$ are the ground states of $H(h_0)$ in the sectors with even/odd numbers of fermions respectively, see Appendix A.4. For finite system size L , the state (112) is a particular linear combination of the ground state and first excited state of the Hamiltonian $H(h_0)$. On the other hand, in the thermodynamic limit $L \rightarrow \infty$ (112) becomes the symmetry broken ground state of H_0 . As is shown in Appendix B the time-evolved initial state

$$|\Psi_0(t)\rangle = e^{-iH(h)t} |\Psi_0\rangle \quad (113)$$

can be expressed in terms of eigenstates of $H(h)$ as

$$|\Psi_0(t)\rangle = \frac{1}{\sqrt{2}} \left[\frac{|B(t)\rangle_{\text{NS}}}{\sqrt{\langle B|B\rangle_{\text{NS}}}} + \frac{|B(t)\rangle_{\text{R}}}{\sqrt{\langle B|B\rangle_{\text{R}}}} \right], \quad (114)$$

where

$$|B(t)\rangle_{\mathbf{a}} = e^{-iE_0^{\mathbf{a}}t} \exp \left[i \sum_{0 < p \in \mathbf{a}} K(p) e^{-2i\varepsilon_p t} b_{-p}^\dagger b_p^\dagger \right] |0; h\rangle_{\mathbf{a}}, \quad \mathbf{a} = \text{R, NS}. \quad (115)$$

For the choice of basis underlying (109) the function $K(k)$ is given by

$$K(k) = \frac{\sin(k) (h - h_0)}{\varepsilon_{h_0}(k) \varepsilon_h(k) (2J)^{-2} + 1 + hh_0 - (h + h_0) \cos(k)}. \quad (116)$$

We note that this agrees with what would be obtained using the choice of fermions presented in (Appendix A). The expectation value of σ_ℓ^x is then given by

$$\langle \Psi_0(t) | \sigma_\ell^x | \Psi_0(t) \rangle = \frac{\text{R} \langle B(t) | \sigma_\ell^x | B(t) \rangle_{\text{NS}} + \text{NS} \langle B(t) | \sigma_\ell^x | B(t) \rangle_{\text{R}}}{2 \sqrt{\text{R} \langle B|B \rangle_{\text{R}} \text{NS} \langle B|B \rangle_{\text{NS}}}}. \quad (117)$$

We note that the diagonal contributions vanish

$$\mathbf{a} \langle B(t) | \sigma_\ell^x | B(t) \rangle_{\mathbf{a}} = 0, \quad \mathbf{a} = \text{R, NS}, \quad (118)$$

because

$$e^{-i\pi \hat{N}} \sigma_\ell^x e^{i\pi \hat{N}} = -\sigma_\ell^x, \quad (119)$$

where \hat{N} is the fermion number operator (A.6).

The normalization is readily evaluated using the explicit representation (115)

$$\begin{aligned} {}_{\text{NS}}\langle B|B\rangle_{\text{NS}} &= \exp\left[\sum_{0 < q \in \text{NS}} \log(1 + K^2(q))\right], \\ {}_{\text{R}}\langle B|B\rangle_{\text{R}} &= \exp\left[\sum_{0 < p \in \text{R}} \log(1 + K^2(p))\right], \end{aligned} \quad (120)$$

so that, for large L , the norms ${}_{\text{R,NS}}\langle B|B\rangle_{\text{R,NS}}$ are approximately equal (we note that $K(0) = K(\pi) = 0$)

$${}_{\text{R}}\langle B|B\rangle_{\text{R}} \approx {}_{\text{NS}}\langle B|B\rangle_{\text{NS}} \approx \exp\left(L \int_0^\pi \frac{dk}{2\pi} \log(1 + K^2(k))\right). \quad (121)$$

Importantly we have

$$\frac{{}_{\text{R}}\langle B|B\rangle_{\text{R}}}{{}_{\text{NS}}\langle B|B\rangle_{\text{NS}}} = 1 + \mathcal{O}(e^{-\alpha L}), \quad (122)$$

where α is a positive constant. Eqn (122) allows us to simplify the expression (117) for the 1-point function to

$$\langle \Psi_0(t) | \sigma_\ell^x | \Psi_0(t) \rangle = \text{Re} \frac{{}_{\text{R}}\langle B(t) | \sigma_\ell^x | B(t) \rangle_{\text{NS}}}{{}_{\text{R}}\langle B|B\rangle_{\text{R}}} + \mathcal{O}(L^{-2}). \quad (123)$$

As we are interested in the thermodynamic limit this representation is most convenient and we will use it in the following. The normalization can be expanded in powers of K as

$$\begin{aligned} {}_{\text{R}}\langle B|B\rangle_{\text{R}} &= 1 + \sum_{0 < k \in \text{R}} K^2(k) + \frac{1}{2} \left[\sum_{0 < k \in \text{R}} K^2(k) \right]^2 - \frac{1}{2} \sum_{0 < k \in \text{R}} K^4(k) + \dots \\ &\equiv 1 + \sum_{n=1}^{\infty} \Upsilon_{2n}, \end{aligned} \quad (124)$$

where Υ_{2n} collects all the terms in which $2n$ functions $K(k)$ are multiplied together. The following representation of Υ_{2n} turns out to be particularly useful

$$\Upsilon_{2n} = \frac{1}{n!} \sum'_{0 < k_1, \dots, k_n \in \text{R}} \prod_{j=1}^n K^2(k_j). \quad (125)$$

Here \sum' indicates that the sum is only over terms with $k_l \neq k_m$ for $l \neq m = 1, \dots, n$. Eqn (124) is a formal series expansion as each term grows as L^n , *i.e.* diverges in the thermodynamic limit. The divergences in the normalization (124) are mirrored by infinite volume divergences in the numerator of (117). Using (115) to expand ${}_{\text{NS}}\langle B(t) | \sigma_\ell^x | B(t) \rangle_{\text{R}}$ in powers of the function $K(k)$ gives

$$\begin{aligned} \text{Re} [{}_{\text{NS}}\langle B(t) | \sigma_\ell^x | B(t) \rangle_{\text{R}}] &= 2m_0^x \left\{ 1 + R_1(t) + [R_2(t) + \Upsilon_2] + [R_3(t) + \Upsilon_2 R_1(t)] \right. \\ &\quad \left. + [R_4(t) + \Upsilon_2 R_2(t) + \Upsilon_4] + \dots \right\}, \end{aligned} \quad (126)$$

where $m_0^x \equiv \langle \sigma_\ell^x \rangle_0 / 2$ is the magnetization at the initial time and the $R_n(t)$ are finite in the thermodynamic limit. In terms of the ‘‘connected’’ contributions $R_n(t)$ the order parameter expectation value (123) is expressed as

$$\langle \Psi_0(t) | \sigma_\ell^x | \Psi_0(t) \rangle = 2m_0^x \left[1 + \sum_{n=1}^{\infty} R_n(t) \right]. \quad (127)$$

Eqn (127) constitutes a linked cluster expansion, where the contribution $R_n(t)$ is of order $\mathcal{O}(K^n)$. As is shown in Appendix B (see Eqn (B.12)) physically the formal expansion in powers of $K(q)$ corresponds to a low-density expansion, where the small parameter is the density of excitations of the post-quench Hamiltonian in the initial state.

The next step is to determine the functions $R_n(t)$. Expanding the boundary states in ${}_{\text{NS}}\langle B(t)|\sigma_\ell^x|B(t)\rangle_{\text{R}}$ we obtain

$$\begin{aligned} {}_{\text{NS}}\langle B(t)|\sigma_\ell^x|B(t)\rangle_{\text{R}} &= \sum_{l,n=0}^{\infty} \frac{i^{n-l}}{n! l!} \sum_{\substack{q_1, \dots, q_n \in \text{NS} \\ p_1, \dots, p_l \in \text{R}}} \prod_{j=1}^n K(q_j) \prod_{i=1}^l K(p_i) e^{2it(\sum_{i=1}^n \varepsilon_{q_i} - \sum_{j=1}^l \varepsilon_{p_j})} \\ &\quad \times {}_{\text{NS}}\langle -q_1, q_1, \dots, -q_n, q_n | \sigma_\ell^x | p_1, -p_1, \dots, p_l, -p_l \rangle_{\text{R}} \\ &\equiv \sum_{l,n=0}^{\infty} C_{(n,l)}. \end{aligned} \quad (128)$$

In the following we consider the first few terms in the expansion (128). We will find that most terms exhibit long-time (infrared) divergences, the strongest of which occur in ‘‘diagonal’’ contributions $n = l$. We will determine and then sum these leading singularities to all orders in the expansion (128).

4.2.1. Order $\mathcal{O}(K^0)$ Contribution ($n = l = 0$). The zero-particle contribution in (128) is the ground state (of the post-quench Hamiltonian $H(h)$) expectation value

$$C_{(0|0)} = 2m_0^x = \sqrt{\xi} = (1 - h^2)^{1/8}. \quad (129)$$

4.2.2. Order $\mathcal{O}(K)$ Contributions. At first order in K there are two contributions

$$\begin{aligned} C_{(1|0)} &= i \sum_{0 < q \in \text{NS}} K(q) e^{2it\varepsilon_q} {}_{\text{NS}}\langle -q, q | \sigma_\ell^x | 0 \rangle_{\text{R}} = 4J^2 h \sqrt{\xi} \frac{1}{L} \sum_{0 < q \in \text{NS}} \frac{K(q) \sin q}{\varepsilon_q^2} e^{2it\varepsilon_q}, \\ C_{(0|1)} &= -i \sum_{0 < p \in \text{R}} K(p) e^{-2it\varepsilon_p} {}_{\text{NS}}\langle 0 | \sigma_\ell^x | p, -p \rangle_{\text{R}} = 4J^2 h \sqrt{\xi} \frac{1}{L} \sum_{0 < p \in \text{R}} \frac{K(p) \sin p}{\varepsilon_p^2} e^{-2it\varepsilon_p}. \end{aligned} \quad (130)$$

In the limit $L \rightarrow \infty$ we can turn the momentum sums in (130) into integrals, which gives

$$I(t) = \frac{1}{\sqrt{\xi}} \lim_{L \rightarrow \infty} [C_{(1|0)} + C_{(0|1)}] = 8J^2 h \int_0^\pi \frac{dk}{2\pi} \frac{K(k) \sin k}{\varepsilon_k^2} \cos(2t\varepsilon_k). \quad (131)$$

For late times we can evaluate this integral by a stationary phase approximation

$$I(t) = A_0 \frac{\cos(2\varepsilon_0 t + \frac{3\pi}{4})}{t^{3/2}} - A_\pi \frac{\cos(2\varepsilon_\pi t - \frac{3\pi}{4})}{t^{3/2}} + o(t^{-3/2}), \quad (132)$$

where

$$A_k = \frac{hJ^2 K'(k)}{\sqrt{\pi \varepsilon_k^2 |\varepsilon_k''|^{3/2}}}, \quad k = 0, \pi. \quad (133)$$

Comparison of (128) and (126) then allows us to identify the function $R_1(t)$ in the thermodynamic limit

$$R_1(t) = I(t). \quad (134)$$

4.2.3. *Order $\mathcal{O}(K^2)$ Contributions.* To order $\mathcal{O}(K^2)$ there are two types of contributions. $C_{(2|0)}$ and $C_{(0|2)}$ are finite in the thermodynamic limit and well behaved at late times. They don't play a significant role in the following and we therefore refrain from presenting explicit expressions. The most important contribution to order $\mathcal{O}(K^2)$ is given by

$$C_{(1|1)} = \sum_{\substack{0 < q \in \text{NS} \\ 0 < p \in \text{R}}} K(q)K(p) e^{-2it(\varepsilon_p - \varepsilon_q)}_{\text{NS}} \langle -q, q | \sigma_\ell^x | p, -p \rangle_{\text{R}}. \quad (135)$$

The relevant form factor is, *cf.* eqn (109),

$$\text{NS} \langle -q, q | \sigma_\ell^x | p, -p \rangle_{\text{R}} \simeq \frac{4\sqrt{\xi}}{L^2} \frac{\epsilon_{p,q}^4}{\varepsilon_q^2 \varepsilon_p^2} \sin q \sin p c_{qp}^2, \quad (136)$$

where we have defined

$$c_{kk'} \equiv \frac{1}{\cos k - \cos k'}. \quad (137)$$

For large t and L the momentum sum in the NS-sector can be evaluated using Lemma 1 (D.1) and retaining only the leading terms in t and L . This results in

$$C_{(1|1)} = \sqrt{\xi} \sum_{0 < p \in \text{R}} K^2(p) \left[1 - \frac{4t\varepsilon'_p}{L} \right] + \dots \quad (138)$$

Crucially, this contribution exhibits an *infinite volume* divergence (for $L \rightarrow \infty$) as well as an *infrared* divergence (for $t \rightarrow \infty$). To $\mathcal{O}(1)$ (in both L and t) (138) can be expressed as

$$C_{(1|1)} = \sqrt{\xi} \Upsilon_2 - \sqrt{\xi} \int_0^\pi \frac{dk}{\pi} K^2(k) 2t\varepsilon'_k + \dots, \quad (139)$$

where Υ_2 is defined in (124). By comparing (139) to (126) we can determine the function $R_2(t)$ for large t

$$R_2(t) = - \int_0^\pi \frac{dk}{\pi} K^2(k) 2t\varepsilon'_k + \dots, \quad (140)$$

where the dots denote terms that are subleading in t at late times. We note the leading term (140) arises from the region $p \approx q$ in (135). This observation will be important in what follows.

4.2.4. *Order $\mathcal{O}(K^3)$ Contributions.* To this order there are several contributions. $C_{(3|0)}$ and $C_{(0|3)}$ are completely regular and do not play an important role in the following. The evaluation of the other contributions follows closely the calculation for $C_{(1|1)}$ and results in

$$\begin{aligned} C_{(1|2)} + \text{h.c.} &= \text{Re} \sum_{0 < k_{1,2} \in \text{NS}} \sum_{0 < p \in \text{R}} iK(k_1)K(k_2)K(p) e^{2it[\varepsilon_{k_1} + \varepsilon_{k_2} - \varepsilon_p]} \\ &\quad \times \text{NS} \langle -k_1, k_1, -k_2, k_2 | \sigma_m^x | p, -p \rangle_{\text{R}} \\ &= \text{Re}(C_{(0|1)}) \left[\Upsilon_2 - \frac{1}{L} \sum_{0 < p \in \text{R}} 4t\varepsilon'_p K^2(p) \right] + \dots, \\ C_{(2|1)} + \text{h.c.} &= \text{Re} \sum_{0 < k_{1,2} \in \text{R}} \sum_{0 < p \in \text{NS}} iK(k_1)K(k_2)K(p) e^{2it[\varepsilon_{k_1} + \varepsilon_{k_2} - \varepsilon_p]} \\ &\quad \times \text{R} \langle -k_1, k_1, -k_2, k_2 | \sigma_m^x | p, -p \rangle_{\text{NS}} \\ &= \text{Re}(C_{(1|0)}) \left[\Upsilon_2 - \frac{1}{L} \sum_{0 < p \in \text{NS}} 4t\varepsilon'_p K^2(p) \right] + \dots \end{aligned} \quad (141)$$

Comparison with (126) then gives

$$R_3(t) = -I(t) \int_0^\pi \frac{dp}{\pi} 2t\varepsilon'_p K^2(p) + \dots, \quad (142)$$

where the dots indicate contributions that are subleading in t . We note that (142) arises from the regions $k_{1,2} \approx p$ in (141).

4.2.5. *Order $\mathcal{O}(K^4)$ Contribution $C_{(2|2)}$.* The most important contribution at order $\mathcal{O}(K^4)$ is $C_{(2|2)}$ and we now discuss its evaluation in some detail. From (128) we have

$$C_{(2|2)} = \frac{1}{2!^2} \sum_{\substack{0 < q \neq q' \in \text{NS} \\ 0 < p \neq p' \in \text{R}}} K(q)K(q')K(p)K(p') e^{-2it(\varepsilon_p + \varepsilon_{p'} - \varepsilon_q - \varepsilon_{q'})} \\ \times \text{NS} \langle -q, q, -q', q' | \sigma_\ell^x | p, -p, p', -p' \rangle_{\text{R}}, \quad (143)$$

where the form factor is given by

$$\text{NS} \langle -q, q, -q', q' | \sigma_\ell^x | p, -p, p', -p' \rangle_{\text{R}} = \frac{16\sqrt{\xi}}{L^4} \frac{\varepsilon_{q,p}^4 \varepsilon_{q,p'}^4 \varepsilon_{q',p}^4 \varepsilon_{q',p'}^4}{\varepsilon_q^2 \varepsilon_{q'}^2 \varepsilon_p^2 \varepsilon_{p'}^2 \varepsilon_{q,q'}^4 \varepsilon_{p,p'}^4} \\ \times \sin q \sin q' \sin p \sin p' \frac{c_{qp}^2 c_{qp'}^2 c_{q'p}^2 c_{q'p'}^2}{c_{qq'}^2 c_{pp'}^2}. \quad (144)$$

Each factor $c_{qq'}$ is associated with a singularity in the thermodynamic limit and it is useful to isolate these poles as functions of the NS-sector momenta, e.g.

$$c_{pq} c_{p'q} = c_{pp'} (c_{p'q} - c_{pq}), \\ c_{pq}^2 c_{p'q}^2 = c_{pp'}^2 \left[c_{pq}^2 + c_{p'q}^2 - 2c_{pp'} (c_{p'q} - c_{pq}) \right], \\ \frac{c_{qp}^2 c_{qp'}^2 c_{q'p}^2 c_{q'p'}^2}{c_{qq'}^2 c_{pp'}^2} = c_{qp}^2 c_{q'p'}^2 + c_{qp'}^2 c_{q'p}^2 - 2c_{pp'}^2 (c_{p'q} - c_{pq})(c_{p'q'} - c_{pq'}). \quad (145)$$

Using the symmetry of (143) under exchange of p and p' the contribution of the last term in (145) can be reexpressed by substituting

$$\frac{c_{qp}^2 c_{qp'}^2 c_{q'p}^2 c_{q'p'}^2}{c_{qq'}^2 c_{pp'}^2} \rightarrow 2c_{qp}^2 c_{q'p'}^2 - 4c_{pp'}^2 c_{pq} c_{p'q'} + 4c_{pp'}^2 c_{pq} c_{p'q'}. \quad (146)$$

The sums over the NS momenta can then be carried out using Lemmas 1 (D.1) and 5 (D.10). We begin with the contribution due to the first term in (146), which we denote by $C_{(2|2)}^{[2,2]}$. Here the superscript indicates the pole structure, namely two double poles. The NS sector momentum sums in (143) are performed by using (D.1) and retaining only the leading terms in L and t , which gives

$$C_{(2|2)}^{[2,2]} = \frac{\sqrt{\xi}}{2} \sum_{0 < p \neq p' \in \text{R}} K^2(p) \left[1 - \frac{4t\varepsilon'_p}{L} \right] K^2(p') \left[1 - \frac{4t\varepsilon'_{p'}}{L} \right] + \dots \\ = \frac{\sqrt{\xi}}{2} [R_2(t) + \Upsilon_2]^2 - \frac{\sqrt{\xi}}{2} \sum_{0 < p \in \text{R}} K^4(p) \left[1 - \frac{8t\varepsilon'_p}{L} \right] + \dots \quad (147)$$

Working out the contributions arising from the other terms in (146) is more involved. Carrying out the sums over q and q' using (D.10) and retaining only the leading contributions in L and t gives

$$\begin{aligned}
 -4c_{pp'}^2 c_{pq} c_{p'q'} &\rightarrow \frac{4\sqrt{\xi}}{L^2} \sum_{0 < p \neq p' \in \mathbb{R}} K^3(p) K(p') e^{-2it(\varepsilon_{p'} - \varepsilon_p)} \frac{\varepsilon_{p,p'}^4}{\varepsilon_p^2 \varepsilon_{p'}^2} \sin p \sin p' c_{pp'}^2, \\
 4c_{pp'}^2 c_{pq} c_{p'q'} &\rightarrow -\frac{4\sqrt{\xi}}{L^2} \sum_{0 < p \neq p' \in \mathbb{R}} K^2(p) K^2(p') \sin p \sin p' c_{pp'}^2.
 \end{aligned} \tag{148}$$

The leading contribution at late times and large L can then be extracted by using Lemma 2a (D.2)

$$C_{(2|2)}^{[1,1]} = -\frac{4\sqrt{\xi}}{L} \sum_{0 < p \in \mathbb{R}} K^4(p) t \varepsilon_p' + \dots \tag{149}$$

Here the superscript $[1, 1]$ indicates that we are considering the contribution from two single poles. Putting everything together we arrive at the following result for $C_{(2|2)}$

$$C_{(2|2)} = C_{(2|2)}^{[2,2]} + C_{(2|2)}^{[1,1]} = \sqrt{\xi} \left[\frac{1}{2} (R_2(t))^2 + \Upsilon_2 R_2(t) + \Upsilon_4 \right] + \dots \tag{150}$$

This allows us to identify the leading contribution to the term $R_4(t)$ in (126) as

$$R_4(t) = \frac{1}{2} (R_2(t))^2 + \dots \tag{151}$$

4.2.6. Exponentiation of the Contributions $C_{(n|n)}$. Our analysis of the first few orders in powers of K reveals the general structure of the expansion (128): at each order (except the very lowest ones) there are late time divergences that become stronger at higher orders. Moreover, the leading singularities are found in the ‘‘diagonal’’ contributions $C_{(n|n)}$ and we will now isolate these singular terms. At order $\mathcal{O}(K^{2n})$ we have

$$\begin{aligned}
 C_{(n|n)} &= \frac{1}{n!^2} \sum'_{\substack{q_1, \dots, q_n \in \text{NS} \\ p_1, \dots, p_n \in \mathbb{R}}} \prod_{j=1}^n K(q_j) K(p_j) e^{2it \sum_{i=1}^n (\varepsilon_{q_i} - \varepsilon_{p_i})} \\
 &\quad \times \text{NS} \langle -q_1, q_1, \dots, -q_n, q_n | \sigma_\ell^x | p_1, -p_1, \dots, p_n, -p_n \rangle_{\mathbb{R}},
 \end{aligned} \tag{152}$$

where the form factor in the limit of large L is given by

$$\begin{aligned}
 \text{NS} \langle -q_1, q_1, \dots, -q_n, q_n | \sigma_\ell^x | p_1, -p_1, \dots, p_n, -p_n \rangle_{\mathbb{R}} &= \\
 \frac{4^n \sqrt{\xi}}{L^{2n}} \left[\prod_{j,l=1}^n \varepsilon_{q_j, p_l}^4 c_{q_j p_l}^2 \right] \left[\prod_{j=1}^n \frac{\sin(q_j) \sin(p_j)}{\varepsilon_{q_j}^2 \varepsilon_{p_j}^2} \right] \left[\prod_{j < j'=1}^n \frac{1}{\varepsilon_{q_j, q_{j'}}^4 \varepsilon_{p_j, p_{j'}}^4 c_{q_j q_{j'}}^2 c_{p_j p_{j'}}^2} \right].
 \end{aligned} \tag{153}$$

The most singular terms at late times arise from the regions in momentum space

$$p_j \approx q_{P(j)}, \tag{154}$$

where P is a permutation of $1, \dots, n$. There are $n!$ such contributions with only double poles and they are all equal. They are determined by replacing

$$\frac{\prod_{j=1}^n \prod_{l=1}^n c_{q_j p_l}^2}{\prod_{j < j'=1}^n c_{q_j q_{j'}}^2 c_{p_j p_{j'}}^2} \rightarrow n! \prod_{i=1}^n c_{q_i p_i}^2 + \dots, \tag{155}$$

and then carrying out the NS-sector momentum sums using (D.1). This gives

$$C_{(n|n)}^{[2,\dots,2]} = \frac{1}{n!} \frac{4^n \sqrt{\xi}}{L^n} \sum'_{0 < p_1, \dots, p_n \in \mathbb{R}} \prod_{i=1}^n K(p_i)^2 \left[\frac{L}{4} - t\varepsilon'_{p_i} \right] + \dots \quad (156)$$

This is in agreement with (138) and (147). Using (125) we see that the t -independent part of (156) equals Υ_{2n} , so that

$$\sum_{n=0}^{\infty} C_{(n|n)}^{[2,\dots,2]} \Big|_{t=0} = \sqrt{\xi} \exp \left[\sum_{0 < p \in \mathbb{R}} \log \left(1 + K^2(p) \right) \right] + \dots \quad (157)$$

For $t > 0$ we may invert the steps used to express (120) in terms of (125), which gives

$$\begin{aligned} \sum_{n=0}^{\infty} C_{(n|n)}^{[2,\dots,2]} &= \sqrt{\xi} \exp \left[\sum_{0 < p \in \mathbb{R}} \log \left(1 + K^2(p) \left[1 - \frac{4t\varepsilon'_p}{L} \right] \right) \right] + \dots \\ &= \sqrt{\xi} \langle B|B \rangle_{\mathbb{R}} \exp \left[-t \int_0^{\pi} \frac{dk}{\pi} \frac{K^2(k)}{1 + K^2(k)} |2\varepsilon'(k)| \right] + \dots \end{aligned} \quad (158)$$

The contribution of all these terms to the 1-point function of the order parameter is thus

$$\text{Re} \sum_{n=0}^{\infty} \frac{C_{(n|n)}}{\langle B|B \rangle_{\mathbb{R}}} = \sqrt{\xi} \exp \left[-t \int_0^{\pi} \frac{dk}{\pi} \frac{K^2(k)}{1 + K^2(k)} |2\varepsilon'(k)| \right] + \dots \quad (159)$$

4.2.7. Exponentiation of the Contributions $C_{(n\pm 1|n)}$. The leading terms (at late times and large L) in $C_{(n\pm 1|n)}$ can be summed to all orders in a similar way to our treatment of $C_{(n|n)}$. The contributions $C_{(n+1|n)}$ are given by

$$\begin{aligned} \text{Re } C_{(n+1|n)} &= \frac{1}{(n+1)!n!} \text{Im} \sum'_{\substack{0 < q_1, \dots, q_n, q \in \text{NS} \\ 0 < p_1, \dots, p_n \in \mathbb{R}}} K(q) \left[\prod_{j=1}^n K(q_j) K(p_j) \right] e^{2it\varepsilon_q + 2it \sum_{i=1}^n (\varepsilon_{q_i} - \varepsilon_{p_i})} \\ &\quad \times \text{NS} \langle -q_1, q_1, \dots, -q_n, q_n, -q, q | \sigma_{\ell}^x | p_1, -p_1, \dots, p_n, -p_n \rangle_{\mathbb{R}}, \end{aligned} \quad (160)$$

where the form factors in the limit of large L are

$$\begin{aligned} \text{NS} \langle -q_1, q_1, \dots, -q_n, q_n, -q, q | \sigma_{\ell}^x | p_1, -p_1, \dots, p_n, -p_n \rangle_{\mathbb{R}} &= -4ihJ^2 \frac{4^n \sqrt{\xi}}{L^{2n+1}} \prod_{j,l=1}^n \epsilon_{q_j, p_l}^4 \prod_{m=1}^n \varepsilon_{q_m}^{-2} \varepsilon_{p_m}^{-2} \\ &\times \prod_{j < j'=1}^n \epsilon_{q_j, q_{j'}}^{-4} \epsilon_{p_j, p_{j'}}^{-4} \prod_{i=1}^n \sin(q_i) \sin(p_i) \frac{\prod_{j,l=1}^n c_{q_j p_l}^2}{\prod_{j < j'=1}^n c_{q_j q_{j'}}^2 c_{p_j p_{j'}}^2} \prod_{j=1}^n \frac{\epsilon_{q, p_j}^4 \sin q}{\epsilon_{q, q_j}^4 \varepsilon_q^2} \prod_{j=1}^n \frac{c_{q p_j}^2}{c_{q_j q}^2}. \end{aligned} \quad (161)$$

Following the same reasoning that led to (155), we focus on the contributions arising from the regions

$$p_j \approx \tilde{q}_j, \quad j = 1, \dots, n, \quad (162)$$

where $(\tilde{q}_1, \dots, \tilde{q}_{n+1})$ is an arbitrary permutation of (q_1, \dots, q_n, q) . All of these contributions are the same and hence the leading behaviour at late times can be extracted by the substitution

$$\frac{\prod_{j=1}^n \prod_{l=1}^n c_{q_j p_l}^2}{\prod_{j < j'=1}^n c_{q_j q_{j'}}^2 c_{p_j p_{j'}}^2} \prod_{j=1}^n \frac{c_{q p_j}^2}{c_{q_j q}^2} \rightarrow (n+1)! \prod_{i=1}^n c_{q_i p_i}^2 + \dots \quad (163)$$

The NS-sector momentum sums can be carried out using (D.1), which gives

$$\begin{aligned} \text{Re } C_{(n+1|n)}^{[2,\dots,2]} &= -\frac{1}{n!} \frac{4^{n+1} h J^2 \sqrt{\xi}}{L^{n+1}} \sum_{\substack{0 < q \in NS \\ 0 < p_1, \dots, p_n \in R}} K(q) \cos(2t\varepsilon_q) \frac{\sin q}{\varepsilon_q^2} \prod_{i=1}^n K(p_i)^2 \left[\frac{L}{4} - t\varepsilon'_{p_i} \right] + \dots \\ &= -4hJ^2 C_{(n|n)}^{[2,\dots,2]} \int_0^\pi \frac{dk}{2\pi} K(k) \cos(2t\varepsilon_k) \frac{\sin k}{\varepsilon_k^2} + \dots \end{aligned} \quad (164)$$

Summing over n then results in

$$\text{Re} \sum_{n=0}^{\infty} C_{(n+1|n)}^{[2,\dots,2]} = \sqrt{\xi} \frac{I(t)}{2} \langle B|B \rangle_R \exp \left[-t \int_0^\pi \frac{dk}{\pi} \frac{K^2(k)}{1+K^2(k)} |2\varepsilon'(k)| \right] + \dots, \quad (165)$$

where $I(t)$ is given by (132). The analysis for the contributions $C_{(n|n+1)}$ is completely analogous and finally leads to the following result

$$\text{Re} \sum_{n=0}^{\infty} \frac{C_{(n+1|n)} + C_{(n|n+1)}}{\langle B|B \rangle_R} = \sqrt{\xi} I(t) \exp \left[-t \int_0^\pi \frac{dk}{\pi} \frac{K^2(k)}{1+K^2(k)} |2\varepsilon'(k)| \right] + \dots \quad (166)$$

We see that by virtue of the extra factor $I(t)$ this is always subleading compared to the ‘‘diagonal’’ contribution (159).

4.2.8. Form Factor Result for the 1-point Function $\langle \Psi_0(t) | \sigma_\ell^x | \Psi_0(t) \rangle$ Combining the results in the previous subsections we conclude that

$$\langle \Psi_0(t) | \sigma_\ell^x | \Psi_0(t) \rangle \sim \sqrt{\xi} [1 + I(t) + \mathcal{O}(t^{-1})] e^{-t/\tau}, \quad (167)$$

where the decay time τ is given by

$$\tau^{-1} = \int_0^\pi \frac{dk}{\pi} K^2(k) [2\varepsilon'(k)] + \mathcal{O}(K^6). \quad (168)$$

Here we have used (151) to infer the absence of $\mathcal{O}(K^4)$ corrections to the decay time. The corrections in the prefactor are expected to be $\mathcal{O}(t^{-1})$ as there are such (subleading) contributions in the various terms $C_{(n|l)}$ we have calculated above. We note that these terms are larger than $I(t)$ at late times as $I(t) \sim t^{-3/2}$.

The result (168) is in agreement with the one obtained by applying the cluster decomposition principle on the asymptotic result for the two-point function obtained in the determinant approach (*cf.* Eq. (69)), which gives

$$\tau^{-1} = \int_0^\pi \frac{dk}{\pi} \log \left| \frac{1+K^2(k)}{1-K^2(k)} \right| \varepsilon'(k). \quad (169)$$

Indeed, expanding (169) in the limit where $K^2(k) \ll 1$ gives precisely (168). We note that (168) is a rather good approximation for a wide range of magnetic fields h_0 and h . For example, for a quench from $h_0 = 0.1$ to $h = 0.8$ the relative error is less than 1%. This shows the effectiveness of the form-factor approach.

4.3. Two-Point Function in the Ordered Phase

We now turn to the time evolution of the two-point function for a quench within the ordered phase. The quantity we want to evaluate is

$$\begin{aligned} \rho^{xx}(t, \ell) &= \langle \Psi_0(t) | \sigma_{m+\ell}^x \sigma_m^x | \Psi_0(t) \rangle \\ &= \frac{\text{R} \langle B(t) | \sigma_{m+\ell}^x \sigma_m^x | B(t) \rangle_{\text{R}}}{2 \text{R} \langle B | B \rangle_{\text{R}}} + \frac{\text{NS} \langle B(t) | \sigma_{m+\ell}^x \sigma_m^x | B(t) \rangle_{\text{NS}}}{2 \text{NS} \langle B | B \rangle_{\text{NS}}}. \end{aligned} \quad (170)$$

In the large- L limit both terms contribute equally, so that

$$\lim_{L \rightarrow \infty} \rho^{xx}(t, \ell) = \lim_{L \rightarrow \infty} \frac{\text{R} \langle B(t) | \sigma_{m+\ell}^x \sigma_m^x | B(t) \rangle_{\text{R}}}{\text{R} \langle B | B \rangle_{\text{R}}}. \quad (171)$$

We note that as a consequence of reflection symmetry the sign of ℓ does not matter, i.e. $\rho^{xx}(t, \ell) = \rho^{xx}(t, -\ell)$. We therefore will assume from now on that

$$\ell \geq 0. \quad (172)$$

The Lehmann representation for the numerator on the right hand side of eqn (171) is

$$\begin{aligned} \text{R} \langle B(t) | \sigma_{m+\ell}^x \sigma_m^x | B(t) \rangle_{\text{R}} &= \sum_{l, n=0}^{\infty} \frac{i^{n-l}}{n! l!} \sum'_{\substack{0 < k_1, \dots, k_n \in \text{R} \\ 0 < p_1, \dots, p_l \in \text{R}}} \sum_{q_1, \dots, q_r \in \text{NS}} \frac{1}{r!} \left[\prod_{j=1}^n K(k_j) \right] \left[\prod_{i=1}^l K(p_i) \right] \\ &\times e^{-2it[\sum_{j=1}^l \varepsilon_{p_j} - \sum_{s=1}^n \varepsilon_{k_s}]} \text{R} \langle -k_1, k_1, \dots, -k_n, k_n | \sigma_{m+\ell}^x | q_1, \dots, q_r \rangle_{\text{NS}} \\ &\times \text{NS} \langle q_r, \dots, q_1 | \sigma_m^x | p_1, -p_1, \dots, p_l, -p_l \rangle_{\text{R}} \\ &\equiv \sum_{l, n, r=0}^{\infty} D_{(2n|r|2l)}. \end{aligned} \quad (173)$$

Like in the case of the 1-point function we focus on the terms with the strongest possible singularities in the form factors for a given order in the formal expansion in powers of $K(p)$. These are obtained by taking $2n = 2l = r$.

4.3.1. Contributions at $\mathcal{O}(K^0)$. These are equal to the ground state two-point function

$$\text{R} \langle 0 | \sigma_{m+\ell}^x \sigma_m^x | 0 \rangle_{\text{R}}. \quad (174)$$

Using a Lehmann representation to evaluate (174) gives rise to contributions

$$D_{(0|2s|0)} = \sum_{0 < q_1, \dots, q_{2s} \in \text{NS}} \frac{1}{(2s)!} \text{R} \langle 0 | \sigma_{m+\ell}^x | q_1, \dots, q_{2s} \rangle_{\text{NS}} \text{NS} \langle q_{2s}, \dots, q_1 | \sigma_m^x | 0 \rangle_{\text{R}}. \quad (175)$$

For $s = 0$ we have

$$D_{(0|0|0)} = (2m_0^x)^2 = \xi = (1 - h^2)^{1/4}, \quad (176)$$

while for $s = 1$ we obtain

$$D_{(0|2|0)} = \frac{2h^2 J^4 \xi}{\pi^2} \int_{-\pi}^{\pi} dq_1 dq_2 \frac{\sin^2\left(\frac{q_1 - q_2}{2}\right)}{\varepsilon_{q_1} \varepsilon_{q_2} \varepsilon_{q_1, q_2}^2} e^{i\ell(q_1 + q_2)} + \mathcal{O}(L^{-1}) \propto h^{2\ell}. \quad (177)$$

We see that at large ℓ $D_{(0|2|0)}$ is exponentially small compared to $D_{(0|0|0)}$. The contributions $D_{(0|2s|0)}$ with $s > 1$ are suppressed by additional exponential factors. We conclude that for large distances ℓ we only need to retain $D_{(0|0|0)}$.

4.3.2. *Contributions at $\mathcal{O}(K^2)$.* At order $\mathcal{O}(K^2)$ the largest contribution at large distances and late times arises from

$$D_{(2|2|2)} = \sum_{0 < k, p \in \mathbb{R}} \frac{1}{2} \sum_{q_1, q_2 \in \text{NS}} K(k)K(p) e^{-2it[\varepsilon_p - \varepsilon_k]} e^{i\ell(q_1 + q_2)} \text{R} \langle -k, k | \sigma_m^x | q_1, q_2 \rangle_{\text{NS}} \\ \times \text{NS} \langle q_2, q_1 | \sigma_m^x | p, -p \rangle_{\text{R}} \equiv D_{(2|2|2)}^{(1)} + D_{(2|2|2)}^{(2)}, \quad (178)$$

where $D_{(2|2|2)}^{(1,2)}$ denote the contributions arising from terms with $k \neq p$ and $k = p$ respectively. Using (D.4) to carry out the summations over $q_{1,2}$ we arrive at

$$D_{(2|2|2)}^{(1)} = \frac{2\xi}{L^2} \sum_{0 < k \neq p \in \mathbb{R}} e^{-2it[\varepsilon_p - \varepsilon_k]} \frac{(\varepsilon_k + \varepsilon_p)^2}{\varepsilon_k^2 \varepsilon_p^2} \frac{K(k)K(p)}{(\cos k - \cos p)^2} \left[\sin k \sin p \varepsilon_{kp}^2 \right. \\ \left. + \varepsilon_k \varepsilon_p \left[\sin^2 \left(\frac{k-p}{2} \right) \cos(\ell(k+p)) - \sin^2 \left(\frac{k+p}{2} \right) \cos(\ell(k-p)) \right] \right] + \dots \quad (179)$$

We note that in this expression there is no singularity if we consider the limit $k-p \rightarrow 0$. Nevertheless for large ℓ and t the leading contribution to the double sum arises from the vicinity of $k = p$. In order to isolate this contribution we turn the sum over k into an integral using the Euler-Maclaurin sum formula and then deform the integration contour into the upper half plane. As $\varepsilon'_p > 0$ for all $p > 0$ the contribution of the first term in square brackets will be negligible for large t . The same holds true for the second contribution as long as $2\varepsilon'_p t \pm \ell > 0$. On the other hand, if $2\varepsilon'_p t \pm \ell < 0$ we need to deform the contour into the lower half-plane (in the variable k). In doing so acquire a contribution from the double pole at $p = k$. The residue is dominated by the factors involving t and ℓ as both of these are assumed to be large, so that we end up with

$$D_{(2|2|2)}^{(1)} = -\frac{4\xi}{L} \sum_{0 < p \in \mathbb{R}} K^2(p) \theta_H(\ell - 2\varepsilon'_p t) [2\varepsilon'_p t - \ell] + \dots, \quad (180)$$

where $\theta_H(x)$ denotes the Heaviside step function. The second contribution $D_{(2|2|2)}^{(2)}$ is given by

$$D_{(2|2|2)}^{(2)} = \frac{8\xi}{L^4} \sum_{0 < k \in \mathbb{R}} \frac{\sin^2(k) K^2(k)}{\varepsilon^4(k)} \sum_{q_1, q_2 \in \text{NS}} \frac{e^{i\ell(q_1 + q_2)} \sin^2 \left(\frac{q_1 - q_2}{2} \right) \varepsilon_{q_1, k}^4 \varepsilon_{q_2, k}^4}{\varepsilon_{q_1} \varepsilon_{q_2} \varepsilon_{q_1, q_2}^2} c_{kq_1}^2 c_{kq_2}^2. \quad (181)$$

Using (D.6) to carry out the summations over $q_{1,2}$ we arrive at

$$D_{(2|2|2)}^{(2)} = \xi \sum_{0 < k \in \mathbb{R}} K^2(k) \left[1 - \frac{4\ell}{L} \right] + \dots \quad (182)$$

where we again have only retained the leading terms at large L and ℓ . Adding the two contributions (180) and (182) we obtain

$$D_{(2|2|2)}(t, \ell) = \xi \left[\Upsilon_2 - \frac{4}{L} \sum_{0 < k \in \mathbb{R}} K^2(k) (\theta_H(\ell - 2t\varepsilon'_k) [2t\varepsilon'_k - \ell] + \ell) \right] + \dots \\ = \xi \left[\Upsilon_2 - \frac{4}{L} \sum_{k > 0} K^2(k) (2t\varepsilon'_k \theta_H(\ell - 2t\varepsilon'(k)) + \ell \theta_H(2t\varepsilon'_k - \ell)) \right] + \dots \quad (183)$$

This contains a part Υ_2 that diverges in the thermodynamic limit, but which will again be compensated by the denominator in (171).

4.4. Exponentiation of $D_{(2n|2n|2n)}$

The dominant contribution at order $\mathcal{O}(K^{2n})$ is again the ‘‘diagonal’’ one

$$\begin{aligned}
D_{(2n|2n|2n)} &= \frac{\xi}{(n!)^2(2n)!} \frac{1}{L^{4n}} \sum'_{\substack{0 < k_1, \dots, k_n \in \mathbb{R} \\ 0 < p_1, \dots, p_n \in \mathbb{R}}} \prod_{r=1}^n \left[\frac{\sin(k_r)K(k_r)e^{2it\varepsilon_{k_r}}}{\varepsilon_{k_r}^2} \frac{\sin(p_r)K(p_r)e^{-2it\varepsilon_{p_r}}}{\varepsilon_{p_r}^2} \right] \\
&\times \prod_{l < l'}^n \frac{1}{4c_{k_l k_{l'}}^2 \epsilon_{k_l, k_{l'}}^4} \frac{1}{4c_{p_l p_{l'}}^2 \epsilon_{p_l, p_{l'}}^4} \sum_{q_1, \dots, q_{2n} \in \text{NS}} \left[\prod_{r=1}^{2n} \frac{e^{i\ell q_r}}{\varepsilon_{q_r}} \right] \\
&\times \prod_{l < l'}^{2n} \frac{\sin^2\left(\frac{q_l - q_{l'}}{2}\right)}{\varepsilon_{q_l, q_{l'}}^2} \prod_{r=1}^n \prod_{s=1}^{2n} 4\epsilon_{k_r, q_s}^2 \epsilon_{p_r, q_s}^2 c_{k_r, q_s} c_{p_r, q_s}.
\end{aligned} \tag{184}$$

In order to extract the large time and distance behaviour of (184) we need to focus on the regions where the form factors exhibit the strongest singularities. For the case $n = 1$ discussed in subsection 4.3.2 these regions were

- $q_1 \approx \pm k$, $q_2 \approx \mp p$ and $p \approx k$,
- $q_2 \approx \pm k$, $q_1 \approx \mp p$ and $p \approx k$.

(185)

For general n we need to focus on the regions

$$\begin{pmatrix} k_{Q_1} \\ \vdots \\ k_{Q_n} \end{pmatrix} \approx \begin{pmatrix} p_1 \\ \vdots \\ p_n \end{pmatrix}, \quad \begin{pmatrix} q_{S_1} \\ \vdots \\ q_{S_{2n}} \end{pmatrix} \approx \begin{pmatrix} \sigma_1 k_{Q_1} \\ -\sigma_1 p_1 \\ \vdots \\ \sigma_n k_{Q_n} \\ -\sigma_n p_n \end{pmatrix}, \tag{186}$$

where $\sigma_j = \pm$ and (Q_1, \dots, Q_n) , (S_1, \dots, S_{2n}) are permutations of $(1, 2, \dots, n)$ and $(1, 2, \dots, 2n)$ respectively. By symmetry all these regions contribute equally, which gives rise to a combinatorial factor of $n!(2n)!$. We therefore focus on the single region where $(Q_1, \dots, Q_n) = (1, \dots, n)$ and $(S_1, \dots, S_{2n}) = (1, \dots, 2n)$, together with all regions obtained by exchanging any pair $S_{2r-1} \leftrightarrow S_{2r}$. We start by expressing (184) in the form

$$\begin{aligned}
D_{(2n|2n|2n)} &= \frac{1}{L^{4n} n! 2^n} \sum'_{\substack{0 < k_1, \dots, k_n \in \mathbb{R} \\ 0 < p_1, \dots, p_n \in \mathbb{R}}} e^{2it \sum_{l=1}^n (\varepsilon_{k_l} - \varepsilon_{p_l})} \sum_{q_1, \dots, q_{2n} \in \text{NS}} f(k_1, \dots, k_n; p_1, \dots, p_n | q_1, \dots, q_{2n}) \\
&\times \prod_{r=1}^n e^{i(q_{2r-1} + q_{2r})\ell} c_{k_r, q_{2r-1}} c_{k_r, q_{2r}} c_{p_r, q_{2r-1}} c_{p_r, q_{2r}},
\end{aligned} \tag{187}$$

where it is understood that the summation only terms arising from the region we consider are retained. We then carry out the sums over the q_s 's using (D.5) and (D.9). When doing this we need to distinguish the cases $k_r \neq p_r$ and $k_r = p_r$ as they give rise to different kinds of singularities in the q_s summations. For $k_r = p_r$ the summation over both q_{2r-1} and q_{2r} gives a leading contribution

$$\begin{aligned}
&\frac{1}{L^3} \sum_{q_{2r-1}, q_{2r} \in \text{NS}} e^{i(q_{2r-1} + q_{2r})\ell} c_{p_r, q_{2r-1}}^2 c_{p_r, q_{2r}}^2 f(k_1, \dots, k_n; p_1, \dots, p_n | q_1, \dots, q_{2n}) \Big|_{p_r = k_r} \\
&= \frac{L}{16} \left(1 - \frac{2\ell}{L}\right)^2 \frac{\tilde{f}(p_r, -p_r) + \tilde{f}(-p_r, p_r)}{\sin^4(p_r)} \Big|_{k_r = p_r} + \dots,
\end{aligned} \tag{188}$$

where we have defined

$$\tilde{f}(p, q) = f(k_1, \dots, k_n; p_1, \dots, p_n | q_1, \dots, q_{2r-2}, p, q, q_{2r+1}, \dots, q_{2n}). \quad (189)$$

The extra factor $1/L$ in (188) is present as we are considering a single term in the sum over k_r . On the other hand, for $p_r \neq k_r$ we obtain

$$\begin{aligned} & \frac{1}{L^3} \sum_{0 < k_r \in \mathbb{R}} e^{2it[\varepsilon_{k_r} - \varepsilon_{p_r}]} \sum_{q_{2r-1}, q_{2r} \in \text{NS}} e^{i(q_{2r-1} + q_{2r})\ell} c_{k_r, q_{2r-1}} c_{k_r, q_{2r}} c_{p_r, q_{2r-1}} c_{p_r, q_{2r}} \\ & \quad \times f(k_1, \dots, k_n; p_1, \dots, p_n | q_1, \dots, q_{2n}) \\ = & \frac{1}{L} \sum_{0 < k_r \in \mathbb{R}} e^{2it[\varepsilon_{k_r} - \varepsilon_{p_r}]} c_{p_r, k_r}^2 \left\{ - \frac{e^{-i\ell(p_r - k_r)} \tilde{f}(-p_r, k_r) + e^{i\ell(p_r - k_r)} \tilde{f}(p_r, -k_r)}{4 \sin k_r \sin p_r} \right. \\ & \quad \left. + \frac{\tilde{f}(p_r, -p_r) + \tilde{f}(-p_r, p_r)}{4 \sin^4(p_r)} + p_r \leftrightarrow k_r \right\} + \dots \end{aligned} \quad (190)$$

Similarly to our treatment of the $n = 1$ case in subsection 4.3.2 we can now carry out the summation over k_r with the result

$$- \theta_H(\ell - 2t\varepsilon'_{p_r}) [2t\varepsilon'_{p_r} - \ell] \left. \frac{\tilde{f}(p_r, -p_r) + \tilde{f}(-p_r, p_r)}{4 \sin^4(p_r)} \right|_{k_r = p_r} + \dots \quad (191)$$

Combining the two contributions (188) and (191) we find that the leading terms at large ℓ and t are

$$\left[\frac{L}{4} - \ell - \theta_H(\ell - 2t\varepsilon'_{p_r}) [2t\varepsilon'_{p_r} - \ell] \right] \left. \frac{\tilde{f}(p_r, -p_r) + \tilde{f}(-p_r, p_r)}{4 \sin^4(p_r)} \right|_{k_r = p_r} + \dots \quad (192)$$

Carrying out all q_s and k_l summations in the same way gives

$$\begin{aligned} D_{(2n|2n|2n)} &= \frac{\xi}{n! 2^n L^n} \sum'_{0 < p_1, \dots, p_n \in \mathbb{R}} \prod_{r=1}^n [L - 4\ell - 4\theta_H(\ell - 2t\varepsilon'_{p_r}) [2t\varepsilon'_{p_r} - \ell]] \frac{1}{16 \sin^4(p_r)} \\ & \quad \times \sum_{\sigma_1, \dots, \sigma_n = \pm} f(p_1, \dots, p_n; p_1, \dots, p_n | \sigma_1 p_1, -\sigma_1 p_1, \dots, \sigma_n p_n, -\sigma_n p_n) + \dots \\ &= \frac{\xi}{n!} \sum'_{0 < p_1, \dots, p_n \in \mathbb{R}} \prod_{r=1}^n K^2(p_r) \left[1 - \frac{4\ell}{L} - \frac{4}{L} \theta_H(\ell - 2t\varepsilon'_{p_r}) [2t\varepsilon'_{p_r} - \ell] \right] + \dots \end{aligned} \quad (193)$$

Like for the 1-point function the sum over n can be taken by inverting the steps used to express (120) in terms of (125), which gives

$$\begin{aligned} \sum_{n=0}^{\infty} D_{(2n|2n|2n)} &= \xi \exp \left(\sum_{0 < p \in \mathbb{R}} \ln \left[1 + K^2(p) \left(1 - \frac{4}{L} (\ell + \theta_H(\ell - 2t\varepsilon'_p) [2t\varepsilon'_p - \ell]) \right) \right] \right) + \dots \\ &\simeq \xi_{\text{NS}} \langle B|B \rangle_{\text{NS}} \exp \left[- \frac{4}{L} \sum_{0 < p \in \mathbb{R}} K^2(p) (\ell + \theta_H(\ell - 2t\varepsilon'_p) [2t\varepsilon'_p - \ell]) \right] + \dots \end{aligned} \quad (194)$$

Here we have retained only the $\mathcal{O}(K^2)$ term in the exponent as the higher orders are beyond the accuracy of our calculation. This then gives the desired result for the two-point function (171) in the ordered phase

$$\lim_{L \rightarrow \infty} \rho^{xx}(t, \ell) \simeq (1 - h^2)^{\frac{1}{4}} \exp \left[- 2 \int_0^\pi \frac{dp}{\pi} K^2(p) (\ell + \theta_H(\ell - 2t\varepsilon'_p) [2t\varepsilon'_p - \ell]) \right] + \dots \quad (195)$$

Eqn (195), including the prefactor, is expected to be accurate at late times and large distances as long as we do not quench too close to the critical point.

4.5. Two-Point Function for Quenches in the Disordered Phase $h_0, h > 1$

As a consequence of the \mathbb{Z}_2 symmetry the 1-point function of σ_ℓ^x is identically zero for quenches within the disordered phase, i.e. $h_0, h > 1$. We therefore turn to the two-point function. As shown in Appendix A the ground state in the paramagnetic phase is the NS vacuum $|0; h_0\rangle_{\text{NS}}$. Hence the 2-point function after the quench is equal to

$$\rho^{xx}(t, \ell) = \frac{\text{NS}\langle B(t) | \sigma_{m+\ell}^x \sigma_m^x | B(t) \rangle_{\text{NS}}}{\text{NS}\langle B | B \rangle_{\text{NS}}}. \quad (196)$$

In the basis underlying the expression (109) for the form factors, the boundary states are again given by (115), but now the function $K(k)$ is given by

$$K(k) = -\frac{\sin(k) (h - h_0)}{\varepsilon_{h_0}(k) \varepsilon_h(k) (2J)^{-2} + 1 + hh_0 - (h + h_0) \cos(k)}. \quad (197)$$

The Lehmann representation of the numerator is again given (173) if we replace $\text{R} \rightarrow \text{NS}$. The difference to the ordered phase is that now only form factors with *odd* numbers r of particles in the intermediate states are non-vanishing.

4.5.1. Order $\mathcal{O}(K^0)$ Contributions. The $\mathcal{O}(K^0)$ contribution obtained upon expanding the boundary states in powers of K is

$$\text{NS}\langle 0 | \sigma_{m+\ell}^x(t) \sigma_m^x(t) | 0 \rangle_{\text{NS}} = \text{NS}\langle 0 | \sigma_{m+\ell}^x \sigma_m^x | 0 \rangle_{\text{NS}}. \quad (198)$$

This is equal to the static zero temperature correlator in equilibrium. Inserting a resolution of the identity we conclude that the large- ℓ behaviour in the $L \rightarrow \infty$ limit is determined by one-particle intermediate states

$$D_{(0|1|0)}(t, \ell) = \xi \sqrt{4J^2 h} \frac{1}{L} \sum_{q \in \mathbb{R}} \frac{e^{iq|\ell|}}{\varepsilon_q} = 2J\mathcal{A} \int_{-\pi}^{\pi} \frac{dq}{2\pi} \frac{e^{iq\ell}}{\varepsilon_q} + \mathcal{O}(L^{-1}) \quad (199)$$

where we have defined

$$\mathcal{A} = \xi \sqrt{h}. \quad (200)$$

The integral can be carried out approximately by bending the contour around the branch cut of the energy in the upper half plane, which gives

$$D_{(0|1|0)} \approx \xi \sqrt{\frac{h}{\pi(h^2 - 1)}} \frac{h^{-|\ell|}}{\sqrt{\ell}} \equiv \mathcal{D}(\ell). \quad (201)$$

We conclude that the leading contribution in $K(q)$ is exponentially small, which means that we need to evaluate all subleading terms with the same exponential accuracy as well. The contributions due to 3, 5, ... particle intermediate states are small for large ℓ when compared to (201)

$$D_{(0|2s+1|0)} \propto h^{-(2s+1)|\ell|}, \quad (202)$$

and can hence be ignored for our purposes.

4.5.2. $\mathcal{O}(K)$ Contributions. The leading contributions to order K are obtained by taking single-particle intermediate states into account only. This gives

$$D_{(2|1|0)} + D_{(0|1|2)} = \frac{4J\mathcal{A}}{L} \sum_k \frac{K(k)}{\varepsilon_k} \sin(2t\varepsilon_k - k\ell) + \dots \quad (203)$$

The corrections to the rhs of (203) can be evaluated using contour techniques but are negligible at large distances. As a function of t for fixed n $D_{(2|1|0)} + D_{(0|1|2)}$ displays oscillatory behaviour on top of a slow $t^{-3/2}$ power-law decay in time. This can be seen by turning the sum in (203) into an integral and evaluating the latter by means of a saddle-point approximation, which gives

$$D_{(2|1|0)} + D_{(0|1|2)} \simeq \frac{2J\mathcal{A}}{\sqrt{\pi}} \sum_{a=\pm} \frac{K(k_a)}{\varepsilon_{k_a}} \text{Im} \left[\frac{e^{2it\varepsilon_{k_a} - ik_a\ell}}{\sqrt{-i\varepsilon_{k_a}'' t}} \right], \quad (204)$$

where

$$k_{\pm} = \arccos \left[\frac{x^2 \pm \sqrt{x^4 - x^2(1+h^2) + h^2}}{h} \right], \quad x = \frac{\ell}{4Jt}. \quad (205)$$

In the limit $\ell/t \rightarrow 0$ this can be simplified further

$$\begin{aligned} D_{(2|1|0)} + D_{(0|1|2)} \simeq & -\frac{\ell}{(2Jt)^{3/2}} \left[\frac{h+1}{h-1} \right]^{1/4} \frac{h-h_0}{4h(h_0-1)\sqrt{\pi}} \sin \left(4Jt(h-1) + \frac{\pi}{4} - \frac{h-1}{4hJ} \frac{\ell^2}{t} \right) \\ & - \frac{\ell}{(2Jt)^{3/2}} \left[\frac{h-1}{h+1} \right]^{1/4} \frac{h-h_0}{4h(h_0+1)\sqrt{\pi}} \sin \left(4Jt(h+1) - \frac{\pi}{4} + \frac{h+1}{4hJ} \frac{\ell^2}{t} \right). \end{aligned} \quad (206)$$

4.5.3. $\mathcal{O}(K^2)$ contributions. The next contributions we need to consider are second order in $K(k)$ and arise from

$$\sum_{0 < k, p \in \text{NS}} K(k)K(p)_{\text{NS}} \langle -k, k | \sigma_{m+\ell}^x(t) \sigma_m^x(t) | p, -p \rangle_{\text{NS}}. \quad (207)$$

Inserting a resolution of the identity between the spin operators we see that for large ℓ and t the dominant contributions are generated by 1-particle and 3-particle intermediate states. The former is given by

$$\begin{aligned} D_{(2|1|2)} = & \sum_{k, p > 0} \sum_q K(k)K(p)_{\text{NS}} \langle -k, k | \sigma_{m+\ell}^x(t) | q \rangle_{\text{R}} \\ & \times {}_{\text{R}} \langle q | \sigma_m^x(t) | p, -p \rangle_{\text{NS}}. \end{aligned} \quad (208)$$

Like in our analysis of the 2-point function for quenches within the ordered phase we again have to consider the two cases $k \neq p$ and $k = p$ separately. Denoting the corresponding contributions by $D_{(2|1|2)}^{(1)}$ and $D_{(2|1|2)}^{(2)}$ respectively, we find in the limit of large ℓ , t and $L \rightarrow \infty$

$$D_{(2|1|2)}^{(2)} = \frac{2J\mathcal{A}}{L} \sum_{k \in \text{NS}} K^2(k) \frac{e^{ik|\ell|}}{\varepsilon_k} + \dots, \quad (209)$$

$$\begin{aligned} D_{(2|1|2)}^{(1)} = & \frac{8J\mathcal{A}}{L^2} \sum_{0 < k \neq p \in \text{NS}} \frac{K(k)K(p)}{\varepsilon_k^2 \varepsilon_p^2} \epsilon_{k,p}^2 \frac{\sin(k) \sin(p)}{\cos(k) - \cos(p)} \left[\frac{\varepsilon_k \sin(k\ell)}{\sin(k)} - \frac{\varepsilon_p \sin(p\ell)}{\sin(p)} \right] e^{2it[\varepsilon_k - \varepsilon_p]} \\ & + \dots \end{aligned} \quad (210)$$

In the thermodynamic limit (210) can be written as a double integral, but we have not succeeded in simplifying it in a useful way. The contribution $D_{(2|1|2)}^{(2)}$ is time independent and exponentially small in ℓ . In contrast to this, $D_{(2|1|2)}^{(1)}$ displays power-law decay in t for fixed ℓ

$$D_{(2|1|2)}^{(1)} \propto t^{-3}. \quad (211)$$

We now turn to the $\mathcal{O}(K^2)$ contribution involving 3-particle intermediate states

$$D_{(2|3|2)} = \frac{1}{6} \sum_{0 < k, p \in \text{NS}} \sum_{q_1, q_2, q_3 \in \text{R}} K(k)K(p) \text{NS} \langle -k, k | \sigma_{m+\ell}^x(t) | q_1, q_2, q_3 \rangle_{\text{R}} \\ \times \text{R} \langle q_3, q_2, q_1 | \sigma_m^x(t) | p, -p \rangle_{\text{NS}}. \quad (212)$$

We denote the contributions from $k \neq p$ and $k = p$ by $D_{(2|3|2)}^{(1)}$ and $D_{(2|3|2)}^{(2)}$ respectively. After some lengthy calculations we find

$$D_{(2|3|2)}^{(2)} = D_{(0|1|0)} \sum_{0 < k \in \text{NS}} K^2(k) \left[1 - \frac{4\ell}{L} \right] \\ + \frac{4J\mathcal{A}}{L} \sum_{0 < k \in \text{NS}} \frac{K^2(k)}{\varepsilon_k} \cos(\ell k) - 4(h^2 - 1)\mathcal{D}(\ell) \frac{1}{L} \sum_{0 < k \in \text{NS}} \frac{4J^2 K^2(k)}{\varepsilon_k^2} + \dots \quad (213)$$

This is time independent and contains a piece that diverges with the volume as expected.

The contribution $D_{(2|3|2)}^{(1)}$ is given by

$$D_{(2|3|2)}^{(1)} = \frac{2J\mathcal{A}}{L^5} \sum_{0 < k \neq p \in \text{NS}} K(k)K(p) \frac{\sin(k) \sin(p)}{\varepsilon_k^2 \varepsilon_p^2} \cos(2t[\varepsilon_k - \varepsilon_p]) \\ \times \frac{1}{6} \sum_{q_1, q_2, q_3 \in \text{R}} \left[\prod_{j < l} \frac{\sin^2(\frac{q_j - q_l}{2})}{\varepsilon_{q_j, q_l}^2} \right] \left[\prod_{m=1}^3 \frac{\varepsilon_{k, q_m}^2 \varepsilon_{p, q_m}^2 e^{iq_m n}}{\varepsilon_{q_m}} 4c_{q_m k} c_{q_m p} \right]. \quad (214)$$

Carrying out the sums over q_j using the same techniques as for the other contributions we eventually arrive at

$$D_{(2|3|2)}^{(1)} = \frac{8J\mathcal{A}}{L^2} \sum_{0 < k \neq p \in \text{NS}} \frac{K(k)K(p)}{\varepsilon_k^2 \varepsilon_p^2} \varepsilon_{k,p}^2 \frac{\sin(k) \sin(p)}{\cos(k) - \cos(p)} \left[\frac{\varepsilon_k \sin(k\ell)}{\sin(k)} - \frac{\varepsilon_p \sin(p\ell)}{\sin(p)} \right] e^{2it[\varepsilon_k - \varepsilon_p]} \\ + \dots \quad (215)$$

The large time and distance behaviour is thus the same as for $D_{(2|1|2)}$.

In summary, the combined $\mathcal{O}(K^2)$ contributions can be divided into two categories:

(i) Time-independent contributions

$$4J\mathcal{A} \int_{-\pi}^{\pi} \frac{dk}{2\pi} \frac{K^2(k)}{\varepsilon_k} e^{ik\ell} + D_{(0|1|0)} \left[\Upsilon_2 - 4\ell \int_0^{\pi} \frac{dk}{2\pi} K^2(k) \right] \\ - 4(h^2 - 1)\mathcal{D}(\ell) \int_0^{\pi} \frac{dk}{2\pi} \frac{4J^2 K^2(k)}{\varepsilon^2(k)}. \quad (216)$$

(ii) Time-dependent oscillatory contributions

$$4J\mathcal{A} \int_0^{\pi} \frac{dk dp}{\pi^2} \frac{K(k)K(p)}{\varepsilon^2(k)\varepsilon^2(p)} \varepsilon_{k,p}^2 \frac{\sin(k) \sin(p)}{\cos(k) - \cos(p)} \left[\frac{\varepsilon_k \sin(k\ell)}{\sin(k)} - \frac{\varepsilon_p \sin(p\ell)}{\sin(p)} \right] e^{2it[\varepsilon_k - \varepsilon_p]}. \quad (217)$$

4.5.4. $\mathcal{O}(K^3)$ contributions. In order to infer the structure of higher-order oscillatory contributions we determine the following $\mathcal{O}(K^3)$ term

$$D_{(4|3|2)} + D_{(2|3|4)} = \frac{J\mathcal{A}}{3L^6} \text{Re} \sum_{\substack{0 < k_{1,2}, p \in \text{NS} \\ q_{1,2,3} \in \mathbb{R}}} K(k_1)K(k_2)K(p) \frac{\sin k_1 \sin k_2 \sin p}{\varepsilon_{k_1}^2 \varepsilon_{k_2}^2 \varepsilon_p^2} g_{k_1, k_2}^2 g_{k_1, -k_2}^2 \\ \times \frac{g_{q_1, q_2}^2 g_{q_1, q_3}^2 g_{q_2, q_3}^2}{\varepsilon_{q_1} \varepsilon_{q_2} \varepsilon_{q_3}} e^{2it[\varepsilon_{k_1} + \varepsilon_{k_2} - \varepsilon_p]} \prod_{j=1}^3 2\varepsilon_{p, q_j}^2 c_{p q_j} e^{i\ell q_j} \prod_{l=1}^2 2\varepsilon_{k_l, q_j}^2 c_{k_l q_j}, \quad (218)$$

where we have defined

$$g_{p, k} = \frac{2 \sin\left(\frac{p-k}{2}\right)}{\varepsilon_p + \varepsilon_k}. \quad (219)$$

(i) Contributions for $p \neq k_{1,2}$. We first consider only the contributions with $p \neq k_{1,2}$ and denote them by $D_{(4|3|2)}^{(1)} + D_{(2|3|4)}^{(1)}$. In order to carry out the sums over q_j it is useful to rewrite the product of pole factors $\prod_{l=1}^3 \prod_{j=1}^3 2c_{k_l q_j}$ using the identity

$$c_{k_1 q} c_{k_2 q} c_{p q} = c_{k_2 k_1} \left\{ c_{p k_1} [c_{k_1 q} - c_{p q}] - c_{p k_2} [c_{k_2 q} - c_{p q}] \right\}. \quad (220)$$

The fully decomposed expression reads

$$\prod_{j=1}^3 8c_{k_1 q_j} c_{k_2 q_j} c_{p q_j} = [8c_{k_2 k_1}]^3 \left\{ -c_{p k_1}^3 \left[\frac{1}{2} \tilde{\mathcal{C}}_{k_1, k_1, p} - \mathcal{C}_{k_1, k_1, k_1} - \frac{1}{2} \tilde{\mathcal{C}}_{p, p, k_1} + \mathcal{C}_{p, p, p} \right] \right. \\ \left. + c_{p k_1}^2 c_{p k_2} \left[\tilde{\mathcal{C}}_{k_1, k_2, p} - \tilde{\mathcal{C}}_{k_1, p, p} + 3\mathcal{C}_{p, p, p} - \frac{1}{2} \tilde{\mathcal{C}}_{p, p, k_2} + \frac{1}{2} \tilde{\mathcal{C}}_{k_1, p, k_1} - \frac{1}{2} \tilde{\mathcal{C}}_{k_1, k_1, k_2} \right] - \{k_1 \leftrightarrow k_2\} \right\}, \quad (221)$$

where we have defined

$$\mathcal{C}_{k_1, k_2, k_3} = \prod_{j=1}^3 c_{k_j, q_j}, \quad \tilde{\mathcal{C}}_{k_1, k_2, k_3} = \sum_{P \in S_3} \mathcal{C}_{k_{P_1}, k_{P_2}, k_{P_3}}. \quad (222)$$

We then can carry out the sums over q_j using Lemma 4 (D.6) and retaining only the pole contributions.

A. The combined contributions to (218) arising from $c_{p k_1}^3 \tilde{\mathcal{C}}_{k_1, k_1, p}$, $c_{p k_2}^3 \tilde{\mathcal{C}}_{k_2, k_2, p}$, $c_{p k_1}^2 c_{p k_2} \tilde{\mathcal{C}}_{k_1, p, k_1}$ and $c_{p k_2}^2 c_{p k_1} \tilde{\mathcal{C}}_{k_2, p, k_2}$ in the decomposition (221) are of the form

$$D_{(4|3|2)}^{(1,1)} + D_{(2|3|4)}^{(1,1)} = \frac{16J\mathcal{A}}{L^3} \sum_{0 < k_{1,2} \neq p \in \text{NS}} K(k_1)K(k_2)K(p) e^{2it[\varepsilon(k_1) + \varepsilon(k_2) - \varepsilon_p]} \\ \times \frac{\varepsilon_{k_1, p}^2 \varepsilon_{k_2, p}^2 c_{k_2 k_1}}{\varepsilon_{k_1}^2 \varepsilon_{k_2}^2 \varepsilon_p} [c_{p k_1} - c_{p k_2}] \sin(\ell p) + \text{h.c.} + \dots \quad (223)$$

B. The contributions due to $c_{p k_1}^3 \tilde{\mathcal{C}}_{p, p, k_1}$ and $c_{p k_2}^3 \tilde{\mathcal{C}}_{p, p, k_2}$ in (221) are

$$D_{(4|3|2)}^{(1,2)} + D_{(2|3|4)}^{(1,2)} = -\frac{8J\mathcal{A}}{L^3} \sum_{0 < k_{1,2} \neq p \in \text{NS}} \frac{K(k_1)K(k_2)K(p)}{\varepsilon_{k_1}^2 \varepsilon_{k_2}^2 \varepsilon_p^2} e^{2it[\varepsilon(k_1) + \varepsilon(k_2) - \varepsilon_p]} \frac{\varepsilon_{k_1, p}^2 \varepsilon_{k_2, p}^2}{\varepsilon_{k_1, k_2}^2} c_{k_2 k_1} \\ \times \sin p \left[\sin(\ell k_1) \sin k_2 \varepsilon_{k_1} \varepsilon_{k_2, p}^2 c_{p k_1} - \{k_1 \leftrightarrow k_2\} \right] + \text{h.c.} + \dots \quad (224)$$

C. The contributions of the $c_{pk_1}^2 c_{pk_2} \tilde{C}_{p,p,k_1}$ and $c_{pk_1} c_{pk_2}^2 \tilde{C}_{p,p,k_2}$ terms are

$$D_{(4|3|2)}^{(1,3)} + D_{(2|3|4)}^{(1,3)} = \frac{16J\mathcal{A}}{L^3} \sum_{0 < k_{1,2} \neq p \in \text{NS}} \frac{K(k_1)K(k_2)K(p)}{\varepsilon_{k_1} \varepsilon_{k_2} \varepsilon_p^2} e^{2it[\varepsilon(k_1) + \varepsilon(k_2) - \varepsilon_p]} \frac{\epsilon_{k_1,p}^2 \epsilon_{k_2,p}^2}{\epsilon_{k_1,k_2}^2} \\ \times c_{k_2 k_1} \sin p \left[\sin(\ell k_1) \sin k_2 \frac{\epsilon_{k_2,p}^2}{\varepsilon_{k_2}} c_{pk_2} - \{k_1 \leftrightarrow k_2\} \right] + \text{h.c.} + \dots \quad (225)$$

D. The contributions of the $c_{pk_1}^2 c_{pk_2} \tilde{C}_{p,p,k_2}$ and $c_{pk_1} c_{pk_2}^2 \tilde{C}_{p,p,k_1}$ terms are

$$D_{(4|3|2)}^{(1,4)} + D_{(2|3|4)}^{(1,4)} = -\frac{8J\mathcal{A}}{L^3} \sum_{0 < k_{1,2} \neq p \in \text{NS}} \frac{K(k_1)K(k_2)K(p)}{\varepsilon_{k_1} \varepsilon_{k_2} \varepsilon_p^2} e^{2it[\varepsilon(k_1) + \varepsilon(k_2) - \varepsilon_p]} \frac{\epsilon_{k_1,p}^2 \epsilon_{k_2,p}^2}{\epsilon_{k_1,k_2}^2} \\ \times c_{k_2 k_1} \sin p \left[\sin(\ell k_1) \sin k_2 \frac{\epsilon_{k_2,p}^2}{\varepsilon_{k_2}} \frac{c_{pk_2}^2}{c_{pk_1}} - \{k_1 \leftrightarrow k_2\} \right] + \text{h.c.} + \dots \quad (226)$$

E. The contributions of the $c_{pk_1}^2 c_{pk_2} \tilde{C}_{k_1,k_1,k_2}$ and $c_{pk_1} c_{pk_2}^2 \tilde{C}_{k_2,k_2,k_1}$ terms are

$$D_{(4|3|2)}^{(1,5)} + D_{(2|3|4)}^{(1,5)} = \frac{8J\mathcal{A}}{L^3} \sum_{0 < k_{1,2} \neq p \in \text{NS}} \frac{K(k_1)K(k_2)K(p)}{\varepsilon_{k_1} \varepsilon_{k_2} \varepsilon_p^2} e^{2it[\varepsilon(k_1) + \varepsilon(k_2) - \varepsilon_p]} \frac{\epsilon_{k_1,p}^2 \epsilon_{k_2,p}^2}{\epsilon_{k_1,k_2}^2} \\ \times \frac{c_{pk_1} c_{pk_2}}{c_{k_1 k_2}} \sin p \left[\sin(\ell k_2) \sin k_1 \frac{\epsilon_{k_1,p}^2}{\varepsilon_{k_1}} c_{pk_1} - \{k_1 \leftrightarrow k_2\} \right] + \text{h.c.} + \dots \quad (227)$$

F. Finally, the contributions of the $c_{pk_1}^2 c_{pk_2} \tilde{C}_{k_1,k_2,p}$ and $c_{pk_2}^2 c_{pk_1} \tilde{C}_{k_2,k_1,p}$ terms are

$$D_{(4|3|2)}^{(1,6)} + D_{(2|3|4)}^{(1,6)} = -\frac{32J\mathcal{A}}{L^3} \sum_{k_{1,2} \neq p \in \text{NS}} \frac{K(k_1)K(k_2)K(p)}{\varepsilon_{k_1} \varepsilon_{k_2} \varepsilon_p} \cos(2t[\varepsilon_{k_1} + \varepsilon_{k_2} - \varepsilon_p]) \\ \times \epsilon_{k_1,p}^4 \epsilon_{k_2,p}^4 c_{k_1 p}^2 c_{k_2 p}^2 g_{k_1,k_2}^2 g_{k_1,p}^2 g_{k_2,p}^2 \sin(\ell(k_1 + k_2 + p)), \quad (228)$$

where here the momentum sums are over the entire Brillouin zone.

The contributions from all other terms are subleading. We observe that the leading terms at large ℓ and t in (224),(225),(226) and (227) combine to

$$\sum_{a=2}^5 D_{(4|3|2)}^{(1,a)} + D_{(2|3|4)}^{(1,a)} \sim -\frac{64J\mathcal{A}}{L^3} \sum_{0 < k_{1,2} \neq p \in \text{NS}} \frac{K(k_1)K(k_2)K(p)}{\varepsilon_{k_1} \varepsilon_{k_2} \varepsilon_p^2} \cos(2t[\varepsilon_{k_1} + \varepsilon_{k_2} - \varepsilon_p]) \\ \times \frac{\epsilon_{k_1,p}^2 \epsilon_{k_2,p}^4}{\epsilon_{k_1,k_2}^2} \sin k_2 \sin p c_{pk_2} [c_{pk_2} - c_{pk_1}] \sin(\ell k_1) + \dots \quad (229)$$

Both (229) and (228) can be simplified further, because for large t and ℓ the dominant contributions arise from the ‘‘double pole’’ factors and can be extracted using Lemmas 2a and 2b of Appendix D. This leaves us with

$$D_{(4|3|2)}^{(1,6)} + D_{(2|3|4)}^{(1,6)} = -\frac{16J\mathcal{A}}{L^2} \sum_{0 < p \in \text{NS}} \sum_{k \in \text{NS}} \frac{K(k)}{\varepsilon_k} \sin(2t\varepsilon_k - \ell k) K^2(p) \\ \times \left[\frac{L}{6} - [\ell + (2t\varepsilon'_p - \ell)\theta_H(2t\varepsilon'_p - \ell)] \right] + \dots, \quad (230)$$

$$\sum_{a=2}^5 D_{(4|3|2)}^{(1,a)} + D_{(2|3|4)}^{(1,a)} = \frac{16JA}{L^2} \sum_{0 < p \in \text{NS}} \sum_{k \in \text{NS}} \frac{K(k)}{\varepsilon_k} \sin(2t\varepsilon_k - \ell k) K^2(p) \left[\frac{L}{6} - 2t\varepsilon'_p \right] + \dots \quad (231)$$

Combining (230) and (231) we arrive at our final result for the leading asymptotics of the $p \neq k_{1,2}$ contributions to (218)

$$\begin{aligned} D_{(4|3|2)}^{(1)} + D_{(2|3|4)}^{(1)} &= \left[\frac{4JA}{L} \sum_{k \in \text{NS}} \frac{K(k)}{\varepsilon_k} \sin(2t\varepsilon_k - \ell k) \right] \left[-\frac{4}{L} \sum_{0 < p \in \text{NS}} K^2(p) [2t\varepsilon'_p - \ell] \theta_H(\ell - 2t\varepsilon'_p) \right] \\ &\quad + \dots \\ &= [D_{(2|1|0)} + D_{(0|1|2)}] \left[-\frac{4}{L} \sum_{0 < p \in \text{NS}} K^2(p) [2t\varepsilon'_p - \ell] \theta_H(\ell - 2t\varepsilon'_p) \right] + \dots \quad (232) \end{aligned}$$

(ii) *Contributions with $p = k_1$ or $p = k_2$.* Using the symmetry under $k_1 \leftrightarrow k_2$ we can express these contributions in the form

$$\begin{aligned} D_{(2|3|4)}^{(2)} + D_{(4|3|2)}^{(2)} &= -\frac{i}{6} \sum_{0 < k_{1,2} \in \text{NS}} \sum_{q_{1,2,3} \in \text{R}} K^2(k_1) K(k_2) e^{2it\varepsilon(k_2)} \\ &\quad \times {}_{\text{NS}} \langle -k_1, k_1, -k_2, k_2 | \sigma_{m+\ell}^x | q_1, q_2, q_3 \rangle_{\text{R}} {}_{\text{R}} \langle q_3, q_2, q_1 | \sigma_m^x | k_1, -k_1 \rangle_{\text{NS}} + \text{h.c.} \quad (233) \end{aligned}$$

In order to carry out the q_j sums we rewrite the pole factors as

$$\begin{aligned} \prod_{j=1}^3 8c_{k_1 q_j}^2 c_{k_2 q_j} &= (8c_{k_2 k_1})^3 \left\{ \mathcal{C}^2(k_1, k_1, k_1) - c_{k_2 k_1} b(k_1, k_2 | q_1) c_{k_1 q_2}^2 c_{k_1 q_3}^2 - c_{k_2 k_1} c_{k_1 q_1}^2 b(k_1, k_2 | q_2) c_{k_1 q_3}^2 \right. \\ &\quad - c_{k_2 k_1} c_{k_1 q_1}^2 c_{k_1 q_2}^2 b(k_1, k_2 | q_3) + c_{k_1 k_2}^2 c_{k_1 q_1}^2 b(k_1, k_2 | q_2) b(k_1, k_2 | q_3) \\ &\quad + c_{k_1 k_2}^2 c_{k_1 q_2}^2 b(k_1, k_2 | q_1) b(k_1, k_2 | q_3) + c_{k_1 k_2}^2 c_{k_1 q_3}^2 b(k_1, k_2 | q_1) b(k_1, k_2 | q_2) \\ &\quad \left. - c_{k_2 k_1}^3 b(k_1, k_2 | q_1) b(k_1, k_2 | q_2) b(k_1, k_2 | q_3) \right\}, \quad (234) \end{aligned}$$

where we have defined

$$b(k_1, k_2 | q) = c_{k_1 q} - c_{k_2 q}. \quad (235)$$

The various terms in (234) contribute in qualitatively different ways, depending on their structure when viewed as functions of (the complex variables) q_1, q_2 and q_3 .

1. *Terms with only simple poles* give rise to contributions of order $\mathcal{O}(L^{-1})$ and can be ignored.
2. *Terms with only double poles* arise from the first contribution on the r.h.s. of (234). Using (D.6) to carry out the sums over q_j we obtain after some calculations

$$\begin{aligned} D_{(4|3|2)}^{(2,1)} + D_{(2|3|4)}^{(2,1)} &= \frac{1}{L} \left[1 - \frac{4\ell}{L} \right] \mathcal{D}(\ell) \sum_{0 < k_{1,2} \in \text{NS}} K^2(k_1) K(k_2) \cos(2t\varepsilon_{k_2}) c_{k_2, k_1} \\ &\quad + \frac{4JA}{L} \sum_{k \in \text{NS}} \frac{K^3(k)}{\varepsilon_k} \sin(2t\varepsilon_k - \ell k) + \dots, \quad (236) \end{aligned}$$

which can be simplified further if required.

3. *Terms with only one double pole* arise from the fifth, sixth and seventh contributions on the r.h.s. of (234). Using (D.6) and (D.4) to carry out the sums over q_j we obtain after some calculations

$$D_{(4|3|2)}^{(2,2)} + D_{(2|3|4)}^{(2,2)} = \frac{16J\mathcal{A}}{L^2} \sum_{0 < k_1 \neq k_2 \in \text{NS}} K^2(k_1)K(k_2) \cos(2t\varepsilon_{k_2}) \sin(k_2) \cos(k_1\ell) \\ \times c_{k_2 k_1} \frac{\varepsilon_{k_1, k_2}^2}{\varepsilon_{k_1} \varepsilon_{k_2}^2} + \dots \quad (237)$$

Here we can carry out the k_1 sum using Lemma 3 D.4, which gives

$$D_{(4|3|2)}^{(2,2)} + D_{(2|3|4)}^{(2,2)} = \frac{4J\mathcal{A}}{L} \sum_{k \in \text{NS}} \frac{K^3(k)}{\varepsilon_k} \sin(2t\varepsilon_k - \ell k) + \dots \quad (238)$$

4. *Terms with two double poles* arise from the second, third and fourth contributions on the r.h.s. of (234). Using (D.6) and (D.4) to carry out the sums over q_j we obtain after some calculations

$$D_{(4|3|2)}^{(2,3)} + D_{(2|3|4)}^{(2,3)} = \left[\frac{4J\mathcal{A}}{L} \sum_{k_2 \in \text{NS}} \frac{K(k_2)}{\varepsilon_{k_2}} \sin(2t\varepsilon(k_2) - \ell k_2) \right] \sum_{0 < k_1 \in \text{NS}} K^2(k_1) \left[1 - \frac{4\ell}{L} \right] + \dots \quad (239)$$

This is in fact the leading contribution.

Combining (232) and (239) we arrive at the following result for our $\mathcal{O}(K^3)$ contributions

$$D_{(4|3|2)} + D_{(2|3|4)} = [D_{(2|1|0)} + D_{(0|1|2)}] \frac{4}{L} \sum_{0 < p \in \text{NS}} K^2(p) \left[\frac{L}{4} - \ell - [2t\varepsilon'(p) - \ell] \theta_H(\ell - 2t\varepsilon'(p)) \right] \\ + \frac{8J\mathcal{A}}{L} \sum_{k \in \text{NS}} \frac{K^3(k)}{\varepsilon_k} \sin(2t\varepsilon_k - \ell k) + \dots \quad (240)$$

We see that as expected there is a contribution that diverges in the thermodynamic limit. However, in addition there are terms that become very large for $\ell \gg 1$

4.5.5. Resummation of Leading $D_{(2n+2|2n+1|2n)} + D_{(2n|2n+1|2n+2)}$ Contributions.

The above calculation of the $\mathcal{O}(K^3)$ contribution shows that the dominant contributions arise from the regions

$$k_{Q_1} \approx p, \quad \begin{pmatrix} q_{S_1} \\ q_{S_2} \\ q_{S_3} \end{pmatrix} \approx \begin{pmatrix} \sigma_1 k_{Q_1} \\ -\sigma_1 p \\ \sigma_2 k_{Q_2} \end{pmatrix}, \quad \sigma_j = \pm, \quad (241)$$

where (Q_1, Q_2) and (S_1, S_2, S_3) are permutations of $(1, 2)$ and $(1, 2, 3)$ respectively. Motivated by this observation we therefore consider the analogous regions for the $\mathcal{O}(K^{2n+1})$ contributions $D_{(2n+2|2n+1|2n)}$ and $D_{(2n|2n+1|2n+2)}$. They are

$$\begin{pmatrix} k_{Q_1} \\ \vdots \\ k_{Q_n} \end{pmatrix} \approx \begin{pmatrix} p_1 \\ \vdots \\ p_n \end{pmatrix}, \quad \begin{pmatrix} q_{S_1} \\ q_{S_2} \\ \vdots \\ q_{S_{2n-1}} \\ q_{S_{2n}} \\ q_{S_{2n+1}} \end{pmatrix} \approx \begin{pmatrix} \sigma_1 k_{Q_1} \\ -\sigma_1 p_1 \\ \vdots \\ \sigma_n k_{Q_n} \\ -\sigma_n p_n \\ \sigma_{n+1} k_{Q_{n+1}} \end{pmatrix}, \quad (242)$$

where $\sigma_j = \pm$ and $(Q_1, \dots, Q_{n+1}), (S_1, \dots, S_{2n+1})$ are permutations of $(1, 2, \dots, n+1)$ and $(1, 2, \dots, 2n+1)$ respectively. Our goal is to determine the contribution of the regions (242) to

$$\begin{aligned}
D_{(2n+2|2n+1|2n)} + \text{h.c.} &= \mathcal{C} \operatorname{Re} \sum'_{\substack{k_1, \dots, k_{n+1} \in \text{NS} \\ p_1, \dots, p_n \in \text{NS}}} \left[\prod_{r=1}^{n+1} \frac{\sin(k_r) K(k_r) e^{2it\varepsilon_{k_r}}}{\varepsilon_{k_r}^2} \right] \left[\prod_{s=1}^n \frac{\sin(p_s) K(p_s) e^{-2it\varepsilon_{p_s}}}{\varepsilon_{p_s}^2} \right] \\
&\times \prod_{l < l'}^{n+1} \frac{4}{c_{k_l k_{l'}}^2 \varepsilon_{k_l, k_{l'}}^4} \prod_{m < m'}^n \frac{4}{c_{p_m p_{m'}}^2 \varepsilon_{p_m, p_{m'}}^4} \sum_{q_1, \dots, q_{2n} \in \text{NS}} \left[\prod_{r=1}^{2n+1} \frac{e^{ilq_r}}{\varepsilon_{q_r}} \right] \prod_{l < l'}^{2n+1} g_{q_l q_{l'}}^2 \\
&\times \prod_{s=1}^{2n+1} 2\varepsilon_{k_{n+1}, q_s}^2 c_{k_{n+1} q_s} c_{k_{n+1} q_s} \left[\prod_{r=1}^n 4\varepsilon_{k_r, q_s}^2 \varepsilon_{p_r, q_s}^2 c_{k_r q_s} c_{p_r q_s} \right], \tag{243}
\end{aligned}$$

where the constant \mathcal{C} is

$$\mathcal{C} = \frac{4JA}{L^{4n+2}(n+1)!n!(2n+1)!}. \tag{244}$$

As all regions (242) contribute equally, we focus on the case $(Q_1, \dots, Q_{n+1}) = (1, \dots, n+1)$, $(S_1, \dots, S_{2n+1}) = (1, \dots, 2n+1)$ and multiply the result by a combinatorial factor $(n+1)!(2n+1)!$. We first carry out the summations over q_1, \dots, q_{2n} and k_1, \dots, k_n by following the analogous calculation for the ordered phase, see section 4.4. Finally, we carry out the sum over q_{2n+1} using (D.4). This results in

$$\begin{aligned}
D_{(2n+2|2n+1|2n)} + \text{h.c.} &= -\frac{2\mathcal{A}}{n!} \sum'_{p_1, \dots, p_n \in \text{NS}} \prod_{r=1}^n K^2(p_r) \left[1 - \frac{4\ell}{L} - \frac{4}{L} \theta_H(\ell - 2t\varepsilon'_{p_r}) [2t\varepsilon'_{p_r} - \ell] \right] \\
&\times \frac{4J}{L} \sum_{0 < k_{n+1} \in \text{NS}} \frac{K(k_{n+1})}{\varepsilon_{k_{n+1}}} \sin(k_{n+1}\ell) \cos(2t\varepsilon_{k_{n+1}}) + \dots \\
&= \frac{1}{n!} \sum'_{p_1, \dots, p_n \in \text{NS}} \prod_{r=1}^n K^2(p_r) \left[1 - \frac{4\ell}{L} - \frac{4}{L} \theta_H(\ell - 2t\varepsilon'_{p_r}) [2t\varepsilon'_{p_r} - \ell] \right] \\
&\times [D_{(2|1|0)} + D_{(0|1|2)}] + \dots \tag{245}
\end{aligned}$$

The sum over n can be again taken by inverting the steps used to express (120) in terms of (125), which gives

$$\begin{aligned}
&\sum_{n=0}^{\infty} D_{(2n+2|2n+1|2n)} + \text{h.c.} \\
&= [D_{(2|1|0)} + D_{(0|1|2)}] \exp \left(\sum_{0 < p \in \text{NS}} \ln \left[1 + K^2(p) \left(1 - \frac{4}{L} (\ell + \theta_H(\ell - 2t\varepsilon'_p) [2t\varepsilon'_p - \ell]) \right) \right] \right) + \dots \\
&\approx [D_{(2|1|0)} + D_{(0|1|2)}]_{\text{NS}} \langle B|B \rangle_{\text{NS}} \exp \left[-\frac{4}{L} \sum_{0 < p \in \text{NS}} K^2(p) (\ell + \theta_H(\ell - 2t\varepsilon'_p) [2t\varepsilon'_p - \ell]) \right]. \tag{246}
\end{aligned}$$

In the last step we have only retained the $\mathcal{O}(K^2)$ term in the exponent in order not to exceed the accuracy of our calculation.

4.5.6. Full Answer For the 2-Point Function in the Disordered Phase

The above results suggests that the two-point function consists of two parts

$$\lim_{L \rightarrow \infty} \rho^{xx}(t, \ell) = F_1(\ell) + F_2(t, \ell). \quad (247)$$

The two kinds of contributions are

- An oscillating time dependent contribution arising from the terms $D_{(2n+2|2n+1|2n)} + \text{h.c.}$

$$F_2(t, \ell) \simeq 2JA \int_{-\pi}^{\pi} \frac{dk}{\pi} \frac{K(k)}{\varepsilon_k} \sin(2t\varepsilon_k - k\ell) \times \exp \left[-2 \int_0^{\pi} \frac{dp}{\pi} K^2(p) (\ell + \theta_H(\ell - 2t\varepsilon'_p)[2t\varepsilon'_p - \ell]) \right]. \quad (248)$$

- An exponentially small, time-independent contribution arising from the “diagonal” terms

$$F_1(\ell) = \frac{1}{\text{NS} \langle B|B \rangle_{\text{NS}}} \sum_{n=0}^{\infty} \frac{1}{n!} \sum'_{0 < k_1, \dots, k_n \in \text{NS}} \left[\prod_{j=1}^n K^2(k_j) \right] \times \text{NS} \langle -k_n, k_n, \dots, -k_1, k_1 | \sigma_{m+\ell}^x \sigma_m^x | k_1, -k_1, \dots, k_n, -k_n \rangle_{\text{NS}}. \quad (249)$$

The $\mathcal{O}(K^0)$ and $\mathcal{O}(K^2)$ have been evaluated in sections 4.5.1 and 4.5.3 respectively and are given by

$$F_1(\ell) \approx 2JA \int_{-\pi}^{\pi} \frac{dq}{2\pi} \frac{e^{iq\ell}}{\varepsilon_q} \left[1 + 2K^2(q) - 4\ell \int_0^{\pi} \frac{dk}{2\pi} K^2(k) \right] - 4(h^2 - 1) \int_0^{\pi} \frac{dk}{2\pi} \frac{4J^2 K^2(k)}{\varepsilon^2(k)} \mathcal{D}(\ell). \quad (250)$$

It is shown in Appendix E that the “pair ensemble” average (249) is equal to the average in the generalized Gibbs ensemble, which was previously calculated in [71]. Hence we conclude that

$$F_1(\ell) \simeq \mathcal{C}_{\text{PP}}(\ell) \exp \left(-\frac{\ell}{\xi} \right), \quad \xi^{-1} = \ln(\min[h_0, h_1]) - \ln \left[\frac{1 + hh_0 + \sqrt{(h^2 - 1)(h_0^2 - 1)}}{2hh_0} \right], \quad (251)$$

where $h_1 = \frac{1 + hh_0 + \sqrt{(h^2 - 1)(h_0^2 - 1)}}{h + h_0}$ and the large distance behaviour of $\mathcal{C}_{\text{PP}}(\ell)$ is determined in paper II.

5. Scaling Limit of the Ising Model

So far we have focussed on the quench dynamics in the transverse field Ising lattice model. In the vicinity of the quantum critical point at $h = 1$ a quantum field theory description applies, see e.g. [99]. As quantum quenches in integrable fields theories are of great current interest, we now present explicit expressions for the quench dynamics in the field theory limit.

The scaling limit of the transverse field Ising chain is (a_0 is the lattice spacing) [99]

$$J \rightarrow \infty, \quad h \rightarrow 1, \quad a_0 \rightarrow 0, \quad (252)$$

while keeping fixed both the gap Δ and the velocity v

$$2J|1 - h| = \Delta, \quad 2Ja_0 = v. \quad (253)$$

In this limit the dispersion and Bogoliubov angle become

$$\varepsilon(q) = \sqrt{\Delta^2 + v^2q^2}, \quad (254)$$

$$\theta_h(q) \rightarrow \arctan\left(\frac{vq}{\Delta}\right). \quad (255)$$

In our quench problem both the initial and the final magnetic field are scaled to the critical point, i.e. we need to take

$$h_0 \rightarrow 1, \quad J(1 - h_0) = \Delta_0 = \text{fixed}. \quad (256)$$

In this limit K -matrix turns into

$$K(q) = \tan \left[\frac{\arctan\left(\frac{vq}{\Delta}\right) - \arctan\left(\frac{vq}{\Delta_0}\right)}{2} \right]. \quad (257)$$

Here the physical momentum is defined as

$$q = \frac{k}{a_0}, \quad -\infty < q < \infty. \quad (258)$$

The Hamiltonian describing the scaling limit is expressed in terms of Majorana fermions as

$$H = \int_{-\infty}^{\infty} \frac{dx}{2\pi} \left[\frac{iv}{2} (\bar{\psi} \partial_x \bar{\psi} - \psi \partial_x \psi) - i\Delta \psi \bar{\psi} \right]. \quad (259)$$

The order parameter in the scaling limit must be defined as

$$\sigma(x) \propto (1 - h^2)^{-\frac{1}{8}} \sigma_n^x. \quad (260)$$

where $x = na_0$. It is customary to choose the normalization of the field $\sigma(x)$ such that

$$\lim_{x \rightarrow 0} \langle 0 | \sigma(x) \sigma(0) | 0 \rangle = \frac{1}{|x|^{\frac{1}{4}}}, \quad (261)$$

which implies that

$$\sigma_j^x \rightarrow 2^{1/24} e^{1/8} \mathcal{A}^{-3/2} a_0^{1/8} \sigma(x), \quad (262)$$

where

$$\mathcal{A} = 1.28242712910062\dots \quad (263)$$

5.1. Ordered Phase

The result for the 2-point function after a quench within the ordered phase in the scaling limit is

$$\frac{\langle \psi_0(t) | \sigma(x) \sigma(0) | \psi_0(t) \rangle}{\langle \psi_0 | \psi_0 \rangle} \propto \exp \left(\int_0^\infty \frac{dq}{\pi} \ln \left[\frac{1 - K^2(q)}{1 + K^2(q)} \right] [x\theta(2\varepsilon'(q)t - x) + 2\varepsilon'(q)t\theta(x - 2\varepsilon'(q)t)] \right), \quad (264)$$

where $x = na_0$. This expression is well-defined because at large q we have

$$K(q) \sim \frac{\Delta - \Delta_0}{2vq}. \quad (265)$$

In the stationary state we have

$$\lim_{t \rightarrow \infty} \frac{\langle \psi_0(t) | \sigma(x) \sigma(0) | \psi_0(t) \rangle}{\langle \psi_0 | \psi_0 \rangle} \propto \exp\left(-\frac{x}{\zeta}\right), \quad (266)$$

where

$$\zeta^{-1} = \frac{\Delta + \Delta_0}{2v} - \frac{\sqrt{\Delta\Delta_0}}{v}. \quad (267)$$

5.2. Disordered Phase

For quenches within the disordered phase we can take the scaling limits of the results (248) and (249), which give

$$\frac{\langle \psi_0(t) | \sigma(x) \sigma(0) | \psi_0(t) \rangle}{\langle \psi_0 | \psi_0 \rangle} \propto \mathcal{F}_1(x) + \mathcal{F}_2(t, x), \quad (268)$$

where the time-dependent part dominates except at very late times and is given by

$$\begin{aligned} \mathcal{F}_2(t, x) \approx & 2v \int_{-\infty}^{\infty} \frac{dq}{2\pi} \frac{K(q)}{\varepsilon(q)} \sin(2t\varepsilon(q) - qx) \\ & \times \exp\left(\int_0^{\infty} \frac{dq}{\pi} \ln\left[\frac{1 - K^2(q)}{1 + K^2(q)}\right] [x\theta(2\varepsilon'(q)t - x) + 2\varepsilon'(q)t\theta(x - 2\varepsilon'(q)t)]\right). \end{aligned} \quad (269)$$

The stationary state component is

$$\mathcal{F}_1(x) \propto \exp\left(-\frac{x}{\tilde{\zeta}}\right), \quad (270)$$

where now

$$\tilde{\zeta}^{-1} = \frac{\Delta + \Delta_0}{2v} - \frac{\sqrt{\Delta\Delta_0}}{v} + \frac{\min(\Delta_0, \sqrt{\Delta\Delta_0})}{v}. \quad (271)$$

6. Conclusions

In this work we have derived analytic expressions for the time evolution of one and two point functions in the transverse field Ising chain after a sudden quench of the magnetic field. To do so we have developed two novel methods based on determinants and form factor sums respectively. The former is applicable to quenches in models with free fermionic spectrum and our analysis generalizes straightforwardly e.g. to the spin-1/2 XY chain in a magnetic field [88]. Results obtained by this method are *exact* for asymptotically large times and distances in what we call the space-time-scaling limit ($t, \ell \rightarrow \infty$ keeping their ratio fixed). The form factor approach is applicable more generally to integrable quenches [32] in integrable quantum field theories [100] such as the sine-Gordon model. It is furthermore straightforwardly extended to the study of non-equal time correlation functions [101]. The form factor method provides approximate results that become exact in the limit of small quenches, defined by the requirement that the density of excitations (of the post-quench Hamiltonian) in the initial state is low. We observe that the difference of the form factor and exact results for quenches within either the ferromagnetic or paramagnetic phase are generally very small, except for quenches originating or terminating in the close vicinity of the quantum critical point.

Acknowledgments

We thank John Cardy, Dirk Schuricht and Alessandro Silva for helpful discussions. This work was supported by the EPSRC under grant EP/I032487/1 (FHLE and MF), the ERC under the Starting Grant n. 279391 EDEQS (PC), and by the ESF network INSTANS (PC and MF). We thank the Galileo Galilei Institute for Theoretical Physics for the hospitality and the INFN for partial support during the completion of this work.

Appendix A. Diagonalization of the Transverse Field Ising Model

In this Appendix we summarize the diagonalization of the TFIM [102] with periodic boundary conditions

$$H(h) = -J \sum_{j=1}^L [\sigma_j^x \sigma_{j+1}^x + h \sigma_j^z], \quad (\text{A.1})$$

where l is even, σ_j^α are the Pauli matrices at site j and

$$\sigma_{L+1}^\alpha = \sigma_1^\alpha, \quad \alpha = x, y, z. \quad (\text{A.2})$$

The dimensionless constant h describes the coupling with an external magnetic field Jh . The quantum Ising chain is mapped to a model of spinless fermions by means of a Jordan-Wigner transformation. Defining $\sigma_j^\pm = (\sigma_j^x \pm i\sigma_j^y)/2$ we construct spinless fermion creation and annihilation operators by

$$c_l^\dagger = \prod_{j=1}^{l-1} \sigma_j^z \sigma_l^-, \quad \{c_j, c_l^\dagger\} = \delta_{j,l}. \quad (\text{A.3})$$

The inverse transformation is

$$\sigma_j^z = 1 - 2c_j^\dagger c_j, \quad \sigma_j^x = \prod_{l=1}^{j-1} (1 - 2c_l^\dagger c_l) (c_j + c_j^\dagger). \quad (\text{A.4})$$

The Hamiltonian can be expressed in terms of the fermions as

$$\begin{aligned} H(h) = & -J \sum_{j=1}^{L-1} [c_j^\dagger - c_j][c_{j+1} + c_{j+1}^\dagger] - Jh \sum_{j=1}^L c_j c_j^\dagger - c_j^\dagger c_j \\ & - J e^{i\pi \hat{N}} (c_L - c_L^\dagger)(c_1 + c_1^\dagger), \end{aligned} \quad (\text{A.5})$$

where

$$\hat{N} = \sum_{j=1}^L c_j^\dagger c_j. \quad (\text{A.6})$$

As $[H, e^{i\pi \hat{N}}] = 0$ we may diagonalize the two operators simultaneously. The Hamiltonian is block diagonal $H = H_e \oplus H_o$, where $H_{e/o}$ act on the subspaces of the Fock space with an even/odd number of fermions respectively.

Appendix A.1. Even Fermion Number

In the sector with an even number of fermions we have $e^{i\pi\hat{N}} = 1$ and the Hamiltonian can be written in the form

$$H_e(h) = -J \sum_{j=1}^L [c_j^\dagger - c_j][c_{j+1} + c_{j+1}^\dagger] - Jh \sum_{j=1}^L c_j c_j^\dagger - c_j^\dagger c_j, \quad (\text{A.7})$$

where we have imposed antiperiodic boundary conditions on the fermions

$$c_{L+1} = -c_1. \quad (\text{A.8})$$

The Hamiltonian H_e is diagonalized by going to Fourier space

$$c(k_n) = \frac{1}{\sqrt{L}} \sum_{j=1}^L c_j e^{ik_n j}, \quad (\text{A.9})$$

where k_n are quantized according to (A.8)

$$k_n = \frac{2\pi(n+1/2)}{L}, \quad n = -\frac{L}{2}, \dots, \frac{L}{2} - 1. \quad (\text{A.10})$$

The antiperiodic sector is commonly referred to as Neveu-Schwarz (NS) sector. Following this nomenclature we introduce the notation $k \in \text{NS}$ to describe the set (A.10). Introducing Bogoliubov fermions by

$$\begin{aligned} c(k_n) &= \cos(\theta_{k_n}/2) \alpha_{k_n} + i \sin(\theta_{k_n}/2) \alpha_{-k_n}^\dagger, \\ c^\dagger(-k_n) &= i \sin(\theta_{k_n}/2) \alpha_{k_n} + \cos(\theta_{k_n}/2) \alpha_{-k_n}^\dagger, \end{aligned} \quad (\text{A.11})$$

where the Bogoliubov angle fulfils

$$e^{i\theta_k} = \frac{h - e^{ik}}{\sqrt{1 + h^2 - 2h \cos k}}, \quad (\text{A.12})$$

the Hamiltonian becomes diagonal

$$H_e(h) = \sum_{n=-\frac{L}{2}}^{\frac{L}{2}-1} \varepsilon(k_n) \left[\alpha_{k_n}^\dagger \alpha_{k_n} - \frac{1}{2} \right]. \quad (\text{A.13})$$

Here the dispersion relation is

$$\varepsilon_k = 2J \sqrt{1 + h^2 - 2h \cos(k)}. \quad (\text{A.14})$$

A basis for the Fock space in the sector with even fermion number is then given by

$$|k_1, \dots, k_{2m}; h\rangle_{\text{NS}} = \prod_{j=1}^{2m} \alpha_{k_j}^\dagger |0; h\rangle_{\text{NS}}, \quad k_j \in \text{NS}, \quad (\text{A.15})$$

where the fermion vacuum $|0; h\rangle_{\text{NS}}$ is the state annihilated by all α_{k_j} ($j = -\frac{L}{2}, \dots, \frac{L}{2} - 1$).

Appendix A.2. Odd Fermion Number

In the sector with an odd number of fermions we have $e^{i\pi\hat{N}} = -1$. The Hamiltonian can again be written in the form

$$H_o(h) = -J \sum_{j=1}^L [c_j^\dagger - c_j][c_{j+1} + c_{j+1}^\dagger] - Jh \sum_{j=1}^L c_j c_j^\dagger - c_j^\dagger c_j, \quad (\text{A.16})$$

but now we have to impose periodic boundary conditions on the fermions

$$c_{L+1} = c_1. \quad (\text{A.17})$$

In Fourier space we therefore now have

$$c(p_n) = \frac{1}{\sqrt{L}} \sum_{j=1}^L c_j e^{ip_n j}, \quad (\text{A.18})$$

where p_n are quantized according to (A.17)

$$p_n = \frac{2\pi n}{L}, \quad n = -\frac{L}{2}, \dots, \frac{L}{2} - 1. \quad (\text{A.19})$$

The periodic sector is known as Ramond sector and we will denote the set (A.19) by $p_n \in \mathbb{R}$. Defining Bogoliubov fermions α_{p_n} for $p_n \neq 0$ by

$$\begin{aligned} c(p_n) &= \cos(\theta_{p_n}/2) \alpha_{p_n} + i \sin(\theta_{p_n}/2) \alpha_{-p_n}^\dagger, \\ c^\dagger(-p_n) &= i \sin(\theta_{p_n}/2) \alpha_{p_n} + \cos(\theta_{p_n}/2) \alpha_{-p_n}^\dagger, \end{aligned} \quad (\text{A.20})$$

we can express the Hamiltonian as

$$H_o(h) = \sum_{\substack{n=-\frac{L}{2} \\ n \neq 0}}^{\frac{L}{2}-1} \varepsilon(p_n) \left[\alpha_{p_n}^\dagger \alpha_{p_n} - \frac{1}{2} \right] - 2J(1-h) \left[\alpha_0^\dagger \alpha_0 - \frac{1}{2} \right]. \quad (\text{A.21})$$

A basis of the subspace of the Fock space with odd fermion numbers is then given by

$$|p_1, \dots, p_{2m+1}; h\rangle = \prod_{j=1}^{2m+1} \alpha_{p_j}^\dagger |0; h\rangle_{\text{R}}, \quad p_j \in \mathbb{R}, \quad (\text{A.22})$$

where the fermion vacuum $|0\rangle_{\text{R}}$ is the state annihilated by all α_{p_j} ($j = -\frac{L}{2}, \dots, \frac{L}{2} - 1$).

Appendix A.3. Paramagnetic Phase $h > 1$

Here the ground state is

$$|0\rangle_{\text{NS}}. \quad (\text{A.23})$$

A complete set of states is then given by

$$\begin{aligned} |p_1, \dots, p_{2m+1}; h\rangle_{\text{R}} &= \prod_{k_j \in \mathbb{R}}^{2m+1} \alpha_{p_j}^\dagger |0; h\rangle_{\text{R}}, \\ |k_1, \dots, k_{2m}; h\rangle_{\text{NS}} &= \prod_{p_j \in \text{NS}}^{2m} \alpha_{k_j}^\dagger |0; h\rangle_{\text{NS}}. \end{aligned} \quad (\text{A.24})$$

The Hamiltonians can be written as

$$\begin{aligned} H_e(h) &= \sum_{k_n \in \text{NS}} \varepsilon(k_n) \alpha_{k_n}^\dagger \alpha_{k_n} + E_0^{\text{NS}}(h), \\ H_o(h) &= \sum_{p_n \in \text{R}} \varepsilon(p_n) \alpha_{p_n}^\dagger \alpha_{p_n} + E_0^{\text{R}}(h), \end{aligned} \quad (\text{A.25})$$

where $E_0^{\text{a}}(h) = -\frac{1}{2} \sum_{q \in \text{a}} \varepsilon(q)$, $\text{a} = \text{R}, \text{NS}$.

Appendix A.4. Ferromagnetic Phase $h < 1$

As the zero momentum mode has negative energy it is useful to perform a particle-hole transformation

$$\alpha_0 \longrightarrow \alpha_0^\dagger. \quad (\text{A.26})$$

Redefining the Ramond vacuum as the state that is annihilated by all α_{p_n} after the particle-hole transformation we can construct a complete set of states as

$$\begin{aligned} |k_1, \dots, k_{2m}; h\rangle_{\text{R}} &= \prod_{k_j \in \text{R}}^{2m} \alpha_{k_j}^\dagger |0; h\rangle_{\text{R}}, \\ |p_1, \dots, p_{2m}; h\rangle_{\text{NS}} &= \prod_{p_j \in \text{NS}}^{2m} \alpha_{p_j}^\dagger |0; h\rangle_{\text{NS}}. \end{aligned} \quad (\text{A.27})$$

The Hamiltonians are then again given by (A.25). For large L we have $E_0^{\text{NS}}(h) - E_0^{\text{R}}(h) = \mathcal{O}(L^{-1})$, so that there are two low-energy states

$$|0; h\rangle_{\text{R}}, \quad |0; h\rangle_{\text{NS}}. \quad (\text{A.28})$$

As long as L is finite the ground state is $|0; h\rangle_{\text{NS}}$. On the other hand, in the thermodynamic limit the states (A.28) become degenerate and by spontaneous symmetry breaking one of the two combinations

$$\frac{1}{\sqrt{2}} [|0; h\rangle_{\text{R}} \pm |0; h\rangle_{\text{NS}}] \quad (\text{A.29})$$

is selected as the ground state.

Appendix B. Initial State

As described in Appendix A the Hamiltonian $H(h_0)$ can be diagonalized by a Bogoliubov transformation. Let us denote the corresponding Bogoliubov fermions by $\tilde{\alpha}_k$, the Bogoliubov angle by θ_k^0 and the NS vacuum by $|0; h_0\rangle_{\text{NS}}$. Similarly the Hamiltonian $H(h)$ is diagonalized by the Bogoliubov transformation (A.11) and its lowest energy state in the even fermion sector is $|0; h\rangle_{\text{NS}}$. As both sets of Bogoliubov fermions are given in terms of the same spinless fermions c_j and c_j^\dagger ($j = 1, \dots, L$), they can be expressed in terms of one another by

$$\tilde{\alpha}_{k_n} = \cos\left(\frac{\theta_{k_n} - \theta_{k_n}^0}{2}\right) \alpha_{k_n} + i \sin\left(\frac{\theta_{k_n} - \theta_{k_n}^0}{2}\right) \alpha_{-k_n}^\dagger. \quad (\text{B.1})$$

As both sets of fermions can be used to construct a basis of the even Fock space we can express $|0; h_0\rangle_{\text{NS}}$ in the form

$$|0; h_0\rangle_{\text{NS}} = \sum_{n=0}^{\infty} \sum_{k^{(1)}, \dots, k^{(n)} \in \text{NS}} f_{k^{(1)}, \dots, k^{(n)}} \prod_{j=1}^n \alpha_{k^{(j)}}^\dagger |0; h\rangle_{\text{NS}} \quad (\text{B.2})$$

Using the expression (B.1) in the condition

$$\tilde{\alpha}_{k_n} |0; h_0\rangle_{\text{NS}} = 0, \quad (\text{B.3})$$

allows determination of the coefficients $f_{k^{(1)}, \dots, k^{(n)}}$. A simple calculation gives

$$|0; h_0\rangle_{\text{NS}} = \frac{1}{\mathcal{N}_{\text{NS}}} \exp \left[i \sum_{p \in \text{NS}} K(p) \alpha_{-p}^\dagger \alpha_p^\dagger \right] |0; h\rangle_{\text{NS}}, \quad (\text{B.4})$$

where \mathcal{N}_{NS} is a normalization constant and the function $K(k)$ is given by

$$K(k) = \tan \left(\frac{\theta_k - \theta_k^0}{2} \right). \quad (\text{B.5})$$

The equations of motion for α_k imply that

$$\alpha_k(t) = e^{it\varepsilon_k} \alpha_k(0), \quad (\text{B.6})$$

so that [61]

$$e^{-itH_e(h)} |0; h_0\rangle_{\text{NS}} = \frac{|B(t)\rangle_{\text{NS}}}{\sqrt{\text{NS} \langle B|B \rangle_{\text{NS}}}}, \quad (\text{B.7})$$

where

$$|B(t)\rangle_{\text{NS}} = e^{-itE_0^{\text{NS}}} \exp \left[i \sum_{0 < p \in \text{NS}} e^{-2it\varepsilon_p} K(p) \alpha_{-p}^\dagger \alpha_p^\dagger \right] |0; h\rangle_{\text{NS}}. \quad (\text{B.8})$$

Similarly one can show that

$$e^{-itH_o(h)} |0; h_0\rangle_{\text{R}} = \frac{|B(t)\rangle_{\text{R}}}{\sqrt{\text{R} \langle B|B \rangle_{\text{R}}}}, \quad (\text{B.9})$$

where

$$|B(t)\rangle_{\text{R}} = e^{-itE_0^{\text{R}}} \exp \left[i \sum_{0 < p \in \text{R}} e^{-2it\varepsilon_p} K(p) \alpha_{-p}^\dagger \alpha_p^\dagger \right] |0; h\rangle_{\text{R}}. \quad (\text{B.10})$$

The states (B.8) and (B.10) are of the same form as *boundary states* in integrable scattering theories [94, 9].

A physical interpretation of the function $K(k)$ (B.5) is obtained as follows. The density of post-quench Bogoliubov fermions $\alpha_k^\dagger \alpha_k$ in the initial state is given by

$$\begin{aligned} \text{a} \langle 0; h_0 | \alpha_k^\dagger \alpha_k | 0; h_0 \rangle_{\text{a}} &= \frac{1}{\mathcal{N}_{\text{a}}^2} \text{a} \langle 0; h | \prod_{k \in \text{a}} (1 - iK(k) \alpha_k \alpha_{-k}) \alpha_k^\dagger \alpha_k (1 + iK(k) \alpha_{-k}^\dagger \alpha_k^\dagger) | 0; h \rangle \\ &= \frac{K^2(k)}{1 + K^2(k)}, \quad \text{a} = \text{NS, R}. \end{aligned} \quad (\text{B.11})$$

This implies that in the case where $K(k)$ is uniformly small in k we have

$$\langle \Psi_0 | \alpha_k^\dagger \alpha_k | \Psi_0 \rangle = K^2(k) + \mathcal{O}(K^4), \quad (\text{B.12})$$

where $|\Psi_0\rangle$ is the initial state of our quantum quench. Physically the small parameter characterizing the expansion in powers of $K(k)$ is therefore the density of excitations of the post-quench Hamiltonian $H(h)$ induced by the quantum quench.

Appendix C. Proof of the product formula

We need to evaluate the product of the 2×2 matrices

$$\Pi_{2n}(\{a_i\}) \equiv \prod_{i=1}^{2n} \mathbb{M}(a_i), \quad \text{with } \mathbb{M}(a) = A\sigma_x + B\sigma_y e^{ia\sigma_x}. \quad (\text{C.1})$$

Compared to Eq. (85) in the main text we have $A = n_x(k_0)$, $B = |\vec{n}_\perp(k_0)|$, $a_i = 2\epsilon_{i-1}t$ and we choose (without loss of generality) $\hat{n}_\perp = \hat{y}$. Using the algebra of the Pauli matrices, it is straightforward to calculate

$$\Pi_2(a_1, a_2) = \mathbb{M}(a_1) \cdot \mathbb{M}(a_2) = A^2 \mathbb{I} + B^2 e^{i(a_2 - a_1)\sigma_x} + iAB\sigma_z (e^{ia_2\sigma_x} - e^{ia_1\sigma_x}), \quad (\text{C.2})$$

where \mathbb{I} is the 2 by 2 identity matrix. A slightly longer exercise is required to calculate Π_4 and to obtain

$$\begin{aligned} \Pi_4 = & A^4 \mathbb{I} + iA^3 B \sigma_z \sum_{j=1}^4 (-1)^j e^{ia_j \sigma_x} + A^2 B^2 \sum_{1 \leq j_1 < j_2 \leq 4} (-1)^{j_1 + j_2 + 1} e^{i(a_{j_2} - a_{j_1})\sigma_x} \\ & + iAB^3 \sigma_z \sum_{1 \leq j_1 < j_2 < j_3 \leq 4} (-1)^{j_1 + j_2 + j_3 + 1} e^{i(a_{j_3} - a_{j_2} + a_{j_1})\sigma_x} + B^4 e^{i(a_4 - a_3 + a_2 - a_1)\sigma_x}. \end{aligned} \quad (\text{C.3})$$

From these two first examples, it should be clear that the general structure of Π_{2n} is

$$\Pi_{2n} = \sum_{p=0}^{2n} A^{2n-p} B^p (i\sigma_z)^p \sum_{1 \leq j_1 < j_2 < \dots < j_p \leq 2n} (-1)^{\sum_{k=1}^p j_k} \exp\left(i \sum_{k=1}^p (-1)^{p-k} a_{j_k} \sigma_x\right). \quad (\text{C.4})$$

Having this conjecture, it is straightforward (but require some algebra) to prove it by induction showing that it is compatible with the recurrence relation

$$\Pi_{2n+2}(a_1, \dots, a_{2n+2}) = \Pi_{2n}(a_1, \dots, a_{2n}) \cdot \Pi_2(a_{2n+1}, a_{2n+2}). \quad (\text{C.5})$$

Appendix D. Useful relations

Lemma 1: For any function $f(z)$ that is 2π periodic and analytic in a strip around the real axis we have for $0 < k \in \mathbb{R}$

$$\begin{aligned} \frac{1}{L} \sum_{q_n \in \text{NS} > 0} \frac{f(q_n) e^{2it\varepsilon(q_n)}}{(\cos k - \cos q_n)^2} = & \left[\frac{L}{4} - t\varepsilon'(k) \right] \frac{e^{2it\varepsilon_k} f(k)}{\sin^2 k} + i \frac{e^{2i\varepsilon_k t} f'(k)}{2 \sin^2(k)} \\ & - \oint \frac{dz}{2\pi} \frac{f(z) e^{2i\varepsilon(z)t}}{(\cos z - \cos k)^2 (1 + e^{iLz})}, \end{aligned} \quad (\text{D.1})$$

where the integration is along a closed contour encircling the interval $[0, \pi]$.

Lemma 2a: For any function $f(z)$ that is 2π periodic and analytic in a strip around the real axis we have for $0 < k \in \mathbb{R}$

$$\begin{aligned} \frac{1}{L} \sum_{\substack{q_n \in \mathbb{R} > 0 \\ q_n \neq k}} \frac{f(q_n) e^{2it\varepsilon(q_n)}}{(\cos k - \cos q_n)^2} &= \left[\frac{L}{12} \left(1 - \frac{6i \cot k}{L} \right) - t\varepsilon'(k) \right] \frac{e^{2it\varepsilon_k} f(k)}{\sin^2 k} \\ &+ i \frac{e^{2i\varepsilon_k t} f'(k)}{2 \sin^2(k)} - \oint \frac{dz}{2\pi} \frac{f(z) e^{2i\varepsilon(z)t}}{(\cos z - \cos k)^2 (1 - e^{iLz})} + \mathcal{O}(L^{-1}). \end{aligned} \quad (\text{D.2})$$

The analogous equation for momenta in the NS sector is

Lemma 2b: For any function $f(z)$ that is 2π periodic and analytic in a strip around the real axis we have for $0 < k \in \text{NS}$

$$\begin{aligned} \frac{1}{L} \sum_{\substack{q_n \in \text{NS} > 0 \\ q_n \neq k}} \frac{f(q_n) e^{2it\varepsilon(q_n)}}{(\cos k - \cos q_n)^2} &= \left[\frac{L}{12} \left(1 - \frac{6i \cot k}{L} \right) - t\varepsilon'(k) \right] \frac{e^{2it\varepsilon_k} f(k)}{\sin^2 k} \\ &+ i \frac{e^{2i\varepsilon_k t} f'(k)}{2 \sin^2(k)} - \oint \frac{dz}{2\pi} \frac{f(z) e^{2i\varepsilon(z)t}}{(\cos z - \cos k)^2 (1 + e^{iLz})} + \mathcal{O}(L^{-1}). \end{aligned} \quad (\text{D.3})$$

Lemma 3: For large $j \gg 1$ and any function $f(z) = f(z + 2\pi)$ that is analytic in a strip around the real axis we have ($k \in \mathbb{R}$)

$$\lim_{L \rightarrow \infty} \frac{1}{L} \sum_{q_n \in \text{NS}} \frac{f(q_n) e^{ijq_n}}{\cos k - \cos q_n} = \frac{e^{-ikj} f(-k) - e^{ikj} f(k)}{2i \sin k} + \mathcal{O}(e^{-\gamma j}), \quad (\text{D.4})$$

where γ is a positive constant.

Proof: Using contour integration we have

$$\begin{aligned} \frac{1}{L} \sum_{q_n} \frac{f(q_n) e^{ijq_n}}{\cos k - \cos q_n} &= \oint \frac{dz}{2\pi} \frac{f(z) e^{ijz}}{(\cos z - \cos k)(1 + e^{iLz})} \\ &+ \frac{e^{-ikj} f(-k) - e^{ikj} f(k)}{2i \sin k}, \end{aligned} \quad (\text{D.5})$$

where we have used the quantization conditions (A.10), (A.19) and where the integration is along a counterclockwise contour encircling the interval $[-\pi, \pi]$ in a manner such that no singularities of $f(z)$ lie within it. The contribution of the part of the contour below the real axis tends to zero in the limit $L \rightarrow \infty$ because $|e^{iz(L \pm j)}| \gg 1$. As $j > 0$ the part of the contour above the real axis can be deformed as shown in Fig. D1. The contributions of the pieces parallel to the imaginary axis

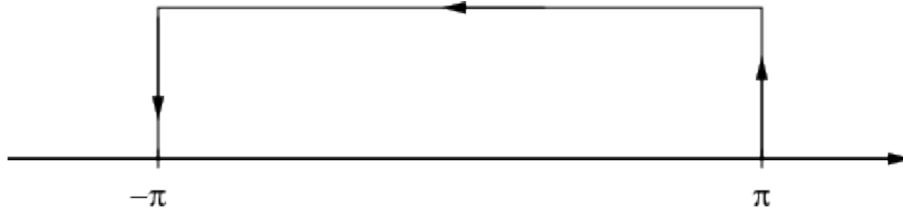


Figure D1. Deformed integration contour.

cancel due to the periodicity of $f(z)$, while the remaining part has the exponentially small bound given in (D.4).

Lemma 4: For any function $f(z)$ that is 2π periodic and analytic in a strip around the real axis we have

$$\begin{aligned} \frac{1}{L} \sum_{q_n \in \text{NS}} \frac{f(q_n) e^{ijq_n}}{(\cos k - \cos q_n)^2} &= -\frac{e^{-ikj} f'(-k) + e^{ikj} f'(k)}{2i \sin^2 k} \\ &+ \left[\frac{L}{4} - \frac{j}{2} \right] \frac{e^{-ikj} f(-k) + e^{ikj} f(k)}{\sin^2 k} + \mathcal{O}(e^{-\gamma j}). \end{aligned} \quad (\text{D.6})$$

Proof: Using contour integration we have

$$\begin{aligned} \frac{1}{L} \sum_{q_n \in \text{NS}} \frac{f(q_n) e^{ijq_n}}{(\cos k - \cos q_n)^2} &= \frac{e^{-ikj} f(-k) + e^{ikj} f(k)}{\sin^2(k)} \left[\frac{L}{4} - \frac{j}{2} \right] \\ &+ i \frac{e^{-ikj} f'(-k) + e^{ikj} f'(k)}{2 \sin^2(k)} - \oint \frac{dz}{2\pi} \frac{f(z) e^{ijz}}{(\cos z - \cos k)^2 (1 + e^{iLz})}, \end{aligned} \quad (\text{D.7})$$

where the integration is along a closed contour encircling the interval $[-\pi, \pi]$. As for $\text{Im}(z) < 0$ we have

$$\lim_{L \rightarrow \infty} e^{i(j-L)z} = 0, \quad (\text{D.8})$$

only the upper part of the contour contributes in the $L \rightarrow \infty$ limit. Using that $f(z)$ is analytic in some strip around the real axis the part of the contour above the real axis can be deformed as shown in Fig. D1. The contributions of the pieces parallel to the imaginary axis cancel due to the periodicity of $f(z)$, while the remaining part is exponentially small in j . In the limit of large L and j the first term in (D.6) can be neglected, so that

$$\frac{1}{L} \sum_{q_n} \frac{f(q_n) e^{ijq_n}}{(\cos k - \cos q_n)^2} \approx \frac{e^{-ikj} f(-k) + e^{ikj} f(k)}{\sin^2(k)} \left[\frac{L}{4} - \frac{j}{2} \right]. \quad (\text{D.9})$$

Lemma 5: For any function $f(z)$ that is 2π periodic and analytic in a strip around the real axis we have

$$\lim_{L \rightarrow \infty} \frac{1}{L} \sum_{0 < q \in \text{NS}} \frac{f(q) e^{2i\sigma\varepsilon(q)t}}{\cos k - \cos q} = \frac{i\sigma f(k) e^{2i\sigma\varepsilon_k t}}{2 \sin k} + \int_{\sigma i 0}^{\pi + \sigma i 0} \frac{dz}{2\pi} \frac{f(z) e^{2i\sigma\varepsilon(z)t}}{\cos k - \cos z}, \quad (\text{D.10})$$

where $\sigma = \pm$ and $0 < k \in \mathbb{R}$.

Appendix E. “Pair Ensemble” Averages

The “diagonal” terms in the Lehmann representation based on the eigenstates of the post quench Hamiltonian $H(h)$ give rise to a *time-independent* contribution to the expectation value $\langle \Psi_0(0) | \mathcal{O} | \Psi_0(0) \rangle$, which we call “pair ensemble”. It is defined as the average

$$\begin{aligned} \langle \mathcal{O} \rangle_{\text{PE}} &\equiv \frac{1}{\text{NS} \langle B | B \rangle_{\text{NS}}} \sum_{n=0}^{\infty} \frac{1}{n!} \sum'_{0 < k_1, \dots, k_n \in \text{NS}} \left[\prod_{j=1}^n K^2(k_j) \right] \\ &\times \text{NS} \langle -k_n, k_n, \dots, -k_1, k_1; h | \mathcal{O} | k_1, -k_1, \dots, k_n, -k_n; h \rangle_{\text{NS}}. \end{aligned} \quad (\text{E.1})$$

Averages of the form (E.1) can be represented using a density matrix as $\langle \mathcal{O} \rangle_{\text{PE}} = \text{tr}(\rho_{\text{PE}} \mathcal{O})$, where

$$\rho_{\text{PE}} = (1 - n_0)(1 - n_\pi) \prod_{0 < k \in \text{NS}} \left(\frac{\mathbb{I}_k \mathbb{I}_{-k} - n_k \mathbb{I}_{-k} - \mathbb{I}_k n_{-k}}{1 + K^2(k)} + n_k n_{-k} \right). \quad (\text{E.2})$$

Here $n_q = \alpha_q^\dagger \alpha_q$ are the Bogoliubov fermion number operators in momentum space and \mathbb{I}_k is the identity in the subspace with momentum k . The only non-vanishing expectation values of the pair ensemble are

$$\langle n_{q_1} n_{q_2} \dots n_{q_m} \rangle_{\text{PE}} = \prod_{|q_j| \in S} \frac{K^2(|q_j|)}{1 + K^2(|q_j|)}, \quad (\text{E.3})$$

where S is the set of all momenta q_j with *mutually distinct* magnitudes, i.e.

$$0 < |q_r| \neq |q_s| < \pi \quad \forall q_r, q_s \in S. \quad (\text{E.4})$$

We note that $\langle n_k n_{-k} \mathcal{O} \rangle = \langle n_k \mathcal{O} \rangle$ since the ensemble describes pairs of particles with opposite momenta.

As shown in section 3 lattice spin operators can be expressed as products of the Majorana fermions a_j^x, a_j^y , which are related to the Bogoliubov fermions diagonalizing the post-quench Hamiltonian $H(h)$ by

$$\begin{aligned} a_j^x &= \frac{1}{\sqrt{L}} \sum_k e^{-ikj} e^{i\theta_k/2} [\alpha_k + \alpha_{-k}^\dagger], \\ a_j^y &= \frac{1}{\sqrt{L}} \sum_k e^{-ikj} e^{-i\theta_k/2} i [\alpha_{-k}^\dagger - \alpha_k]. \end{aligned} \quad (\text{E.5})$$

As the only non-zero expectation values in the pair ensemble are of the form (E.3) we can express a general average in the form

$$\left\langle \prod_{r=1}^{2n} a_{j_r}^{b_r} \right\rangle_{\text{PE}} = \frac{1}{L^n} \sum_{k_1, \dots, k_n} \sum_{s=0}^n \chi_b^{(s)}(k_1, \dots, k_n | \vec{j}) \left\langle \prod_{u=1}^s n_{k_u} \right\rangle_{\text{PE}}, \quad (\text{E.6})$$

where $\chi_b^{(s)}(k_1, \dots, k_n | \vec{j})$ are well-behaved functions of the momenta.

The generalized Gibbs ensemble for the Ising model is defined as

$$\langle \mathcal{O} \rangle_{\text{GGE}} \equiv \frac{1}{Z_{\text{GGE}}} \text{tr} \left[e^{-\sum_q \lambda_q n_q} \mathcal{O} \right], \quad (\text{E.7})$$

where $Z_{\text{GGE}} = \text{tr} \left[e^{-\sum_q \lambda_q n_q} \right]$ and

$$\lambda_q = -\log(K^2(q)). \quad (\text{E.8})$$

By taking the trace over a basis of eigenstates of $H(h)$ we conclude that the only non-zero averages are

$$\langle n_{q_1} n_{q_2} \dots n_{q_m} \rangle_{\text{GGE}} = \prod_{j=1}^m \frac{K^2(q_j)}{1 + K^2(q_j)}. \quad (\text{E.9})$$

The corresponding density matrix is

$$\rho_{\text{GGE}} = \prod_{k \in \text{NS}} \frac{\mathbb{I}_k - (1 - K^2(k)) n_k}{1 + K^2(k)}. \quad (\text{E.10})$$

We observe that $\langle n_{k_1} n_{k_2} \cdots n_{k_m} \rangle_{\text{GGE}} = \langle n_{k_1} \rangle_{\text{GGE}} \langle n_{k_2} \cdots n_{k_m} \rangle_{\text{GGE}}$ for any set of distinct momenta k_1, k_2, \dots, k_m , and unlike in the pair ensemble Wick's theorem applies in the generalized Gibbs ensemble. General averages can be expressed as

$$\left\langle \prod_{r=1}^{2n} a_{j_r}^{b_r} \right\rangle_{\text{GGE}} = \frac{1}{L^n} \sum_{k_1, \dots, k_n} \sum_{s=0}^n \chi_{\vec{b}}^{(s)}(k_1, \dots, k_n | \vec{j}) \left\langle \prod_{u=1}^s n_{k_u} \right\rangle_{\text{GGE}}, \quad (\text{E.11})$$

where the functions $\chi_{\vec{b}}^{(s)}(k_1, \dots, k_n | \vec{j})$ are the same as in (E.6). As the averages $\langle \prod_{u=1}^s n_{k_u} \rangle_{\text{GGE}}$ and $\langle \prod_{u=1}^s n_{k_u} \rangle_{\text{PE}}$ are the same unless at least two of the $|k_u|$'s coincide, and such contributions are suppressed by factors of $1/L$, we conclude that

$$\lim_{L \rightarrow \infty} \left\langle \prod_{r=1}^{2n} a_{j_r}^{b_r} \right\rangle_{\text{PE}} = \lim_{L \rightarrow \infty} \left\langle \prod_{r=1}^{2n} a_{j_r}^{b_r} \right\rangle_{\text{GGE}}. \quad (\text{E.12})$$

The above arguments show that averages of operators that are local in space are the same in both ensembles. However, non-local operators have in general different averages, e.g. $\langle n_k n_{-k} \rangle_{\text{GGE}} = \langle n_k n_{-k} \rangle_{\text{PE}}^2$.

References

- [1] M. Greiner, O. Mandel, T. W. Hänsch, and I. Bloch, Collapse and Revival of the Matter Wave Field of a Bose-Einstein Condensate, *Nature* **419** 51 (2002).
- [2] S. Hofferberth, I. Lesanovsky, B. Fischer, T. Schumm, and J. Schmiedmayer, Non-equilibrium coherence dynamics in one-dimensional Bose gases, *Nature* **449**, 324 (2007).
- [3] S. Trotzky Y.-A. Chen, A. Flesch, I. P. McCulloch, U. Schollwöck, J. Eisert, and I. Bloch, Probing the relaxation towards equilibrium in an isolated strongly correlated 1D Bose gas, *Nature Phys.* **XX**, XXX (2012). [1101.2659].
- [4] M. Cheneau, P. Barmettler, D. Poletti, M. Endres, P. Schauss, T. Fukuhara, C. Gross, I. Bloch, C. Kollath, and S. Kuhr, Light-cone-like spreading of correlations in a quantum many-body system, *Nature* **481**, 484 (2012).
- [5] M. Gring, M. Kuhnert, T. Langen, T. Kitagawa, B. Rauer, M. Schreitl, I. Mazets, D. A. Smith, E. Demler, and J. Schmiedmayer, Relaxation Dynamics and Pre-thermalization in an Isolated Quantum System, arXiv:1112.0013.
- [6] T. Kinoshita, T. Wenger, D. S. Weiss, A quantum Newton's cradle, *Nature* **440**, 900 (2006).
- [7] E. H. Lieb and D. W. Robinson, The finite group velocity of quantum spin systems, *Commun. Math. Phys.*, **28**, 251 (1972).
- [8] P. Calabrese and J. Cardy, Evolution of Entanglement Entropy in One-Dimensional Systems, *J. Stat. Mech.* (2005) P04010.
- [9] P. Calabrese and J. Cardy, Time-dependence of correlation functions following a quantum quench, *Phys. Rev. Lett.* **96**, 136801 (2006).
- [10] P. Calabrese and J. Cardy, Entanglement and correlation functions following a local quench: a conformal field theory approach, *J. Stat. Mech.* P10004 (2007).
- [11] S. Sotiriadis and J. Cardy, Quantum quench in interacting field theory: a self-consistent approximation, *Phys. Rev. B* **81**, 134305 (2010).
- [12] J.-M. Stéphan and J. Dubail, Local quantum quenches in critical one-dimensional systems: entanglement, the Loschmidt echo, and light-cone effects, *J. Stat. Mech.* (2011) P08019
- [13] S. R. Manmana, S. Wessel, R. M. Noack, and A. Muramatsu, Time evolution of correlations in strongly interacting fermions after a quantum quench, *Phys. Rev. B* **79**, 155104 (2009).
- [14] A. Laeuchli and C. Kollath, Spreading of correlations and entanglement after a quench in the one-dimensional Bose-Hubbard model, *J. Stat. Mech.* (2008) P05018.
- [15] P. Barmettler, D. Poletti, M. Cheneau, and C. Kollath, Propagation front of correlations in an interacting Bose gas, arXiv:1202.5558.
- [16] M. Ganahl, E. Rabel, F. H. L. Essler, and H. G. Evertz, Observing complex bound states in the spin-1/2 Heisenberg XXZ chain using local quantum quenches, *Phys. Rev. Lett.* **108**, 077206 (2012).

- [17] J. Happola, G. B. Halasz, and A. Hamma, Universality and robustness of revivals in the transverse field XY model, *Phys. Rev. A* **85**, 032114 (2012).
- [18] T. Enss and J. Sirker, Light cone renormalization and quantum quenches in one-dimensional Hubbard models, *New J. Phys.* **14**, 023008 (2012).
- [19] A. Polkovnikov, K. Sengupta, A. Silva, and M. Vengalattore, Nonequilibrium dynamics of closed interacting quantum systems, *Rev. Mod. Phys.* **83**, 863 (2011).
- [20] M. Rigol, V. Dunjko, V. Yurovsky, and M. Olshanii, Relaxation in a completely integrable many-body quantum system: An ab initio study of the dynamics of the highly excited states of lattice hard-core bosons, *Phys. Rev. Lett.* **98**, 50405 (2007).
- [21] M. Rigol, V. Dunjko, and M. Olshanii, Thermalization and its mechanism for generic isolated quantum systems, *Nature* **452**, 854 (2008).
- [22] P. Calabrese and J. Cardy, Quantum quenches in extended systems, *J. Stat. Mech.* (2007) P06008.
- [23] M. A. Cazalilla, Effect of suddenly turning on the interactions in the Luttinger model, *Phys. Rev. Lett.* **97**, 156403 (2006); A. Iucci and M. A. Cazalilla, Quantum quench dynamics of the sine-Gordon model in some solvable limits, *New J. Phys.* **12**, 055019 (2010); A. Iucci and M. A. Cazalilla, Quantum quench dynamics of the Luttinger model, *Phys. Rev. A*, **80**, 063619 (2009).
- [24] S. R. Manmana, S. Wessel, R.M. Noack, and A. Muramatsu, Strongly correlated fermions after a quantum quench, *Phys. Rev. Lett.* **98**, 210405 (2007).
- [25] M. Cramer, C.M. Dawson, J. Eisert, and T.J. Osborne, Quenching, relaxation, and a central limit theorem for quantum lattice systems, *Phys. Rev. Lett.* **100**, 030602 (2008); M. Cramer and J. Eisert A quantum central limit theorem for non-equilibrium systems: Exact local relaxation of correlated states, *New J. Phys.* **12**, 055020 (2010)
- [26] T. Barthel and U. Schollwöck, Dephasing and the steady state in quantum many-particle systems, *Phys. Rev. Lett.* **100**, 100601 (2008).
- [27] M. Cramer, A. Flesch, I. A. McCulloch, U. Schollwöck, and J. Eisert, Exploring local quantum many-body relaxation by atoms in optical superlattices, *Phys. Rev. Lett.* **101**, 063001 (2008); A. Flesch, M. Cramer, I.P. McCulloch, U. Schollwöck, and J. Eisert, Probing local relaxation of cold atoms in optical superlattices, *Phys. Rev. A* **78**, 033608 (2008).
- [28] M. Kollar and M. Eckstein, Relaxation of a one-dimensional Mott insulator after an interaction quench, *Phys. Rev. A* **78**, 013626 (2008).
- [29] S. Sotiriadis, P. Calabrese, and J. Cardy, Quantum Quench from a Thermal Initial State, *EPL* **87**, 20002, (2009).
- [30] G. Roux, Quenches in quantum many-body systems: One-dimensional Bose-Hubbard model reexamined, *Phys. Rev. A* **79**, 021608 (2009); G. Roux, Finite size effects in global quantum quenches: examples from free bosons in an harmonic trap and the one-dimensional Bose-Hubbard model, *Phys. Rev. A* **81**, 053604 (2010).
- [31] S. Sotiriadis, D. Fioretto, and G. Mussardo, Zamolodchikov-Faddeev Algebra and Quantum Quenches in Integrable Field Theories, *J. Stat. Mech.* (2012) P02017.
- [32] D. Fioretto and G. Mussardo, Quantum Quenches in Integrable Field Theories, *New J. Phys.* **12**, 055015 (2010).
- [33] G. P. Brandino, A. De Luca, R.M. Konik, and G. Mussardo, Quench Dynamics in Randomly Generated Extended Quantum Models, arXiv:1111.6119.
- [34] C. Kollath, A. Laeuchli, and E. Altman, Quench dynamics and non equilibrium phase diagram of the Bose-Hubbard model, *Phys. Rev. Lett.* **98**, 180601 (2007).
- [35] G. Biroli, C. Kollath, and A. Laeuchli, Effect of Rare Fluctuations on the Thermalization of Isolated Quantum Systems, *Phys. Rev. Lett.* **105**, 250401 (2010).
- [36] M. C. Banuls, J. I. Cirac, and M. B. Hastings, Strong and weak thermalization of infinite non-integrable quantum systems, *Phys. Rev. Lett.* **106**, 050405 (2011).
- [37] C. Gogolin, M. P. Mueller, and J. Eisert, Absence of Thermalization in Nonintegrable Systems, *Phys. Rev. Lett.* **106**, 040401 (2011).
- [38] M. Rigol and M. Fitzpatrick, Initial-state dependence of the quench dynamics in integrable quantum systems, *Phys. Rev. A* **84**, 033640 (2011).
- [39] T. Caneva, E. Canovi, D. Rossini, G. E. Santoro, and A. Silva, Applicability of the generalized Gibbs ensemble after a quench in the quantum Ising chain, *J. Stat. Mech.* (2011) P07015.
- [40] M. A. Cazalilla, A. Iucci, and M.-C. Chung, Thermalization and Quantum Correlations in Exactly Solvable Models, *Phys. Rev. E* **85**, 011133 (2012).
- [41] M. Rigol and M. Srednicki, Alternatives to Eigenstate Thermalization, *Phys. Rev. Lett.* **108**, 110601 (2012).
- [42] J. M. Zhang, F. C. Cui, and J. Hu, The generalized Gibbs ensemble as a pseudo-initial state: its predictive power revealed in a second quench, arXiv:1109.5904.
- [43] L. F. Santos, A. Polkovnikov, and M. Rigol, Entropy of Isolated Quantum Systems after a Quench, *Phys. Rev. Lett.* **107**, 040601 (2011).

- [44] J. Mossel and J.-S. Caux, Exact time evolution of space- and time-dependent correlation functions after an interaction quench in the 1D Bose gas, arXiv:1201.1885.
- [45] P. Grisins and I. E. Mazets, Thermalization in a one-dimensional integrable system, Phys. Rev. A **84**, 053635 (2011).
- [46] J.-S. Caux and R. M. Konik, Numerical renormalization based on integrable theories: quantum quenches and their corresponding generalized Gibbs ensembles, 1203.0901.
- [47] J. Mossel and J.-S. Caux, Generalized TBA and generalized Gibbs, 1203.1305.
- [48] E. Canovi, D. Rossini, R. Fazio, G. E. Santoro, and A. Silva, Quantum Quenches, Thermalization and Many-Body Localization, Phys. Rev. B **83**, 094431 (2011).
- [49] E. Altman and A. Auerbach, Oscillating Superfluidity of Bosons in Optical Lattices, Phys. Rev. Lett. **89**, 250404 (2002).
- [50] R. A. Barankov and L. S. Levitov, Synchronization in the BCS Pairing Dynamics as a Critical Phenomenon, Phys. Rev. Lett. **96**, 230403 (2006); E. A. Yuzbashyan and M. Dzero, Dynamical vanishing of the order parameter in a fermionic condensate, Phys. Rev. Lett. **96**, 230404 (2006). E. A. Yuzbashyan, O. Tsypliyatyev, and B. L. Altshuler, Relaxation and persistent oscillations of the order parameter in fermionic condensate, Phys. Rev. Lett. **96**, 097005 (2006).
- [51] B. Sciola and G. Biroli, Quantum quenches and off-equilibrium dynamical transition in the infinite dimensional Bose Hubbard model, Phys. Rev. Lett. **105**, 220401 (2010); B. Sciola and G. Biroli, Dynamical transitions and quantum quenches in mean-field models, J. Stat. Mech. (2011) P11003.
- [52] M. Eckstein, M. Kollar, P. Werner, Phys. Rev. Lett. **103**, 056403 (2009).
- [53] M. Schirò and M. Fabrizio, Time-Dependent Mean Field Theory for Quench Dynamics in correlated electron systems, Phys. Rev. Lett. **105**, 076401 (2010); M. Schirò and M. Fabrizio, Quantum Quenches in the Hubbard Model: Time Dependent Mean Field Theory and The Role of Quantum Fluctuations, Phys. Rev. B **83**, 165105 (2011).
- [54] A. Gambassi and P. Calabrese, Quantum quenches as classical critical films, EPL **95** (2011) 66007.
- [55] V. Balasubramanian, A. Bernamonti, J. de Boer, N. B. Copland, B. Craps, E. Keski-Vakkuri, B. Muller, A. Schafer, M. Shigemori, and W. Staessens, Thermalization of Strongly Coupled Field Theories, Phys. Rev. Lett. **106**, 191601(2011); V. Balasubramanian, A. Bernamonti, J. de Boer, N. B. Copland, B. Craps, E. Keski-Vakkuri, B. Muller, A. Schafer, M. Shigemori, and W. Staessens, Holographic Thermalization, Phys. Rev. D **84**, 026010 (2011).
- [56] J. Abajo-Arastia, J. Aparicio, and E. Lopez, Holographic Evolution of Entanglement Entropy, JHEP **1011**, 149 (2010); J. Aparicio and E. Lopez, Evolution of Two-Point Functions from Holography, arXiv:1109.3571.
- [57] S. R. Das, T. Nishioka, and T. Takayanagi, Probe branes, time-dependent couplings and thermalization in AdS/CFT, JHEP **1007** (2010) 071; A. Allais and E. Tonni, Holographic evolution of the mutual information, JHEP **1201**, 102 (2012); V. Balasubramanian, A. Bernamonti, N. Copland, B. Craps, and F. Galli, Thermalization of mutual and tripartite information in strongly coupled two dimensional conformal field theories, Phys. Rev. D. **84**, 105017 (2011); V. Keranen, E. Keski-Vakkuri, and L. Thorlacius, Thermalization and entanglement following a nonrelativistic holographic quench, Phys. Rev. D **85**, 026005 (2012).
- [58] S. Sachdev, Quantum Phase Transitions, Cambridge University Press, 2001.
- [59] R. Coldea, D.A. Tennant, E.M. Wheeler, E. Wawrzynska, D. Prabhakaran, M. Telling, K. Habicht, P. Smeibidl, K. Kiefer, Quantum criticality in an Ising chain: experimental evidence for emergent E8 symmetry, Science **327**, 177 (2010).
- [60] J. Simon, W. S. Bakr, R. Ma, M. E. Tai, P. M. Preiss, and M. Greiner, Quantum simulation of antiferromagnetic spin chains in an optical lattice, Nature **472**, 307 (2011).
- [61] D. Rossini, A. Silva, G. Mussardo, and G. Santoro, Effective thermal dynamics following a quantum quench in a spin chain, Phys. Rev. Lett. **102**, 127204 (2009); D. Rossini, S. Suzuki, G. Mussardo, G. E. Santoro, and A. Silva, Long time dynamics following a quench in an integrable quantum spin chain: local versus non-local operators and effective thermal behaviour, Phys. Rev. B **82**, 144302 (2010).
- [62] E. Barouch, B. McCoy, and M. Dresden, Statistical Mechanics of the XY Model. I, Phys. Rev. A **2**, 1075 (1970); E. Barouch and B. McCoy, Statistical Mechanics of the XY Model. II, Phys. Rev. A **3**, 786 (1971); E. Barouch and B. McCoy, Statistical Mechanics of the XY Model. III, Phys. Rev. A **3**, 2137 (1971).
- [63] F. Igloi and H. Rieger, Long-Range correlations in the nonequilibrium quantum relaxation of a spin chain, Phys. Rev. Lett. **85**, 3233 (2000).
- [64] F. Igloi and H. Rieger, Quantum relaxation after a quench in systems with boundaries, Phys. Rev. Lett. **106**, 035701 (2011).
- [65] K. Sengupta, S. Powell, S. Sachdev, Quench dynamics across quantum critical points, Phys. Rev. A **69** 053616 (2004).
- [66] M. Fagotti and P. Calabrese, Evolution of entanglement entropy following a quantum quench: Analytic results

- for the XY chain in a transverse magnetic field, Phys. Rev. A **78**, 010306 (2008).
- [67] A. Silva, The statistics of the work done on a quantum critical system by quenching a control parameter, Phys. Rev. Lett. **101**, 120603 (2008); A. Gambassi and A. Silva, Statistics of the Work in Quantum Quenches, Universality and the Critical Casimir Effect, 1106.2671.
- [68] L. Campos Venuti and P. Zanardi, Unitary equilibrations: Probability distribution of the Loschmidt echo, Phys. Rev. A **81**, 022113 (2010); L. Campos Venuti, N. T. Jacobson, S. Santra, and P. Zanardi, Exact Infinite-Time Statistics of the Loschmidt Echo for a Quantum Quench, Phys. Rev. Lett. **107**, 010403 (2011).
- [69] L. Foini, L. F. Cugliandolo, and A. Gambassi, Fluctuation-dissipation relations and critical quenches in the transverse field Ising chain, Phys. Rev. B **84**, 212404 (2011).
- [70] H. Rieger and F. Iglói, Semiclassical theory for quantum quenches in finite transverse Ising chains, Phys. Rev. B **84**, 165117 (2011).
- [71] P. Calabrese, F.H.L. Essler and M. Fagotti, Quantum Quench in the Transverse Field Ising Chain, Phys. Rev. Lett. **106**, 227203 (2011).
- [72] F. A. Smirnov, *Form factors in completely integrable models of quantum field theory* (World Scientific, Singapore, 1992).
- [73] J. L. Cardy and G. Mussardo, Form factors of descendent operators in perturbed conformal field theories, Nucl. Phys. **B340**, 387 (1990); V. P. Yurov and Al. B. Zamolodchikov, Correlation functions of integrable 2-D* models of relativistic field theory. Ising model, Int. Jour. Mod. Phys. **A6**, 3419 (1991); S. Lukyanov, Free Field Representation For Massive Integrable Models, Commun. Math. Phys. **167**, 183 (1995); H. Babujian, A. Fring, M. Karowski and A. Zapletal, Exact Form Factors in Integrable Quantum Field Theories: the Sine-Gordon Model, Nucl. Phys. B **538**, 535 (1999).
- [74] G. Delfino, Integrable field theory and critical phenomena. The Ising model in a magnetic field, J. Phys. A: Math. Gen. **37**, R45 (2004).
- [75] G. Mussardo, "Statistical Field Theory, An Introduction to Exactly Solved Models in Statistical Physics" (Oxford University Press, Oxford 2009).
- [76] F.H.L. Essler and R.M. Konik, Applications of Massive Integrable Quantum Field Theories to Problems in Condensed Matter Physics, in Ian Kogan Memorial Collection "From Fields to Strings: Circumnavigating Theoretical Physics", eds M. Shifman, A. Vainshtein and J. Wheeler, World Scientific Singapore 2005 [cond-mat/0412421].
- [77] P. Barmettler, M. Punk, V. Gritsev, E. Demler, and E. Altman, Relaxation of antiferromagnetic order in spin-1/2 chains following a quantum quench, Phys. Rev. Lett. **102**, 130603 (2009); P. Barmettler, M. Punk, V. Gritsev, E. Demler, and E. Altman, Quantum quenches in the anisotropic spin-1/2 Heisenberg chain: different approaches to many-body dynamics far from equilibrium, New J. Phys. **12**, 055017 (2010).
- [78] A. Faribault, P. Calabrese, and J.-S. Caux, Quantum quenches from integrability: the fermionic pairing model, J. Stat. Mech., P03018 (2009); Bethe Ansatz approach to quench dynamics in the Richardson model, J. Math. Phys. **50**, 095212 (2009).
- [79] V. Gritsev, T. Rostunov, and E. Demler Exact methods in analysis of nonequilibrium dynamics of integrable models: application to the study of correlation functions in nonequilibrium 1D Bose gas, J. Stat. Mech., P05012 (2010).
- [80] R. Ng and E. S. Sorensen, Exact real-time dynamics of quantum spin systems using the positive-P representation, J. Phys. A **44**, 065305 (2011).
- [81] P. Calabrese, F.H.L. Essler and M. Fagotti, Quantum Quench in the Transverse Field Ising chain II: Stationary State Properties, in preparation.
- [82] G. Vidal, J. I. Latorre, E. Rico, and A. Kitaev, Entanglement in quantum critical phenomena, Phys. Rev. Lett. **90**, 227902 (2003); J. I. Latorre, E. Rico, and G. Vidal, Ground state entanglement in quantum spin chains, Quant. Inf. and Comp. **4**, 048 (2004).
- [83] M. E. Fisher and R. E. Hartwig, Toeplitz determinants: some applications, theorems, and conjectures, Adv. Chem. Phys. **15**, 333 (1968); H. Au-Yang and B. McCoy, Theory of layered Ising models. II. Spin correlation functions parallel to the layering, Phys. Rev. B **10**, 3885 (1974); E. L. Basor and C. A. Tracy, The Fisher-Hartwig conjecture and generalizations, Physica A **177**, 167 (1991); P. J. Forrester and N. E. Frankel, Applications and generalizations of Fisher-Hartwig asymptotics, J. Math. Phys. **45**, 2003 (2004); A. Yu Karlovich, Asymptotics of block Toeplitz determinants generated by factorable matrix functions with equal partial indices, Math. Nachr. **280**, 1118 (2007); P. Deift, A. Its, and I. Krasovsky, Asymptotics of Toeplitz, Hankel, and Toeplitz+Hankel determinants with Fisher-Hartwig singularities, Ann. Math. **174**, 1243 (2011).
- [84] A. Boettcher and H. Widom, Szegő via Jacobi, Lin. Alg. Appl., **419**, 656 (2006).
- [85] M. Fagotti and P. Calabrese, Entanglement entropy of two disjoint blocks in XY chains, J. Stat. Mech. (2010) P04016.
- [86] R. Wong, Asymptotic Approximations of Integrals (SIAM ed., 2001).

- [87] S. Servadio, Unitarity constraint on the "truly 3 body" scattering .1, *Nuovo Cimento B* **100**, 565 (1988); S. Servadio, Unitarity constraint on the "truly 3 body" scattering .2, *Nuovo Cimento B.* **100**, 587 (1988).
- [88] M. Fagotti, unpublished.
- [89] F. H. L. Essler and R. M. Konik, Finite-temperature lineshapes in gapped quantum spin chains, *Phys. Rev. B* **78**, 100403 (2008); F. H. L. Essler and R. M. Konik, Finite Temperature Dynamical Correlations in Massive Integrable Quantum Field Theories, *J. Stat. Mech.* P09018 (2009).
- [90] M. Kormos and B. Pozsgay, One-point functions in massive integrable QFT with boundaries, *JHEP* 04 (2010) 112; B. Pozsgay and G. Takacs, Form factor expansion for thermal correlators, *J. Stat. Mech.* P11012 (2010).
- [91] B. Doyon, Finite-temperature form factors in the free Majorana theory, *J. Stat. Mech.* P11006 (2005); B. Doyon, Finite-Temperature Form Factors: a Review, *Sigma* **3**, 11 (2007);
- [92] A. Leclair, F. Lesage, S. Sachdev and H. Saleur, *Nucl. Phys.* **B482**, 579 (1996); A. LeClair, G. Mussardo, *Nucl. Phys. B* **552**, 624 (1999); R.M. Konik, *Phys. Rev. B* **68**, 104435 (2003); S.A. Reyes, A. Tsvetlik, *Phys. Rev. B* **73**, 220405(R) (2006); A.J.A. James, F.H.L. Essler and R.M. Konik, Finite Temperature Dynamical Structure Factor of Alternating Heisenberg Chains, *Phys. Rev. B* **78**, 094411 (2008); W. D. Goetze, U. Karahasanovic and F.H.L. Essler, Low-Temperature Dynamical Structure Factor of the Two-Leg Spin-1/2 Heisenberg Ladder, *Phys. Rev. B* **82**, 104417 (2010).
- [93] B. Pozsgay and G. Takacs, Form factors in finite volume I: form factor bootstrap and truncated conformal space, *Nucl. Phys. B.* **788**, 167 (2008); B. Pozsgay and G. Takacs, Form factors in finite volume II: disconnected terms and finite temperature correlators *Nucl. Phys. B.* **788**, 209 (2008).
- [94] S. Ghoshal and A. B. Zamolodchikov, Boundary S-Matrix and Boundary State in Two-Dimensional Integrable Quantum Field Theory, *Int. J. Mod. Phys. A* **9**, 3841 (1994); *ibid.* **9**, E4353 (1994).
- [95] B. L. Altshuler, R. M. Konik, and A. M. Tsvetlik, Low temperature correlation functions in integrable models: Derivation of the large distance and time asymptotics from the form factor expansion, *Nucl. Phys. B* **739**, 311 (2006).
- [96] A. Bugrij, Correlation function of the two-dimensional Ising model on the finite lattice. I, *Theor. Math. Phys.* **127**, 528 (2001); A. Bugrij and O. Lisovyy, Spin matrix elements in 2D Ising model on the finite lattice, *Phys. Lett. A* **319**, 390 (2003).
- [97] G. von Gehlen, N. Iorgov, S. Pakuliak, V. Shadura and Y. Tykhyy, Form-factors in the Baxter-Bazhanov-Stroganov model II: Ising model on the finite lattice, *J. Phys. A* **41**, 095003 (2008).
- [98] N. Iorgov, V. Shadura and Yu. Tykhyy, Spin operator matrix elements in the quantum Ising chain: fermion approach, *J. Stat. Mech.* (2011) P02028.
- [99] see e.g. C. Itzykson and J.-M. Drouffe, *Statistical Field Theory*, Cambridge University Press, Cambridge (1989).
- [100] D. Schuricht and F.H.L. Essler, arXiv:1203.5080.
- [101] F.H.L. Essler, S. Evangelisti and M. Fagotti, in preparation.
- [102] E. Lieb, T. Schultz, and D. Mattis, Two soluble models of an antiferromagnetic chain, *Ann. Phys. (N.Y.)* **16**, 407 (1961); P. Pfeuty, The one-dimensional Ising model with a transverse field, *Ann. Phys. (N.Y.)* **57**, 79 (1970).